TECHNISCHE UNIVERSITÄT MÜNCHEN

Lehrstuhl für Experimentelle Genetik

The role of TGFβ1 and microRNAs in skeletal muscle cell metabolism and differentiation

Selina Höckele

Vollständiger Abdruck der von der TUM School of Life Sciences der Technischen Universität München zur Erlangung des akademischen Grades eines

Doktors der Naturwissenschaften

genehmigten Dissertation.

Vorsitzende:	Prof. Dr. Veronika Somoza
Prüfer der Dissertation:	1. Prof. Dr. Dr. h. c. mult. Martin Hrabe de Angelis
	2. Prof. Dr. Nina Henriette Uhlenhaut

Die Dissertation wurde am 24.06.2020 bei der Technischen Universität München eingereicht und durch die TUM School of Life Sciences am 08.12.2020 angenommen.

Table of Contents

I. Publications

I.I. Publications related to this thesis in peer reviewed journals

Hoffmann, C., Höckele, S., Kappler, L., Hrabe de Angelis, M., Häring, H. U., & Weigert, C. (2018). The effect of differentiation and TGFβ on mitochondrial respiration and mitochondrial enzyme abundance in cultured primary human skeletal muscle cells. Sci Rep, 8(1), 737. doi:10.1038/s41598-017-18658-3

Jeske, T., Huypens, P., Stirm, L., Höckele, S., Wurmser, C. M., Böhm, A., Weigert, C., Staiger, H., Klein, C., Beckers, J., & Hastreiter, M. (2019). DEUS: an R package for accurate small RNA profiling based on differential expression of unique sequences. Bioinformatics. doi:10.1093/bioinformatics/btz495

I.II. Poster presentations related to this thesis

Höckele, S., Hoffmann, C., Irmler, M., Böhm, A., Beckers, J., Häring, H.U., Hrabe de Angelis, M., Weigert, C. Role of human intramuscular fibroblasts in the metabolic adaption to physical exercise. Danish Diabetes Academy summer school 2017, Eberup, Denmark.

Höckele, S., Huypens, P., Hoffmann, C., Jeske, T. Hastreiter, M., Böhm, A., Beckers, J., Häring, H.U., Hrabe de Angelis, M., Weigert, C. TGFß regulates Metabolism of Human Skeletal Muscle Cells by miRNAs. Diabetes Kongress der Deutschen Diabetes-Gesellschaft 2018, Berlin.

Höckele, S., Huypens, P., Hoffmann, C., Jeske, T. Hastreiter, M., Böhm, A., Beckers, J., Häring, H.U., Hrabe de Angelis, M., Weigert, C. TGFß regulates Metabolism of Human Skeletal Muscle Cells by miRNAs. Exercise Metabolism Cell Symposium 2019, Sitges, Spain.

II. Abbreviations

AKT	AKT serine/threonine kinase 1 and 2; protein kinase B (PKB)
ALDOA	aldolase, fructose-bisphosphate A
AMP	adenosine monophosphate
AMPKα2	AMP-activated catalytic subunit alpha 2
ANOVA	analysis of variance
ATP	adenosine triphosphate
ATP5A	ATP synthase
BMI	body mass index
BSA	bovine serum albumine
CARMN	cardiac mesoderm enhancer-associated non-coding RNA
CD56	neural cell adhesion molecule (NCAM)
cDNA	complementary DNA
COL18A1	collagen type XVIII alpha 1 chain
COL6A1	collagen type VI alpha 1 chain
COX6A2	cytochrome c oxidase subunit 6A2
CPT1B	carnitine palmitoyltransferase 1B
Cy3	cyanine dye 3
DEUS	differential expression of unique sequences
DMEM	Dulbecco's modified Eagle's medium
DMSO	dimethyl sulfoxide
DPBS	Dulbecco's phosphate-buffered saline
DSMZ	deutsche Sammlung von Mikroorganismen und Zellkulturen
EDTA	ethylenediaminetetraacetic acid
FBN1	fibrillin 1
FBS	fetal bovine serum
FC	fold change
FNDC5	fibronectin type III domain containing 5
GAPDH	glyceraldehyde-3-phosphate dehydrogenase
GLUT4	solute carrier family 2 member 4, glucose transporter type 4
HADHA	hydroxyacyl-CoA dehydrogenase trifunctional multienzyme complex subunit alpha
HDAC4	histone deacetylase 4
HRE	High responder
IGFBP5	insulin like growth factor binding protein 5
IPA	Ingenuity pathway analysis
IRS1	insulin receptor substrate 1
KEGG	kyoto encyclopedia of genes and genomes
LDLRAD4	low-density lipoprotein receptor class A domain-containing protein 4
LNA	locked nucleic acid

MACS	magnetic-activated cell sorting
MALDI-TOF MS	Matrix-assisted laser desorption ionization time-of-flight mass spectrometry
MAPK	mitogen activated protein kinase
MEF2C	myocyte enhancer factor 2C
MEOX2	mesenchyme homeobox 2
MIR143HG	microRNA-143 host gene
miRNA	microRNA
Mrf4	Myf6, myogenic factor 6
mRNA	messenger RNA
MSTN	myostatin
mTOR	mammalian target of rapamycin
mTORC1	mammalian target of rapamycin complex 1
Myf5	myogenic factor 5
MYH	myosin heavy chain
MyoD1	myogenic differentiation 1
MyoG	myogenin
NF-κB	nuclear factor-kappa B
NRE	non-responder
nt	nucleotides
OGTT	oral glucose tolerance test
ORP8	oxysterol binding protein like 8
PAX3	paired box 3
PBS	phosphate-buffered saline
PDE2A	phosphodiesterase 2A
PGC1α	PPARγ coactivator 1 alpha, gene name PPARGC1A
PKB	protein kinase B, see also AKT
PPARGC1A	PPARγ coactivator 1 alpha, protein name PGC1α
PPARγ	peroxisome proliferative activated receptor, gamma
Pri-miRNA	primary or precursor miRNA
PRKAA2	protein kinase AMP-activated catalytic subunit alpha 2, protein name AMPKα2
qPCR	quantitative real-time PCR
RIPA	radioimmunoprecipitation assay buffer
RNU6	RNA, U6A small nuclear
ROS	reactive oxigen species
RPS13	ribosomal protein S13
RRAGD	ras related GTP binding D
SD	standard deviation
siRNA	small interfering RNA
SMAD	mothers against decapentaplegic homolog

sncRNA	small non-coding RNA
TBP	TATA-Box Binding Protein
TFAM	transcription factor A, mitochondrial
TGFBI	transforming growth factor beta induced
TGFß	transforming growth factor beta
TSS	transcription start site
VMP1	vacuole membrane protein 1
VO_{2peak}	maximal oxygen uptake
α-MEM	minimum essential medium, alpha modification

III. Summary

The prevention of type 2 diabetes by exercise intervention is a promising path to battle the rising incidents. However, the wide range in the individual response to exercise, in particular the lack of a beneficial outcome in glycemic control and insulin sensitivity, needs to be understood in order to be able to prescribe individualized training programs. A possible upstream regulator involved in non-response to exercise is TGFβ1. The aim of this thesis was to investigate the molecular effects of TGFβ1 in human primary skeletal muscle cells, its effects on metabolic regulators and on microRNAs.

We stimulated CD56-positive, primary human skeletal myoblasts with TGFβ1, and subsequently differentiated them to myotubes. The collected samples were investigated by small and long RNA sequencing. Candidate regulators and miRNAs were further analyzed using qPCR or western blot. To study underlying mechanisms, we transfected a mix of TGFβ1-repressed miRNAs into human primary skeletal muscle cells to compensate the effects of TGFβ1, or transfected TGFβ1-induced miRNAs to examine if the effects of TGFβ1 are transmitted via upregulated miRNAs. Furthermore, we investigated different timepoints of myo-differentiation. Lastly, we repeated the preconfluent TGFβ1-stimulation in the murine cell line C2C12 and quantified regulators and miRNAs we previously found differentially expressed in human primary cells by qPCR.

In primary human skeletal muscle cells, TGFβ1 induced persistent effects which were detected after 5 days of myo-differentiation. We validated the upregulation of RNAs of extracellular matrix proteins and the inhibition of markers of differentiated skeletal muscle. Almost all mitochondrially encoded genes were repressed, together with a downregulation of *PGC1α*, ATP5A protein, and the insulin effect on the phosphorylation of threonine 308 of AKT. Regulated miRNAs could be distinguished into differentiation-dependent and -independent miRNAs. Differentiation-independent miRNAs, miR-21, miR-31, miR-143, miR-145, and miR-181a2, were acutely upregulated by TGFβ1 stimulation and were still increased after 5 days of myo-differentiation. In contrast, miRNAs, which were upregulated during myo-differentiation, were downregulated by TGFβ1. We could not show compensatory effects on the TGFβ1-induced repression of myo-differentiation when four of the differentiation-dependent miRNAs (miR-133b, miR-206, miR-208, and miR-499a) were supplemented by transfection of the respective miRNA mimics. Among the miRNAs upregulated by TGFβ1, miR-31 mimics reduced insulin-stimulated phosphorylation of threonine 308 of AKT. Furthermore, we discovered, that the murine cell line C2C12 does not show the prolonged regulation of e.g. PGC1α in myotubes after TGFβ1 treatment of myoblasts.

Our results confirmed, that TGFβ1 is an important regulator in skeletal muscle metabolism. TGFβ1 treatment of primary human skeletal muscle cells regulated the abundance of several miRNAs, which may be implicated in the regulation of insulin signaling and myo-differentiation. The different results

in C2C12 cells showed that the choice of the used model is essential. Immortalized cell lines are useful tools, however, their use should always be complemented with other models, such as the use of primary cells or *in vivo* data.

To conclude, the prolonged negative impact of TGFβ1 on skeletal muscle metabolism could be regulated via miRNAs. The inhibition of myo-differentiation by TGFβ1 further impairs healthy metabolism in skeletal muscle. Nevertheless, more research is needed to determine the role of miRNAs and molecular mechanisms involved in TGFβ1-induced effects.

IV. Zusammenfassung

Die Prävention von Typ 2 Diabetes durch Sportintervention ist ein vielversprechender Weg, um die ansteigende Inzidenz zu bekämpfen. Allerdings muss dafür die große Bandbreite der individuellen Trainingsreaktionen, insbesondere das Ausbleiben einer Verbesserung der Glukosekontrolle und Insulinsensitivität, verstanden werden, um individualisierte Trainingsprogramme verschreiben zu können. Ein möglicher Upstream-Regulator, der am Ausbleiben einer positiven Trainingsreaktion beteiligt ist, ist TGFβ1. Das Ziel dieser Arbeit war es, die molekularen Auswirkungen von TGFβ1 auf Stoffwechselregulatoren und microRNAs in humane Primärskelettmuskelzellen zu untersuchen.

Wir stimulierten CD56-positive, primäre humane Skeletmuskel-Myoblasten mit TGFβ1 und differenzierten sie anschließend zu Myotuben. Die gesammelten Proben wurden durch Sequenzierung kurzer und langer RNAs untersucht. Kandidatenregulatoren und miRNAs wurden mittels qPKR und Western Blot weiter analysiert. Um die zugrundeliegenden Mechanismen zu erforschen, transfizierten wir einen Mix aus TGFβ1-unterdrückten miRNAs in humane Primärmuskelzellen, um die Effekte von TGFβ1 zu kompensieren, oder transfizierten TGFβ1-induzierte miRNAs, um zu untersuchen, ob die Effekte von TGFβ1 über hochregulierte miRNAs übertragen werden. Darüber hinaus untersuchten wir verschiedene Zeitpunkte der Myodifferenzierung. Zuletzt wiederholten wir die präkonfluente TGFβ1-Stimulation in der murinen Zelllinie C2C12 und quantifizierten Regulatoren und miRNAs, die wir zuvor in humanen Primärzellen durch TGFβ1 reguliert gefunden hatten, mit qPKR.

In humanen Primärskelettmuskelzellen induzierte TGFβ1 anhaltende Effekte, die noch nach 5 Tagen Myodifferenzierung gemessen werden konnten. Wir bestätigten die Hochregulation von RNAs extrazellulärer Matrixproteine und die Hemmung von Markern differenzierter Skelettmuskelzellen. Fast alle mitochondrial kodierten Gene wurden unterdrückt, zusammen mit einer Herunterregulierung von *PGC1α*, des ATP5A-Proteins und der Wirkung von Insulin auf die Phosphorylierung von Threonin 308 von AKT. Die regulierten miRNAs konnten in differenzierungsabhängige und differenzierungsunabhängige miRNAs unterteilt werden. Die differenzierungsunabhängigen miRNAs miR-21, miR-31, miR-143, miR-145 und miR-181a2 wurden durch die Stimulation von TGFβ1 akut hochreguliert und waren nach 5 Tagen Myodifferenzierung immer noch erhöht. Im Gegensatz dazu wurden miRNAs, die während der Myodifferenzierung hochreguliert wurden, durch TGFβ1 herunterreguliert. Wir konnten keinen kompensatorischen Effekt auf die TGFβ1-induzierte Unterdrückung der Myodifferenzierung zeigen, wenn vier der differenzierungsabhängigen miRNAs (miR-133b, miR-206, miR-208 und miR-499a) durch Transfektion der entsprechenden miRNA-Mimics supplementiert wurden. Von den miRNAs, die von TGFβ1 hochreguliert wurden, reduzierten miR-31-Mimics die insulinstimulierte Phosphorylierung von Threonin 308 der AKT. Darüber hinaus stellten wir fest, dass die murine Zelllinie C2C12 nach TGFβ1 Behandlung von Myoblasten nicht die anhaltende Regulation von z.B. *PGC1α* in Myotuben zeigt.

Unsere Ergebnisse bestätigten, dass TGFβ1 ein wichtiger Regulator im Skelettmuskelstoffwechsel ist. Die Behandlung von humanen Primärskelettmuskelzellen mit TGFβ1 regulierte die Abundanz verschiedener miRNAs, die möglicherweise an der Regulation der Insulinsignalisierung und der Myodifferenzierung beteiligt sind. Die abweichenden Ergebnisse in C2C12-Zellen zeigten, dass die Wahl des verwendeten Modells von entscheidender Bedeutung ist. Immortalisierte Zelllinien sind nützliche Werkzeuge, ihre Verwendung sollte jedoch immer durch andere Modelle ergänzt werden, wie z.B. die Verwendung von Primärzellen oder *in vivo*-Daten.

Zusammenfassend lässt sich sagen, dass der anhaltende negative Effekt von TGFβ1 auf den Stoffwechsel der Skelettmuskulatur über miRNAs reguliert werden könnte. Die Hemmung der Myodifferenzierung durch TGFβ1 beeinträchtigt den gesunden Stoffwechsel in der Skelettmuskulatur zusätzlich. Dennoch ist weitere Forschung erforderlich, um die Rolle der miRNAs und die molekularen Mechanismen zu bestimmen, die an den TGFβ1-induzierten Effekten beteiligt sind.

1 Background/Introduction

The rising incident of diabetes is a serious burden for economy and society worldwide and needs to be counteracted (Barres and Zierath, 2016; Shubrook et al., 2018; Zheng et al., 2018; Zimmet et al., 2001). The most efficient way to tackle type 2 diabetes is to prevent or delay the onset of disease (Shubrook et al., 2018; Zimmet et al., 2001). The Diabetes prevention program research group showed that lifestyle intervention is more efficient in reducing the incident of type 2 diabetes than metformin treatment (Knowler et al., 2002). Skeletal muscle is the main site of glucose disposal under hyperinsulinemic conditions (DeFronzo et al., 1981), and responsible for the variance in resting metabolic rate (Zurlo et al., 1990). Intervention programs that activate glucose uptake in skeletal muscle and increase skeletal muscle tissue mass are a good measure to fight unbalanced glucose metabolism. It has been shown that physical activity is a major determinant in reducing the risk for type 2 diabetes (Kriska et al., 2003; Solomon and Thyfault, 2013).

Further advantages of regular physical exercise opposed to medication include costs (Neumann et al., 2017), simple implementation (Solomon and Thyfault, 2013), and an overwhelming majority of positive side effects (Pedersen and Saltin, 2015; Ruegsegger and Booth, 2018). However, response to physical exercise depends on the outcome looked at and has a high interindividual variability (Bohm et al., 2016b; Sparks, 2017). To help each subject in finding the best way to prevent disease, we need to understand all aspects on a molecular level in order to be able to judge which interventions will help whom (Samocha-Bonet et al., 2018). Therefore, we want to elucidate the mechanism behind the high interindividual variability in the response of glucose tolerance and insulin sensitivity after exercise interventions.

1.1 Physical exercise as prevention of type 2 diabetes

1.1.1 Type 2 diabetes mellitus – a lifestyle disease

Diabetes mellitus is a disease of disturbed glucose homeostasis and grouped into different types. Type 1 diabetes is an autoimmune disease, resulting in non-functional islet cells and therefore inability to produce sufficient insulin, whereas type 2 diabetes starts with an increasing insensitivity to insulin. Less common types include gestational diabetes, monogenetic diabetes, and secondary diabetes (International Diabetes Federation, 2017).

In this thesis, only type 2 diabetes mellitus, the most common type of diabetes, will be considered. Type 2 diabetes is preceded by prediabetes, a phase of impaired fasting glucose or impaired glucose tolerance during an oral glucose tolerance test (OGTT). In clinical practice in Germany, prediabetes is tackled by informing the patient and introducing lifestyle intervention and regular checkups.

Type 2 diabetes occurs mainly in obese patients (American Diabetes Association, 2014), while obesity itself causes insulin resistance (Thota et al., 2017). Obesity is the highest risk factor for type 2

diabetes, posing a higher risk than a sedentary lifestyle (Goedecke and Micklesfield, 2014). It has been shown, that an increase in visceral fat rather than only increase in body mass index (BMI) is associated with onset of type 2 diabetes (Bjorntorp, 1990; Kuwahara et al., 2017; Smith and Kahn, 2016). Obesity can lead to dysfunctional adipose tissue which in turn leads to disadvantageous distribution of fat in visceral fat instead of subcutaneous fat (Chait and den Hartigh, 2020). Visceral fat constantly releases free fatty acids, contributing to the metabolic syndrome, hyperinsulinemia and systemic inflammation (Bjorntorp, 1990). Lifestyle interventions can potentially reverse these negative effects, since weight loss also leads to loss of visceral fat (Ross, 1997). Exercise without weight loss has been shown to reduce visceral fat in subjects with and without type 2 diabetes (Lee et al., 2005). Thus, prevention of type 2 diabetes should build on prevention of accumulation of visceral fat by avoiding obesity and physical inactivity.

1.1.2 Skeletal muscle, physical exercise, and selected markers

To understand how and why exercise intervention can prevent diabetes or even revert prediabetes, basics about physical exercise and glucose uptake in skeletal muscle need to be understood.

1.1.2.1 Skeletal muscle and myoblast differentiation

Skeletal muscle is needed for motion and support of the body and in contrast to the other two types of muscle, cardiac and smooth muscle, skeletal muscle can be consciously controlled. It is the tissue with the largest tissue mass in the body (Dulloo et al., 2010). Skeletal muscle is a regenerative tissue and its cells are called myocytes. Skeletal muscle cells in cell culture can be distinguished into three differentiation states: Satellite cells, myoblasts and myotubes. As shown in Figure 1, satellite cells, the skeletal muscle precursor cells, can proliferate and are then called myoblasts. Myoblasts have the potential to fuse to differentiated myotubes containing several nuclei. *In vivo*, myotubes further mature into well-aligned myofibers and can be several centimeters long (Chal and Pourquie, 2017). They are the components that make up muscle. Myofibers contain myofibrils and sarcomere structures, mainly composed of actin and myosin (Newsholme et al., 2010). Each muscle fiber is surrounded by endomysium, a specialized basal lamina (Chal and Pourquie, 2017). These fibers are the base of skeletal muscle tissue, together with extracellular matrix, nerves, and blood vessels, they form muscle *in vivo* (Newsholme et al., 2010).

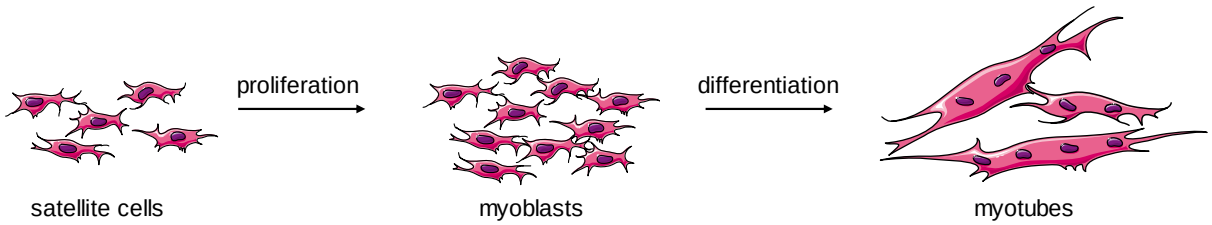

Figure 1. Myo-differentiation of skeletal muscle cells from satellite cells to myotubes.
Skeletal muscle stem cells (satellite cells) are named myoblasts when they proliferate. After differentiation to multinucleate cells, they are called myotubes. Figure was created with the use of Servier medical art creative commons.

1.1.2.2 Adaptations in skeletal muscle after exercise

Physical exercise means contraction of skeletal muscle. For contraction, skeletal muscle needs energy in the form of ATP (adenosine triphosphate). ATP can be generated from intramuscular sources of phosphocreatine, glycogen, triacylglycerol or plasma born fatty acids and glucose. The use of fuel is dependent on exercise intensity, duration and availability of oxygen in the muscle (Newsholme et al., 2010). At low intensity exercise, the bulk of energy needed for exercise is generated by oxidation of free fatty acids from intramuscular triglycerides or plasma while at higher intensities the proportional use of carbohydrates increases (Coyle, 1995; Romijn et al., 1993). At high intensity, e.g. sprints, anaerobe conversion of glucose to lactic acid and phosphocreatine are used (Newsholme et al., 2010). Anaerobe ATP generation from glucose is by far less effective than oxidative degradation of glucose in mitochondria over citric acid cycle but quicker (Newsholme et al., 2010). During prolonged exercise, the availability of glycogen in muscle (Ahlborg et al., 1967) and free glucose from liver glycogen decreases and therefore the contribution of fatty acid oxidation to ATP generation increases (Newsholme et al., 2010).

When exercised regularly, skeletal muscle adjusts to the challenge and takes on multifaceted adaptations. Trained skeletal muscle possesses more mitochondria and thereby a higher substrate oxidation capacity (Gollnick et al., 1973; Holloszy, 1967). It stores more glycogen (Bergstrom et al., 1972) and has increased muscle mass and capillarization providing better infrastructure for glucose and oxygen supply (Ingjer, 1979). Trained individuals also show better processing of glucose with a lower insulin peak, and fast removal of lipids (Bjorntorp et al., 1972). Even a single bout of exercise improves insulin sensitivity for approximately two days (Mikines et al., 1988). Furthermore, exercise has effects on other tissues, for example, increased glucose uptake not only in skeletal muscle but also in adipose tissue was shown in trained rats (James et al., 1985). On the other hand, increased capillarization and increased glucose uptake has been shown in one-leg-training models to be local effects only present in the exercised tissue (Dela et al., 2019; Sjoberg et al., 2017).

The exact mechanisms of improved insulin sensitivity are still under investigation, but several aspects were shown: The resting energy consumption in trained subjects is higher than in sedentary subjects

(Poehlman et al., 1989) and increased mitochondrial content by physical activity brings along an increased capability of ATP generation by mitochondria (Wibom et al., 1992). Trained rats have more glucose transporters in the plasma membrane of skeletal muscle (Goodyear et al., 1992). Overall, more energy in the form of glucose is used by skeletal muscle in trained subjects and glucose uptake rate is increased, leading to quicker glucose clearance. In skeletal muscle, GLUT4 (solute carrier family 2 member 4) is the most important glucose transporter. It is insulin sensitive (Birnbaum, 1989; James et al., 1989) and its abundance in the plasma membrane increases with training status (Goodyear et al., 1992). Interestingly, insulin and exercise are both stimuli for GLUT4 translocation paving the way for increased glucose transport (Lauritzen et al., 2008; Lauritzen et al., 2010). The effects of muscle contraction and insulin are independent and additive, also meaning that GLUT4 translocation by exercise is still functional in insulin resistant individuals (Klip et al., 2019).

Additionally, during exercise, free fatty acids are used as energy source (Ranallo and Rhodes, 1998), and increased lipid turnover and oxidation in athletes compared to sedentary subjects was retained in cultured myoblasts (Lund et al., 2018). This is reflected in loss of visceral fat after aerobic training programs (Ismail et al., 2012; Sabag et al., 2017), but also in both aerobic and resistance reducing hepatic fat independent of dietary changes (Golabi et al., 2016).

As physical exercise seems to be a good measure to achieve higher insulin sensitivity, bettering glucose homeostasis, and reducing fat mass, lifestyle interventions in prediabetics, diabetics and people with high risk for type 2 diabetes might be the solution to the epidemic.

1.1.2.3 Selected parameters to evaluate skeletal muscle cell differentiation and exercise effects on skeletal muscle metabolism

When investigating skeletal muscle, especially in the context of insulin sensitivity, some transcripts and proteins are of specific interest. This paragraph will shortly describe three of the most important measures used in this thesis.

The most obvious attribute of skeletal muscle cells, in contrast to other cells, is the differentiation to multinucleated myotubes. Myosin heavy chain (MYH) transcripts and protein are expressed in adult muscle and increase clearly during myo-differentiation *in vitro*. In humans, there are three myosin heavy chain isoforms encoded by the genes *MYH1*, *MYH2*, and *MYH7* (Schiaffino and Reggiani, 2011). MYH7 protein expression is associated with slow fiber type muscle, whereas MYH1 and MYH2 are associated with fast myosin fiber type (Schiaffino and Reggiani, 2011). The expression of *MYH* transcripts is a valuable measure for functional, differentiated skeletal muscle cells.

PPARγ (peroxisome proliferative activated receptor, gamma) coactivator 1 alpha (PGC1α, gene name PPARGC1A) is a central regulator of metabolism and was first described in adipose tissue and skeletal muscle of mice after cold exposure (Puigserver et al., 1998). In human skeletal muscle,

PGC1α levels increase after acute and regular physical exercise (Pilegaard et al., 2003; Russell et al., 2003). The overexpression of PGC1α leads to higher lipid oxidative capacity, increases genes of mitochondrial function and biogenesis, and decreases expression of a fast fiber type gene marker (Nikolic et al., 2012). Muscle-specific knock out of Pgc1α leads to a switch in fiber-type, exercise intolerance and severe loss of muscle mass in mice (Handschin et al., 2007). Thus, increases or decreases in PGC1α are an insightful measure for metabolic state of skeletal muscle cells.

To investigate insulin sensitivity *in vitro*, measuring the insulin-induced phosphorylation (Thr308 or Ser473) of AKT (AKT serine/threonine kinase 1 and 2 or protein kinase B, PKB) is a valuable tool. AKT is a central kinase in insulin stimulated glucose uptake in skeletal muscle (Ueki et al., 1998). The inhibition of insulin-stimulated activation of AKT in patients with type 2 diabetes has been shown to be maintained in skeletal muscle cell culture (Cozzone et al., 2008). Therefore, insulin-induced phosphorylation of AKT is a useful measure of insulin sensitivity in skeletal muscle cell culture.

1.2 Lifestyle intervention studies

Over the years, many lifestyle intervention studies to reduce the risk of developing type 2 diabetes have been performed. They are different in their kind of intervention, duration, supervision, outcomes, and many more parameters. In the following, a short overview of some of the most relevant studies reaching from general lifestyle intervention studies to supervised and controlled exercise intervention studies will be given.

In a study in Finland, Tuomilehto et al. showed that lifestyle intervention aiming at reducing weight, adapting a healthier diet and exercising could reduce the risk for developing type 2 diabetes by 58% compared to a control group and that the reduced risk was directly associated with changes in lifestyle (Tuomilehto et al., 2001). One of the most known lifestyle intervention studies is the one reported by Knowler et al. as they compared an intensive lifestyle intervention to an intervention with metformin treatment. They showed that lifestyle intervention could reduce the incident of type 2 diabetes more efficiently (-58%) than metformin treatment (-31%) (Knowler et al., 2002). The contribution of physical exercise to the risk for type 2 diabetes was reviewed by Hawley (Hawley, 2004), demonstrating clear associations of physical inactivity and impaired glucose tolerance, leading to a cascade of events resulting in insulin resistance and type 2 diabetes.

Long before, Richter et al. investigated effects of intense and endurance exercise on insulin sensitivity in healthy subjects and subjects with type 2 diabetes. They showed that physical exercise increases metabolic flexibility by enabling muscle to take up and oxidize free fatty acids and increasing lipoprotein lipase activity. The activity of lipoprotein lipase in muscle was further shown to correlate with insulin sensitivity (Richter et al., 1992).

The HERITAGE Family Study investigated sedentary, healthy adults before and after an exercise intervention, aiming to reveal genes and mutations affecting cardiovascular endurance and disease, risk factors for type 2 diabetes, as well as response to regular exercise. Using genome-wide linkage scans, they identified a linkage of changes in fasting insulin in response to exercise intervention with a marker in the leptin gene (Lakka et al., 2003). Another finding was, that even though the mean insulin sensitivity increased by 10% after 20 weeks of endurance exercise intervention, there was a high variability in the changes amongst participants (Boule et al., 2005).

One limitation of most lifestyle interventions studies for type 2 diabetes is that they often motivate subjects with a high risk for type 2 diabetes to adopt a healthier lifestyle including change in diet and increasing physical activity. Both exercise and healthier nutrition, can reduce risk factors for diabetes development, e.g. by decreasing fat mass. Thus, it is hard to dissect which part of the intervention program contributes in which way to an improvement of insulin sensitivity. Additionally, large intervention studies are often not controlled trials and adherence to intervention is only monitored using questionnaires. It is therefore not possible to say if people that are not responding well really did take part in the intervention with the same effort as the ones responding well. The following paragraphs will therefore focus on intervention studies with controlled exercise intervention.

There was scientific consensus that physical activity is beneficial for prevention of type 2 diabetes but also type 2 diabetic patients. Nevertheless, this knowledge was not broadly implemented in clinical practice (Praet and van Loon, 2008). It was suggested, that more detailed understanding of which patient would benefit most from which training regimen was needed to maximize the effects and increase prescription of structured exercise therapy (Praet and van Loon, 2008).

Thus, several studies compared exercise interventions of differing intensity and volume. Bajpeyi et al. compared groups of low and high volume of exercise as well as moderate and vigorous intensity to a sedentary control group. They found insulin sensitivity increased after all exercise intervention plans but a faster decrease of insulin sensitivity back to sedentary values after 15 days in the groups that exercised at low volume but vigorous intensity. They concluded that obese subjects with impaired insulin sensitivity could benefit most from chronic endurance-oriented training and that persistence of the effects varies strongly amongst training modes (Bajpeyi et al., 2009).

In the comparison of aerobic training, resistance training and the combination of both, the combination resulted in greater improvements in insulin sensitivity or HbA1c in two independent studies (AbouAssi et al., 2015; Church et al., 2010). Although all subjects were able to reduce waist circumference, aerobic training and resistance training alone failed to improve maximum oxygen consumption in a 9-month exercise program with patients with type 2 diabetes (Church et al., 2010). In a study with healthy, sedentary, overweight subjects, the 8 months exercise intervention with combination exercise lead to improvements in insulin sensitivity and β-cell function that were partly

retained 14 days after the last bout of exercise. Either aerobic or resistance training alone were not able to improve insulin sensitivity (AbouAssi et al., 2015). Sparks et al. showed different metabolic adaptions by the different training modalities. While 9 months of resistance training increased mitochondrial content in subjects with type 2 diabetes, aerobic training increased octanoate oxidation, and combination training increased both. They also showed changes homogenous amongst all training regiments, such as increase in palmitate, pyruvate, and acetate oxidation. Furthermore, they showed an association between increased mitochondrial DNA and improvements in VO_{2peak} (Sparks et al., 2013).

Exercise intervention studies vary in exercise protocols and measured endpoints. Some compare different types of exercise or frequency of exercise bouts, intensity or duration of exercise, and many different target objectives are investigated (Bohm et al., 2016b; Solomon, 2018; Sparks, 2017). In most renowned diabetes prevention studies, the main target objectives are risk reduction for diabetes (Bouchard et al., 2012). In controlled exercise intervention studies, insulin sensitivity is often used as a parameter of intervention outcome (Roberts et al., 2013). In studies using endurance training, increases between 25% and 50% in insulin sensitivity were observed in different study groups as reviewed by Roberts et al. Similar results were seen for resistance training where improvements in insulin sensitivity and glucose tolerance after resistance training was shown (Roberts et al., 2013). Nevertheless, there are also studies not showing improved glucose handling after resistance training intervention, e.g. in a study comparing aerobic and resistance training and combination of both that only found improvement in the endurance and the combined training groups (Davidson et al., 2009).

One crucial problem with studies like this is that individuals react very different to exercise (Bohm et al., 2016b; Bouchard et al., 2012; Solomon, 2018; Sparks, 2017). While heritable responses to exercise have been described (Lakka et al., 2003), DNA methylation and other epigenetic modifications are also discussed to explain the observed heterogenous response to exercise (Stephens and Sparks, 2015). The understanding of these interpersonal differences is crucial for our comprehension of the individual response to exercise and the development of individualized therapies.

1.3 Exercise non-response

When looking at individuals in exercise intervention studies, there is always a group of people not reaching the desired improvement of the investigated outcome, e.g. no improvement of insulin sensitivity or cardiovascular fitness after exercise intervention (Bohm et al., 2016b; Bouchard et al., 2012; Sparks, 2017). Thereby, it is possible that an individual improves its cardiovascular fitness but not its insulin sensitivity throughout the study period. It is therefore crucial to define the parameter in which the non-response occurred. For the context of type 2 diabetes, non-response with respect to glucose homeostasis should be in focus. As summarized by Bohm et al. and shown in Table 1, non-responders exist in various settings from healthy individuals over prediabetics to diabetics, but also

throughout different types of exercise intervention (Bohm et al., 2016b). Therefore, there does not seem to be one training program that fits all.

Table 1. Amount of non-responders with respect to parameters of glucose homeostasis in different exercise intervention studies.
Adapted from Böhm et al. (Bohm et al., 2016b).

Citation	Population	Intervention	Duration	Outcome	Non-responders (%)[a]
(Boule et al., 2005)	$n = 596$, healthy	Endurance training, 3×/week, 55–75 % VO_2max,	20 weeks	Insulin sensitivity	42
(Borel et al., 2012)	$n = 104$, abdominally obese/dyslipidemic	160 min/week moderate-intensity exercise and −500 kcal per day, pedometer use	12 months	Glucose tolerance status	62.5
(Hagberg et al., 2012)	$n = 110$, healthy	endurance training, 3×/week, 50–70 % VO_2max	26 weeks	Insulin sensitivity	25
(Yates et al., 2014)	$n = 29$, prediabetic	education program with pedometer use	12 months	2-h glucose	7[b]
(Winett et al., 2014)	$n = 159$, prediabetic	Resistance training, 2 ×/week	3 months	2-h OGTT	44[c]
(Stephens et al., 2015)	$n = 42$, diabetic	Aerobic, resistance training, or combination thereof	9 months	Combination of HbA1c, % body fat, BMI, muscle mitochondrial content	21
(Osler et al., 2015)	$n = 14$, prediabetic	Nordic walking, 5 h/week, unsupervised	20 weeks	Glucose tolerance status	36

Quantity of non responders with respect to glucose homeostasis
[a] Meaning no improvement, unless stated otherwise
[b] Adverse response
[c] Estimated from graph

As the percentage of non-responders varies hugely, it has been suggested that non-response can be overcome by training more frequently or more intensely (Montero and Lundby, 2017). This study however, only considered VO_{2peak} as outcome. From this study, we cannot say if all non-response with respect to insulin sensitivity could be abolished by increasing training modalities. However, in a realistic setting for patients, the higher doses of training suggested are most likely not feasible for most in need of exercise intervention. On the other hand, a change in exercise type might be more practicable in a real-life setting. Thus, we need to understand the molecular mechanisms of exercise non-response to be able to judge what changes could help non-responders in becoming responders.

1.4 The NRE Study

To elucidate the mechanisms of non-response to exercise with respect to insulin sensitivity, the non-responder (NRE) study was conducted in Tübingen. It was a controlled exercise intervention study with twenty sedentary men with high risk for type 2 diabetes defined as meeting at least one of the following criteria, BMI > 27 kg/m², or first-degree family history of type 2 diabetes. The exercise intervention was comprised of three supervised exercise sessions per week over 8 weeks. The training sessions were performed at 80% of individual VO_{2peak} and comprised of 30 minutes of ergometer exercise followed by 30 minutes of walking on a treadmill (Bohm et al., 2016a).

Extensive analysis of clinical parameters before and after exercise intervention lead to the grouping into high-responders (HRE) and non-responders (NRE) with regards to change in insulin sensitivity index. RNA from muscle biopsies underwent microarray analysis. When comparing changes by training intervention between NRE and HRE, upregulation of mitochondrial enzymes like carnitine palmitoyltransferase 1B (CPT1B) or ATP synthase (ATP5A) were impaired in non-responders. Furthermore, Ingenuity pathway analysis (IPA) showed an impaired activation of peroxisome proliferator-activated receptor γ coactivator (PGC1α; gene name *PPARGC1A*) in NRE. IPA further showed TGFβ1 (transforming growth factor beta 1) as a possible upstream regulator as it was upregulated in NRE after exercise compared to pre-exercise levels and several TGFβ1 target genes showed a negative correlation with the change in insulin sensitivity in the entire study group. As plasma levels of TGFβ1 were not different before and after training intervention and not different between response groups, Böhm et al. suspect the activation of TGFβ1 signaling to be locally restricted to skeletal muscle (Bohm et al., 2016a).

They further stimulated primary human skeletal muscle cells with TGFβ1 and found decreases in mRNA levels of *PGC1α*, *CPT1B*, *MYH2* and *MYH7*. On protein level, they observed a reduction in protein kinase AMP-activated catalytic subunit alpha 2 (AMPKα2, gene name *PRKAA2*) and ATP5A. All this data taken together suggest that TGFβ1 impairs not only differentiation of myoblasts to myotubes as it already reported (Allen and Boxhorn, 1987, 1989; Massague et al., 1986) but also metabolism and thus could be part of the mechanism of non-response to exercise with respect to insulin sensitivity (Bohm et al., 2016a).

1.5 TGFβ1 in skeletal muscle, diabetes, and exercise

Transforming growth factor beta 1 is a cytokine with broad tissue expression and functions. It belongs to the TGFβ superfamily whose members regulate essential processes in cells such as proliferation, differentiation, cytoskeletal organization, migration and cell death (Weiss and Attisano, 2013). Canonical signaling occurs via SMAD (mothers against decapentaplegic homolog) signaling. TGFβ1 binds to the TGFβ receptor complex which further leads to a phosphorylation of SMAD2/3 proteins, which then associate with SMAD4. This complex is translocated to the nucleus where it can enhance or repress the expression of target genes (Abrigo et al., 2018). TGFβ1 can also act through non-canonical pathways, e.g. activating mitogen activated protein kinases (MAPK), nuclear factor-kappa B (NF-κB), or phosphoinositide 3-kinase-pritein kinase B (PKB) (Abrigo et al., 2018; Zhang, 2009).

TGFβ1's fundamental role for development and physiology was shown with a mouse knockout resulting in inflammatory disorders, wasting syndrome and early death (Shull et al., 1992). TGFβ1 has been described to inhibit myoblast fusion as early as 1986 (Massague et al., 1986; Olson et al., 1986). Elevated levels of TGFβ1 negatively affect muscle regeneration (Allen and Boxhorn, 1987, 1989) and TGFβ1 levels are elevated in different muscle disorders (Bernasconi et al., 1999; Gosselin et al., 2004;

Ishitobi et al., 2000). Taken together, TGFβ1 is involved in the regulation of central physiological processes in skeletal muscle like development and tissue regeneration.

In a meta-analysis, Qiao et al. found that patients with type 2 diabetes show increased levels of TGFβ1 in urine and plasma (Qiao et al., 2017). In children with type 1 diabetes, elevated TGFβ1 levels in urine could be normalized by insulin treatment (Holmquist and Torffvit, 2009). These results indicate a potential role of TGFβ1 in dysfunctional metabolism.

An increase of TGFβ1 levels after exercise was first shown in mice 48 h after eccentric exercise (Barash et al., 2004). In rats, different responses to a single bout of exercise were observed in trained and untrained rats. Trained rats showed decreased TGFβ1 mRNA expression directly after exercise while untrained rats had increased TGFβ1 expression levels directly after exercise. Three hours after exercise, both groups were recovering TGFβ1 levels towards pre-training levels. Furthermore, trained rats showed higher mRNA levels but lower protein levels of TGFβ1 (Czarkowska-Paczek et al., 2009).

In humans, increases in transforming growth factor beta-induced (*TGFBI*) transcript have been shown 4 days after intense exercise in trained individuals (Neubauer et al., 2014). In a different study, moderately active subjects showed clear increases 3 days after eccentric exercise, whereas the increase was higher in younger subjects (Hamada et al., 2005). After acute leg kicking exercise, Heinemeier et al. found *TGFβ1* mRNA levels increased in muscle but not tendon of humans (Heinemeier et al., 2013).

Mechanistically it has been shown in mice and cell culture that SMAD3 (activated by TGFβ1) negatively regulates PGC1α and knock-out of SMAD3 reversely leads to higher levels of PGC1α in skeletal muscle models (Tiano et al., 2015).

SMAD3 also has been shown to be part of the mechanism of TGFβ inhibiting myo-differentiation (Liu et al., 2001). It was shown that TGFβ1 inhibits the myogenic factors MyoD (MyoD1, myogenic differentiation 1), MyoG (myogenin), Myf5 (myogenic factor 5), and Mrf4 (also Myf6, myogenic factor 6) (Brennan et al., 1991; Liu et al., 2001; Martin et al., 1992; Vaidya et al., 1989). In detail, it was shown that the inhibition is transmitted via SMAD3 which inhibits MyoD (Liu et al., 2001). More recently, the inhibitory effect of TGFβ1 on myo-differentiation was proposed to be transmitted by downregulation of miRNAs miR-206 and miR-29 which would otherwise suppress HDAC4 (histone deacetylase 4) (Winbanks et al., 2011). It is therefore possible, that effects of TGFβ1 are mechanistically regulated by changed abundance of miRNAs.

Thus, TGFβ1 signaling plays an important role in skeletal muscle, exercise and diabetes. Its role in non-response to exercise thereby becomes even more plausible. Effects of TGFβ1 might be regulated by miRNAs.

1.6 miRNAs in skeletal muscle and insulin signaling

Only 1-2 % of the human genome is protein coding. It was shown that the complexity of organisms correlates with the proportion of non-protein-coding DNA sequence (Taft and Mattick, 2003). There are non-coding DNA sequences that are not transcribed and there are sequences that are transcribed to RNA but not translated into protein. Of these non-coding RNAs, we generally distinguish between long non-coding RNAs and small non-coding RNAs (sncRNA). The first described function of a sncRNA was in *C. elegans* where lin-4 post-transcriptionally regulates lin-14 by complementary binding. They found an approximately 61 nt long precursor-miRNA and an approximately 22 nt long mature miRNA (Lee et al., 1993; Wightman et al., 1993). With the discovery of small interfering RNA (siRNA) and the possibility to synthetically silence genes using this discovery (Elbashir et al., 2001), the future of miRNA research was paved. Soon, important regulatory functions of miRNAs were described and miRNA pathways were slowly elucidated (Ambros, 2004; Bartel, 2004).

Most miRNAs are derived from longer primary or precursor miRNA transcripts (pri-miRNA) which form imperfect hairpin structures (Bartel, 2004; He and Hannon, 2004; Lai, 2003). They are processed by Drosha and its cofactor to stem-looped structured pre-miRNAs (Lee et al., 2003; Lee et al., 2002) before being transported to the cytoplasm to be cleaved by Dicer to the miRNA duplex consisting of miRNA guide strand and the passenger strand (Grishok et al., 2001; Hutvagner et al., 2001). The miRNA duplex is loaded onto Argonaute proteins (Iwasaki et al., 2010) where one strand, the passenger strand, is retained as the guide strand exits Argonaute to act as mature miRNA by forming the RNA-induced silencing complex (Suzuki, 2018). Both strands have the potential to become guide or passenger strand, however, for each miRNA there is a asymmetry which strand is found as mature miRNA more frequently (Chiang et al., 2010; Suzuki et al., 2015). The more abundant strand is by convention called guide strand or miRNA, while the less abundant strand is called passenger strand or miRNA* (Suzuki, 2018). The respective strands are specified by their location in the pre-miRNA, meaning the 5’ arm would be called miRNA-5p, and the 3’ arm miRNA-3p (Desvignes et al., 2015).

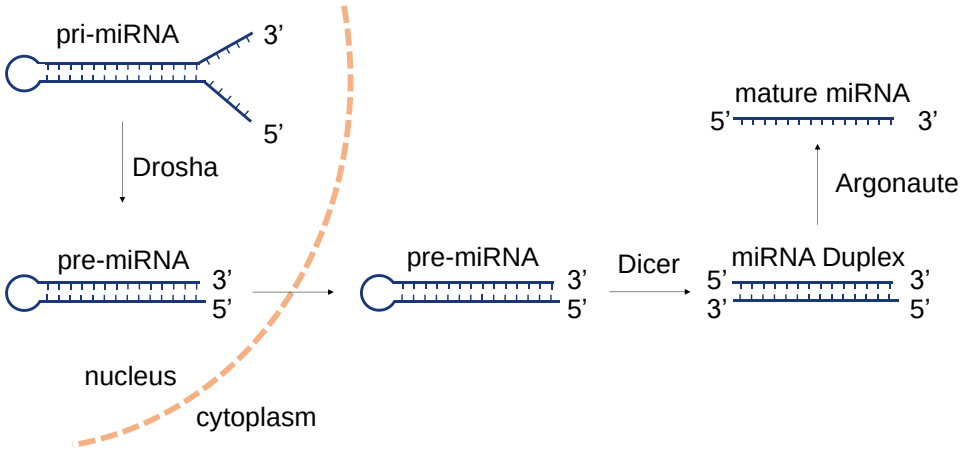

Figure 2. Processing of miRNA.
Simplified visualization of miRNA processing after transcription.

With the rising understanding about miRNAs, it became clear, that expression patterns of miRNAs are tissue specific. Horak et al. reviewed the regulation and function of miRNAs in development of skeletal muscle and identified miR-1, miR-133a, miR-133b, miR-206, miR-208b, miR-486 and miR-499 as muscle-specific microRNAs (Horak et al., 2016). Increased expression of miR-1, miR-133 (Chen et al., 2006; Zhang et al., 2012) and miR-206 (Goljanek-Whysall et al., 2012; Kim et al., 2006) induce satellite cell differentiation, and Winbanks et al. showed an effect of TGFβ1 via miR-206 and miR-29 on myogenic differentiation via regulation of HDAC4 (Winbanks et al., 2011). In a miRNA inhibitor screen, Polesskaya et al. showed that myo-miRNAs are essential for differentiation of skeletal muscle cells (Polesskaya et al., 2013).

The next question to ask was whether miRNAs are regulated by exercise and implicated in the adaption of muscle function to training. In humans, an acute bout of exercise increased expression levels of miR-1, miR-133a, miR-133b, miR-181a and miR-206 and decreased expression levels of miR-9, miR-23a, miR-23b and miR-31 (Russell et al., 2013). An intensive 10-day exercise program lead to continued increase (measured 2 days after end of exercise program) of miR-1, miR-29b and miR-133b in comparison to pre-training levels (Russell et al., 2013). The decrease of miR-31 was also sustained two days after the end of the 10-day training program (Russell et al., 2013). On the other hand, Nielsen et al. found miR-1, miR-133a, miR-133b and miR-206 decreased in muscle tissue after 12 weeks of endurance training (Nielsen et al., 2010). To summarize, muscle specific miRNAs seem to be upregulated after acute or intense exercise bouts in muscle tissue but downregulated in endurance-trained individuals. Furthermore, other miRNAs, such as miR-31 are also regulated after exercise.

In parallel, researchers started to investigate circulating miRNAs, e.g. miRNAs detectable in blood samples. Several studies looked at levels of circulating miRNAs after intense exercise and some found before-mentioned miRNAs upregulated (Sapp et al., 2017). However, the evidence is not consistent (Russell and Lamon, 2015; Sapp et al., 2017) hinting towards a high heterogeneity or individual response to exercise or exercise type.

Among others, one miRNA has gained a lot of attention in metabolism, obesity and diabetes: miR-143 (Fang et al., 2012; Jordan et al., 2011; Li et al., 2018; Muralimanoharan et al., 2016). Jordan et al. demonstrated a mechanism how miR-143 inhibits insulin-stimulated AKT phosphorylation via oxysterol binding protein like 8 (ORP8) in liver of mice (Jordan et al., 2011). Furthermore, miR-143 is needed for differentiation in adipose tissue (Esau et al., 2004).

Interestingly, miR-143 is also described to be upregulated by TGFβ1 stimulation in non-small lung cancer cells (Cheng et al., 2014), and smooth muscle cells (Climent et al., 2015; Long and Miano, 2011). On the other hand, TGFβ was shown to influence the processing of miRNAs by promoting Drosha mediated pri-miRNA processing over SMADs (Davis et al., 2008; Davis et al., 2010). Vice

versa, it was shown that TGFβ signaling is regulated by miRNAs (Suzuki, 2018), for example by miR-21 downregulating TGFBR2 (Yu et al., 2012) or the miR-200 family which were shown to downregulate TGFβ1, TGFβ2 and TGFβ3 expression (Gregory et al., 2011).

Hence, miRNAs are potential regulators in skeletal muscle, in insulin signaling and TGFβ1 signaling and their mechanisms need to be understood to elucidate molecular mechanisms of the effects of TGFβ1 on metabolic regulators and insulin signaling in skeletal muscle.

1.7 Cell culture models for skeletal muscle

For mechanistic studies, cell culture models are commonly used and feasible models. For skeletal muscle, often used cell lines are the murine myoblast cell line C2C12, or L6 myoblasts, a cell line from rat myoblasts. However, we wanted to stay as closely to the human scenario as possible and therefore used primary human skeletal muscle cells. Since the first description in 1981 (Blau and Webster, 1981), the use of primary human skeletal muscle cells in culture became well established. To achieve a clean culture with as little fibroblasts as possible, cells were sorted magnetically for CD56-positive cells as described before (Bohm et al., 2016a) in our experiments. Furthermore, our group showed that myo-differentiation without FBS (instead of 2% FBS or horse serum) leads to higher levels of differentiation markers, reflecting a more homogenous culture, containing less undifferentiated cells (Hoffmann et al., 2018).

Of course, the culture of primary cells leads to changes compared to the *in vivo* situation. However, cultured myotubes show great morphological, metabolic and biochemical similarities to adult *in vivo* skeletal muscle (Gaster et al., 2001; Henry et al., 1995; Thompson et al., 1996). Cultured myoblasts obtained from diabetics or subjects with insulin resistance still show changed metabolism *in vitro* (Henry et al., 1995; Thompson et al., 1996). The most impressive example of maintained phenotype was shown by (McIntyre et al., 2004). McIntyre et al. demonstrated differences in insulin signaling of skeletal muscle cells from diabetics in comparison to controls after 5 passages in culture (McIntyre et al., 2004). To name a more mechanistic example, it was shown that cells from diabetic patients still showed altered phosphorylation of AKT after insulin stimulation *in vitro* compared to cells from healthy controls (Cozzone et al., 2008).

In conclusion, primary human muscle cells after myo-differentiation are a good model to study metabolism and mechanistic effects of skeletal muscle.

1.8 Aims of this thesis

Exercise intervention together with nutritional changes might be the most sustainable way to prevent type 2 diabetes. However, at a given dose, exercise intervention does not lead to improvements of insulin sensitivity in all individuals. Therefore, molecular differences in the adaptations to exercise intervention need to be understood to be able to draw conclusions for individualized exercise programs. TGFβ1 is an important regulator of skeletal muscle morphology and differentiation and its dysregulation might be a key element of non-response to exercise intervention.

Thus, we aimed to elucidate the molecular mechanisms of TGFβ1 on metabolic regulators and insulin signaling with a focus on TGF β1-regulated miRNAs. We used primary skeletal muscle cells to identify TGFβ1-regulated coding and small noncoding RNAs by RNA sequencing as an untargeted approach. Next, we elucidated the regulation of the identified miRNAs during myo-differentiation. We further evaluated the function of identified miRNAs in myo-differentiation, insulin signaling and effect on the abundance of metabolic regulators, e.g. PGC1α. Lastly, we analyzed the methylation of PGC1α promoters after TGFβ1 treatment as potential additional mechanism for the regulation of PGC1α expression by TGFβ1.

2 Materials and Methods

2.1 Materials

2.1.1 Chemicals, reagents and additives

Table 2. Chemicals, reagents and additives.

Chemical or reagent	Supplier	Catalogue number
2-Propanol for molecular biology use	Applichem	A3928
Acrylamide solution (Rotiphorese Gel 30)	Roth	3029.1
Albumin from bovine serum	Sigma	A3311-50G
Ammonium persulfate (APS)	Sigma	A-7460
Amphotericin B ,100 ml	Lonza	17-836E
Chicken Embryo Extract Lyophilized, 10ml	Seralab	CE-650-DL
EDTA	Sigma	ED2SS
Ethanol absolute for molecular biology use	Applichem	A3678
Fetal Bovine Serum	Life technology	A2720801
Gelatin	Merck	1.04070.0500
Geltrex LDEV-free	Life technology	A1413302
Glycerol	Sigma	G 7757-1GA
Glycine	AppliChem	A1067,5000
Human insulin	Sigma	11376497001
Human TGFβ1	R&D systems	100-B-001
IGEPAL CA-630	Sigma	I3021-100ML
L-Carnitine hydrochloride	Sigma	C0283-1G
NaCl	Merck	1.06404.5000
Oleic acid	Sigma	O1008-5G
Palmitic acid	Sigma	P0500-10G
Penicillin-Streptomycin mixture	Lonza	DE17-602E
Phosphatase inhibitor cocktail (PhosSTOP)	Roche	04906837001
Ponceau S solution	Sigma	P7171-1L
Protease inhibitor cocktail (complete)	Roche	05892791001
RNase A	Macherey-Nagel	740505.50
SB431542	Sigma	S4317-5MG
SDS	Sigma	L-5750
Sodium deoxycholate	Sigma	D6750-100G
TRIS	Serva	37190
Triton X100	Sigma	X100-100ML
Trypsin/EDTA 0.05% phenol red	Life technologies	25300054
Tween 20	Sigma	T2700-100ML
TEMED	Roth	2367.3

2.1.2 Buffers and media

Table 3. Buffers and media for cell culture.

Buffer or medium	Supplier	Catalogue number
Albumin, bovine serum 10% solution	Sigma	A1595-50ML
DMEM 4.5 g/L glucose with L-glutamine	Lonza	12-604F
Ham's F-12	Biochrom	FG 0815
MEM Alpha Eagle	Biozym	880110-12
PBS, pH 7.4	Life technology	10010056
TRIS EDTA buffer solution pH 8.0	Sigma	93283-100ML

Table 4. Buffers for Western Blot.

Reagent	Amount	Final concentration
TBS (10x)		
TRIS pH 7.4	250 ml from 1M	250 mM
NaCl	87.66 g	1.5 M
Ultrapure H_2O	Added to a final volume of 1 l	
Diluted 10x using ultrapure H_2O for 1x TBS.		
TBST (1x)		
TBS (10x)	100 ml	25 mM TRIS 0.15 M NaCl
Tween 20	1 ml	0.1%
ultrapure H_2O	Added to a final volume of 1 l	
NET-G (10x)		
Gelatin	25 g	2.5%
NaCl	87.66 g	1.5 M
EDTA	18.61 g	50 mM
TRIS	60.55 g	500 mM
Triton X100	5 ml	0.5%
ultrapure H_2O	Added to a final volume of 1 l	
Diluted 10x using ultrapure H_2O, pH adjusted to 7.4 using HCl, for 1x NET-G.		
Running buffer (10x)		
TRIS	30 g	250 mM
Glycine	144 g	2 M
SDS	10 g	35 mM
ultrapure H_2O	Added to a final volume of 1 l	
Diluted 10x using ultrapure H_2O for 1x running buffer.		

RIPA		
TRIS-HCl pH 7.4	12.5 ml	50 mM
NaCl 5M	7.5 ml	150 mM
IGEPAL CA-630	2.5 ml	1%
Sodium deoxycholate 10% solution	6.25 ml	0.25%
ultrapure H_2O	Added to a final volume of 1 l	
Before use add to every 10 ml:		
Phosphatase inhibitor cocktail	1 tablet	
Protease inhibitor cocktail	1 tablet	
Buffer for resolving gel		
TRIS pH 8.8		1.5 M
SDS		2%
Buffer for stacking gel		
TRIS pH 6.8		0.5 M
SDS		2%

2.1.3 Consumables

Table 5. Consumables.

Consumable	**Supplier**	**Catalogue number**
6 well plates	Corning	CORN3506
8 microTUBE strip	Covaris	520053
FrameStar 384 well	4titude	4ti-0381
Bolt 4-12% Bis-Tris Plus Gels	Life technology	various, e.g. NW04127BOX
Bolt MES SDS Running Buffer 20x	Life technology	B000202
CD56 MicroBeads human	Miltenyi Biotec	130-050-401
Cell scraper	Sarstedt	83.1832
Cell strainer (MACS SmartStrainers 30 µm)	Miltenyi Biotec	130-110-915
Combitips advanced, biopur	Eppendorf	various
ExactaCruz Round Gel Loading Tips in Sterile Rack, 1-200 µl	Santa Cruz	SC-201732
Filter tips (Biosphere)	Sarstedt	various
Gel blotting paper (Whatmann GB005)	GE Healthcare	10426994
High Sensitivity DNA Kit	Agilent	5067-4626
iblot 2 transfer stacks, nitrocellulose	Life technologies	IB23002
LS Columns	Miltenyi Biotec	130-042-401
Nitrocellulose blotting membrane 0.45 µm (Amersham Protran Premium)	GE Healthcare	10600003
Novex Tris-Gycerine SDS Sample Buffer (2X)	Life technologies	LC276
Novex Tris-Gycerine SDS Running Buffer	Life technologies	LC22675

Consumable	Supplier	Catalogue number
qPCR seal sheets	4titude	4ti-0560
Reaction tubes 15 ml and 50 ml	Sarstedt	various
Reaction tubes SafeSeal 0.5 ml, 1.5 ml, 2 ml	Sarstedt	various
RNA 6000 Pico Kit	Agilent	5067-1513
Scepter sensors 60 µm	Merck Millipore	PHCC60050
Serological pipettes 5 ml, 10 ml, 25 ml, 50 ml	Greiner	various
Sterile syringe filter 0.20 µm	Corning	431229
Western blot roller	ThermoFisher Scientific	84747

2.1.4 Kits

Table 6. Kits.

Kit	Supplier	Catalogue number
DC Protein Assay Kit II	Bio-Rad	5000112
EZ DNA Methylation Kit	Zymo Research	D5001
GeneCellin	Bio-Connect	GC5000
HiSeq PE Rapid Cluster Kit v2	Illumina	PE-402-4002
HiSeq Rapid SBS Kit v2 (200 cycles)	Illumina	FC-402-4021
HiSeq Rapid SBS Kit v2 (50 cycles)	Illumina	FC-402-4022
HiSeq Rapid SR Cluster Kit v2	Illumina	GD-402-4002
HiSeq Rapid SBS Kit v2 (50 cycles)	Illumina	FC-402-4022
MinElute PCR Purification Kit	Qiagen	5001328
miScript SYBR Green PCR Kit	Qiagen	218073
miScript II RT Kit	Qiagen	218161
NEBNext Ultra DNA Library Prep Kit for Illumina	New England Biolabs	E7370S
NEBNext Small RNA Library Prep Set for Illumina	New England Biolabs	E7330S
Nucleospin miRNA	Macherey Nagel	740971250
Nucleospin Tissue	Macherey Nagel	740952.50
Ovation RNA-Seq System V2	Nugen	7102
Transcriptor cDNA Synthesis Kit	Roche	4897030001
Viromer BLUE	Biozym	230005
QuantiFast SYBR Green PCR Kit	Qiagen	204057

2.1.5 Antibodies

Table 7. Primary and secondary antibodies for Western Blot.

Antibody against	Host	Clonality	Supplier	Cat. number	Dilution
Myosin (skeletal, fast)	Mouse	monoclonal	Sigma	M4276-100UL	1:1000
Myosin (skeletal, slow)	Mouse	monoclonal	Sigma	M8421-100UL	1:1000
ATP5A	Mouse	monoclonal	Abcam	ab110273	1:1000
p-AKT (Thr308)	Rabbit	polyclonal	Cell signaling	9275S	1:1000
AKT	Mouse	monoclonal	BC biosciences	610861	1:1000
GAPDH	Rabbit	monoclonal	Cell signaling	2118S	1:10000
AMKPα2	Rabbit	polyclonal	Merck Millipore	07-363	1:1000
ORP8	Mouse	monoclonal	Abcam	ab60110	1:200
Secondary antibodies					
IRDye 680 RD anti-mouse	Goat		Li-Cor	926-68070	1:10000
IRDye 800 CW anti-rabbit	Goat		Li-Cor	925-32211	1:10000
Controls					
Chameleon Duo Prestained protein Ladder			Li-Cor	928-60000	

Table 8. Antibody for flow cytometry.

Antibody	Host	Supplier	Catalogue number
Alexa Fluor® 488 Mouse Anti-Human CD56	Mouse	BD-Biosciences	557699

2.1.6 Oligonucleotides

Table 9. Primers for quantitative real-time PCR.
All primer assays were purchased from Qiagen.

Gene Symbol	Primer	Catalogue number
ALDOA	Hs_ALDOA_1_SG	QT00082460
COX6A2	Hs_COX6A2_1_SG	QT00215432
CPT1B	Hs_CPT1B_1_SG	QT00057036
IGFBP5	Hs_IGFBP5_1_SG	QT00047530
LDLRAD4	Hs_LDLRAD4_1_SG	QT01678915
MIR143	Hs_mir-143_PR_1	MP00000917
MYH1	Hs_MYH1_2_SG	QT01671005
MYH2	Hs_MYH2_1_SG	QT00082495
MYH7	Hs_MYH7_1_SG	QT00000602
OSBPL8 (ORP8)	Hs_OSBPL8_1_SG	QT00067102
PPARGC1A	Hs_PPARGC1A_1_SG	QT00095578
Ppargc1a	Mm_Ppargc1b_1_SG	QT00125272
PRKAA2	Hs_PRKAA2_SG	QT00042077
RRAGD	Hs_RRAGD_1_SG	QT00078085
RPS13	Hs_RPS13_3_SG	QT02317532
TBP	Hs_TBP_1_SG	QT00000721

miRNA	miRNA Primer	Catalogue number
hsa-miR-21-5p	Hs_miR-21_2	MS00009079
hsa-miR-31-5p	Hs_miR-31_1	MS00003290
hsa-miR-133b	Hs_miR-133b_2	MS00031430
hsa-miR-139-5p	Hs_miR-139_1	MS00003493
hsa-miR-143-3p	Hs_miR-143_1	MS00003514
hsa-miR-145-5p	Hs_miR-145_1	MS00003528
hsa-miR-146b-5p	Hs_miR-146b_1	MS00003542
hsa-miR-181a-2-3p	Hs_miR-181a-2*_1	MS00008834
hsa-miR-206	Hs_miR-206_1	MS00003787
hsa-miR-208b-5p	Hs_miR-208b_1	MS00009058
hsa-miR-499a-5p	Hs_miR-499_1	MS00004375
hsa-miR-3615	Hs_miR-3615_2	MS00041811
RNU6-1	Hs_RNU6-2_11	MS00033740

Table 10. miRNA Mimics.

miRNA Mimic	Supplier	Catalogue number
Cy3 dye- labeled Pre-miR negative Control	Life technologies	AM17120
hsa-miR-31-5p miRCURY LNA miRNA Mimic	Qiagen	YM00472582
hsa-miR-122-5p miRCURY LNA mi RNA Mimic	Qiagen	YM00470430
hsa-miR-133b miRCURY LNA miRNA Mimic	Qiagen	YM00470608
hsa-miR-143-3p miRCURY LNA miRNA Mimic	Qiagen	YM00470035
hsa-miR-145-5p miRCURY LNA miRNA Mimic	Qiagen	YM00470014
hsa-miR-206 miRCURY LNA miRNA Mimic	Qiagen	YM00472240
hsa-miR-208b-3p miRCURY LNA miRNA Mimic	Qiagen	YM00472072
hsa-miR-499a-5p miRCURY LNA miRNA Mimic	Qiagen	YM00470181

2.1.7 Laboratory equipment

Table 11. Laboratory equipment.

Name	Manufacturer / Supplier
E220 Focused-ultrasonicator	Covaris
Bioanalyzer Instrument 2100	Agilent Technologies
EVOS FL Auto 2	ThermoFisher Scientific
Gradient mixer 2x20ml	LabArt UG & Co. KG
Heraeus Fresco 17 centrifuge	ThermoFisher Scientific
Heraeus Pico 21 centrifuge	ThermoFisher Scientific
iBlot2	ThermoFisher Scientific
LightCycler 480 Instrument II	Roche
Mastercycler gradient	Eppendorf
Micropipettes (various, from series research pro and Xplorer plus)	Eppendorf
Nanodrop ND-1000	NanoDrop Technologies
Odysseyinfrared imaging system 2219	Li-Cor
PerfectBlue double gel system twin ExW S	Peqlab/VWR
Scepter Cell Counter	Merck Millipore
Thermomixer compact	Eppendorf
Ultra Clear UF	Siemens
Varioskan Lux	ThermoFisher Scientific

2.1.8 Software

Table 12. Software.

Name	Supplier	Version
Excel	Microsoft	2016
GraphPad Prism	GraphPad Software	8.3.1
Image Studio Lite	Li-Cor	5.2.5
LightCycler 480 Software	Roche	1.5.0

2.2 Methods

2.2.1 Ethical approval and informed consent.

The Ethical Committee of the Tübingen University Medical Department approved of the study and all donors gave informed written consent.

2.2.2 Human subjects and isolation of primary cells

Cells were isolated by the team at the university hospital in Tübingen as described in (Hoffmann et al., 2018). Briefly, percutaneous needle biopsies were performed on *vastus lateralis* muscle of humans. Collagenase digestion was performed to release cells from tissue. Cells were seeded in six to eight GelTrex coated 15 cm plates, grown to 50% confluency and detached by incubation with trypsin/EDTA at 37°C. Detached cells were passed through a 30 µm cell strainer to remove clumps, washed, and enriched for CD56-positive myoblasts using MACS (magnetic-activated cell sorting) microbeads and LS-columns. The flow-through contained fibroblasts while the eluate contained the myoblast fraction. The manufacturer's protocol was followed except for an increase of bead incubation time to 30 minutes. Cells were kept in liquid nitrogen. Percentage of CD56 positive cells was checked by flow cytometry. Only cells with more than 90% CD56 positive cells were used.

2.2.3 Cell culture

2.2.3.1 Culture of primary human myoblasts

Cells were cultured as described in (Hoffmann et al., 2018). Cells were proliferated in cloning medium (39% α-MEM, 39% Ham's F-12, 20% FBS, 1% chicken extract, 100 U/ml penicillin, 100 µg/ml streptomycin and 0.5 µg/ml amphotericin B) on GelTrex coated (1:300) 6-well plates. Upon confluence, differentiation was induced by serum withdrawal in fusion medium (α-MEM, 100 U/ml penicillin, 100 µg/ml streptomycin, 0.5 µg/ml amphotericin B) containing BSA-coupled fatty acids (final concentrations: 50 µM palmitate, 50 µM oleate, 1.67 mg/ml BSA, 0.05% ethanol, and 100 µM carnitine) or with 2% FBS without additional fatty acids and carnitine. TGFβ1 stimulation was performed by diluting TGFβ1 (2 µg/ml stock in 2 mg/ml BSA in 4 mM HCl solution) to 1 ng/ml in the required amount of medium, aspirating old medium from cell culture plates and pipetting 2 ml of TGFβ1 containing medium to each well of a 6-well plate. The same applies for the TGFβ1 inhibitor SB431542 (solved to 10 mM in DMSO (dimethyl sulfoxide)), which was diluted in medium to 10 µM. As vehicle control, the respective amount of 2 mg/ml BSA in 4 mM HCl or DMSO was diluted in medium. For example, in an experiment with four different treatments, vehicle, TGFβ1 alone, TGFβ1 and inhibitor SB431542, and inhibitor SB431542 alone, all four treatments would end up containing 1 µg/ml BSA, 2 nM HCl and 0.1% DMSO. This means that to the vehicle control, we added 1:2000 2 mg/ml BSA in 4 mM HCl solution and 1:1000 DMSO. To the TGFβ1 solution, only 1:1000 DMSO was added, to the inhibitor solution only 1:2000 2 mg/ml BSA in 4 mM HCl solution

was added and to the solution containing TGFβ1 and the inhibitor no additional vehicle was added. In experiments without inhibitor, no DMSO was used in any stimulating solution.

2.2.3.2 Coupling of fatty acids to BSA

Palmitate and oleate were solved in ethanol at 200 mM. 300 µl of the solution were added to 9.7 ml 10% BSA in DPBS (Dulbecco's phosphate-buffered saline) and incubated over night at 37 °C in a shaking incubator, yielding a solution containing 6 mM fatty acid and 3% ethanol. Carnitine was dissolved at 500 nM in water and filtrated with 20 µm filters for sterilization. Solutions were aliquoted and stored at −20 °C until use. For each fatty acid, a separate stock solution was generated.

2.2.3.3 Transfections of miRNA mimics

Cells were transfected for 24 h using viromer blue according to the manufacturer's instructions. We used the 0.2x transfection scale to achieve a final concentration of 5 nM for the experiments with a mix of miRNA mimics and the 0.4x transfection scale for a final concentration of 10 nM for the transfection of single miRNAs. For experiments requiring a mix of miRNA mimics, a mix of miR-133b, miR-206, miR-208b and miR-499a mimics, each at a concentration of 1.25 nM, leading to a total concentration of 5 nM, was used. Negative control mimic in this experiment was also transfected at 5 nM.

2.2.3.4 Culture of C2C12 cell line

The group of Cora Weigert (University Hospital Tübingen) kindly provided an aliquot of C2C12 cell line (DSMZ, ACC565) in passage 3. Cells were proliferated in DMEM (4.5 g/L glucose with L-glutamine) supplemented with 100 U/ml penicillin, 100 µg/ml streptomycin, 2 mM glutamine and 10% FBS. For passaging, myoblasts were washed once with warm PBS and detached by incubation in trypsin/EDTA at 37 °C for a maximum of 10 minutes. Trypsin activity was stopped by adding twice the volume of proliferation medium. The cell suspension was centrifuged at 160 g for 4 minutes, the supernatant was discarded, and the cell pellet was resuspended in fresh proliferation medium. Cells were counted using the Scepter cell counter and diluted to 50,000 to 500,000 cells/ml. Only cells of passage 8 or lower were used. For differentiation, serum was reduced to 2% FBS. Cells were differentiated to myotubes for 5 days.

2.2.4 Protein isolation and quantification

For protein isolation, cells were washed once with cold PBS, RIPA was added directly to the cell culture dish, and cells were detached using a cell scraper. The RIPA-cell mixture was transferred to reaction tubes and kept at -80°C at least overnight. For protein extraction, the cell-RIPA mixture was thawed on ice and shaken at 4°C for 15 minutes. Afterwards, this lysate was centrifuged (15 min, 4°C, 13000 g) to pellet debris. The supernatant, containing the extracted proteins, was transferred to a new reaction tube.

Protein content was quantified using the DC Protein Assay Kit II using the microplate assay protocol according to the manual's instructions. For the BSA standard, a 1:2 dilution series from 2 mg/ml to 0.06 mg/ml was prepared. Absorbance at 750 nm was read in the Varioskan plate reader.

2.2.5 Western blotting

Two different systems were used for western blotting; either with self-cast sodium dodecyl sulfate polyacrylamide (7.5%-15%) gradient gel electrophoresis followed by semi-dry electroblotting on a nitrocellulose membrane, or with the precast bolt plus polyacrylamide gels and using the iBlot 2 dry blotting system.

2.2.5.1 Gel electrophoresis

For the self-cast gels, the gradient was casted using a gradient mixer and the following recipe per gel:

	15% gel	7% gel	stacking gel
Ultrapure H_2O [ml]	1.42	4.92	3.21
Resolving gel buffer [ml]	2.5	2.5	0
Stacking gel buffer [ml]	0	0	1.25
Glycerol [ml]	1	0	0
Acrylamid solution [ml]	5	2.5	0.5
TEMED [µl]	17	17	8
APS [µl]	67	67	33

The reagents for the respective parts of the gel were combined in one reaction tube each, not adding APS until directly before casting the gel. The gradient was achieved by using the gradient mixer. After casting the separation gel, gels were covered with isopropanol during polymerization (30 minutes). Subsequent to successful polymerization, the isopropanol layer was disposed thoroughly, APS was added to the stacking gel tube, the stacking gel was casted, and the comb carefully pushed into the stacking gel. The stacking gel was left for polymerization for 1 h.

2.2.5.2 Semi-dry electroblotting

Two gel blotting papers and one piece of nitrocellulose membrane were cut into the same size as the gel (usually 6 cm x 18 cm for a full gel) and soaked in transfer buffer. The gel from electrophoresis was prepared by cutting off and discarding the stacking gel and soaking the separating gel in transfer buffer. The first gel blotting paper was put onto the bottom electrode of the blotting apparatus, followed by the nitrocellulose membrane, the gel and a second blotting paper. With a roller, remaining air bubbles were rolled out of the stack. The transfer took place for 3 h at 0.8 mA per cm^2. After transfer, gel and papers were discarded. The membrane was blocked and incubated with antibodies as described below.

2.2.5.3 Precast gels and iBlot dry blotting system

The bolt plus gels and iBlot 2 dry blotting system were used according to the manufacturer's instructions. Only gradient gels (4%-12%) were used. Samples were adjusted to the required concentration either by diluting with the respective amount of RIPA buffer and LSD sample buffer and reducing buffer to a total volume of 15 µl or by acetone precipitation. For acetone precipitation, the required volume of sample was mixed with the same volume of cold acetone and incubated at -20°C for at least 20 minutes. Subsequently, the mixture was centrifuged at 7500 g for 10 minutes at 4°C and the supernatant discarded. The pellet was reconstituted in 15 µl 1x LSD sample buffer containing reducing buffer. The samples were loaded, run, and blotted according to the manufacturer's protocols.

2.2.5.4 Blocking, incubation with antibodies

To control for even loading, membranes were stained with ponceau solution. Membranes were washed and blocked in NET-G buffer (150 mM NaCl, 50 mM Tris/HCl, pH 7.4, 5 mM EDTA, 0.05% Triton X-100, and 0.25% gelatin) for 3 x 10 minutes. The primary antibodies were incubated in NET-G over night at 4°C. After washing thrice, secondary antibodies in NET-G were incubated for 1 h at room temperature. Detection was performed after washing 3 times, first with Net-G, second wash with TBST, and third wash with TBS, on an Odyssey scanner.

2.2.6 RNA isolation

Total RNA was isolated using the NucleoSpin miRNA kit. After washing cells once with warm PBS, the lysis buffer "Buffer ML" was applied directly into the wells, incubated for 5 minutes, and then scratched from the plates, transferred to reaction tubes, and stored at -80°C. After thawing, the column kit was used according to the manufacturer's instructions for the total RNA protocol, adding an extra washing step with 80% ethanol in a new collection tube before eluting with 50 µl of RNase free water. RNA was quantified using a Nanodrop spectrophotometer and stored at -80°C.

For reverse transcription in experiments not looking at miRNAs, the Transcriptor cDNA Synthesis Kit was used with anchored-oligo$(dT)_{18}$ and random hexamer primer as described in the kit's protocol using 500 – 1000 ng input. Obtained cDNA was diluted 1:5 by adding 80 µl RNase free water to 20 µl reaction volume. For all experiments concerning miRNAs, the miScript II RT kit was used according to the manufacturer's instructions using 500 ng RNA input and choosing HiFlex buffer if not stated otherwise. For qPCR (quantitative real-time PCR), miScript cDNA was diluted by adding 100 µl RNase free water to 20 µl reaction volume. Incubation steps of both kits were conducted in an Eppendorf Mastercycler gradient.

2.2.7 Quantitative real-time PCR

Quantitative real-time PCR (qPCR) was performed in a Roche LightCycler 480 using 384 well plates. Standards for targets for all experiments were generated by purifying PCR product with the MinElute

PCR purification kit for each primer, measuring the concentration using a Nanodrop spectrophotometer, and diluting it to a 5 ng/µl stock which was stored in aliquots at -20°C. From this stock, a 1:10 dilution series ranging from 5 pg/µl to 0.5 ag/µl of the specific amplificate was prepared for each plate run with the respective primer. For each reaction, 2.5 µl diluted cDNA or standard was used in a 10 µl qPCR reaction volume and put into the wells first. The remaining 7.5 µl constituted of mastermix, primers and PCR grade water. The components were mixed in a tube for all wells and dispensed into the wells. Depending on the transcript of interest, different mastermixes were used: Quantifast for mRNAs and Quantitect Mastermix for miRNAs.

2.2.7.1 qPCR for mRNA and precursor miRNA

To detect mRNA transcripts, 5 µl Quantifast Mastermix and 1 µl of Quantitect primer assay were used per reaction. In the LightCycler, the first step was the initial activation of the polymerase at 95°C for 5 minutes. Next, 40 cycles of denaturation at 95°C for 10 s and the combined annealing and extension step at 60°C for 30 s with collection of fluorescence data were performed. At the end, the melting curve was recorded from 62 °C to 98 °C with a ramp rate of 0.11 °C/s and continuous acquisition of fluorescence.

It is also possible to detect mRNA transcript using Quantitect Mastermix, however, the run protocol in the LightCycler takes about twice the amount of time. In some cases, it was still useful to use Quantitect Mastermix for mRNA primers in order to detect mRNAs and miRNAs on the same plate and thereby save time. In this case, the run protocol for Quantitect as described below was used in the LightCycler.

2.2.7.2 qPCR for miRNA

For miRNA detection, 5 µl Quantitect Mastermix, 1 µl miScript primer and 1 µl universal reverse primer were used for each 10 µl reaction. The LightCycler run protocol for Quantitect Mastermix starts with an initial activation step of 15 minutes at 95°C to activate the DNA polymerase. Subsequently, samples underwent 45 cycles of denaturation at 94°C for 15 s, annealing at 55°C for 30 s, and extension at 70°C for 30 s with collection of fluorescence data. Finally, the melting curve was detected by increasing the temperature with a ramp rate of 0.11 °C/s up to 95 °C and continuous fluorescence acquisition.

2.2.8 Preparation of libraries and sequencing

Peter Huypens from the group for gene regulation and epigenetics at our institute (Institute of Experimental Genetics) prepared libraries and flow cells for us. For sncRNAs, he used the NEBNext Small RNA Library Prep Set for Illumina. For long RNAs, he used the Ovation RNA-Seq System V2 for cDNA synthesis, amplification and purification. Next, cDNA was fragmented to a size of 200 bp using the Covaris system. Finally, libraries were generated using the NEBNext Ultra DNA Library

Prep Kit for Illumina. Libraries were tested during processing with a Nanodrop spectrophotometer and bioanalyzer. The same controls of quality and quantity were used for final product.

Christine Wurmser from the Technical University Munich performed the sequencing on a HiSeq2500 (Illumina). She used the kits HiSeq PE Rapid Cluster Kit v2, HiSeq Rapid SBS Kit v2 (200) and HiSeq Rapid SBS Kit v2 (50 cycles), all from Illumina for the 2 x 125 bp paired-end sequencing analysis of long RNAs. For small RNAs, she used the HiSeq Rapid SR Cluster Kit v2 and HiSeq Rapid SBS Kit v2 (50 cycles) for single-read 1x 50 bp sequencing. Fastq files were generated with CASAVA BCL2FASTQ Conversion Software.

2.2.9 Analysis of sequencing data

All sequencing data were analyzed using R by two bioinformaticians, Tim Jeske and Max Hastreiter from Helmholtz Zentrum München. Small RNA sequencing data was analyzed as published (Jeske et al., 2019). Briefly, two pipelines were used; as shown in Figure 3, in the classical pipeline, sequences were annotated to the genome before comparing testing conditions. In the DEUS (differential expression of unique sequences) analysis, raw sequences of testing conditions were compared prior to annotation to the genome. Thus, also sequences that cannot be annotated but are differentially expressed can be discovered. The annotation to the known sncRNAs is still performed afterwards, for easier analysis.

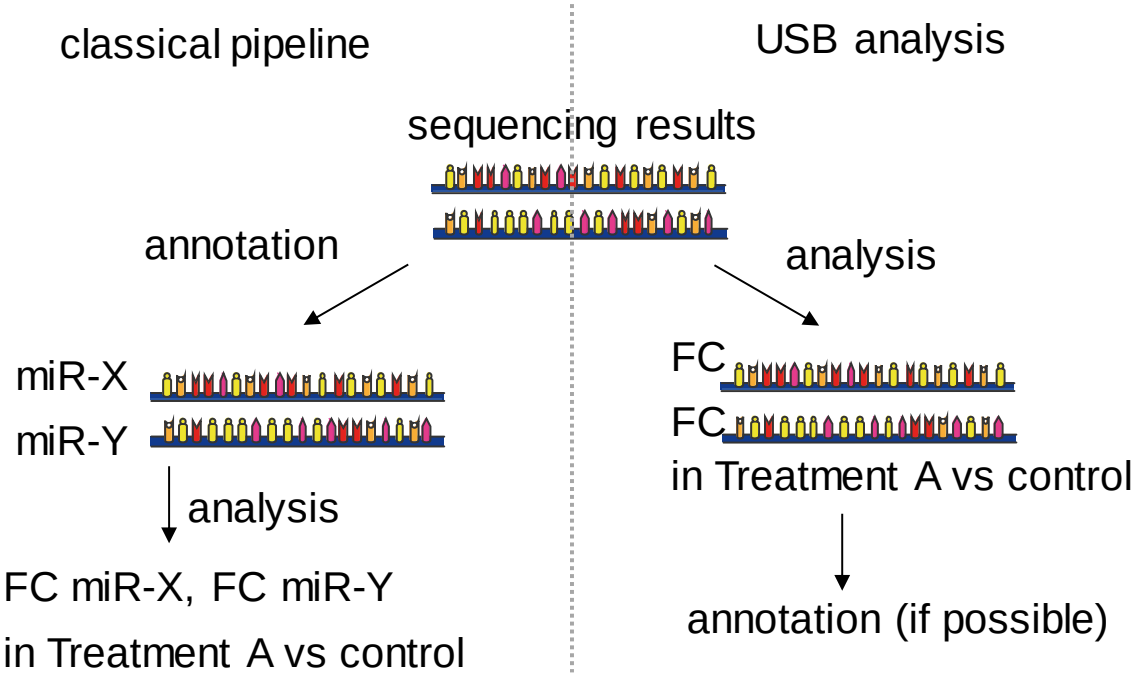

Figure 3. Two approaches to analyze small RNA sequencing results.
Left side: classical pipeline. Individual sequences were annotated to the genome prior to comparison of treatment groups. Right side: DEUS (differential expression of unique sequences) analysis. First individual sequences were compared between treatment groups. Next, sequences were annotated to the genome where possible.

2.2.10 Isolation of DNA

DNA was extracted from cell culture using the Nucleospin Tissue kit. Briefly, cells on 10 cm-dishes were washed with warm PBS once, followed by adding the kit components 200 µl T1 and 200 µl B3 as well as 25 µl proteinase K directly onto the cell culture dish. With a cell scraper, cells were detached and gathered and then transferred after careful mixing by pipetting to a reaction tube. Until further processing, the reactions tubes were stored at -20°C. After thawing, 20 µl RNase A (10 mg/ml) was added and the mixtures was incubated for 5 minutes at room temperature. From here on, the manufacturer's protocol was followed, beginning with the step to adjust DNA binding conditions (adding ethanol). Samples were quantified using the Nanodrop spectrophotometer.

2.2.11 Promoter methylation analysis

In a cooperation with Jennifer Kriebel from the Institute of Epigenetics, promoter methylation of known *PPARGC1A* promoters was analyzed. Primers were designed using EpiDesigner and Primer3 web application.

For bisulfite conversion, she used the EZ DNA Methylation Kit. The obtained bisulfite converted DNA was amplified using PCR, followed by *in vitro* RNA transcription and T-specific cleavage by RNase A. The obtained products were dispensed to a SpectroCHIP using the Mass ARRAY Nanodispenser. For detection with MADLI-TOF MS, chips were ran on a MassARRAY workstation compact with MassCLEAVE settings. Methylation degree was analyzed with EpiTYPER software and exported for further processing.

In Excel, we excluded methylation sides for which one or more positive controls a methylation degree of 0.7 or less was detected. After this additional quality control step, we calculated the mean of all CpG sites for each sample and each promoter.

2.2.12 Data processing and statistics

Immunoblots were analyzed with Image Studio Lite. Results of qPCR experiments were analyzed with the LightCycler480 software using the function for absolute quantification with in-run standard curve. From both programs, data were exported for further processing. For all data, normalization and sorting was performed in Excel and GraphPad Prism was used for further processing such as statistics and creating graphs.

2.2.12.1 Statistical multiple comparison tests in two-way ANOVAs

In our data, we often compared two sets (e.g. myoblasts and differentiated myotubes or TGFβ1-treated and vehicle-treated) that both underwent one or several treatments (in this paragraph called groups). An example is shown in Figure 4A. In two-way ANOVA (analysis of variance), we used Sidak's multiple comparison test when comparing sets within treatment groups, e.g. comparing vehicle-treated myoblasts and vehicle-treated myotubes (Figure 4B). However, for the comparison of

different treatment groups, Tukey's multiple comparison test was used (e.g. comparing negative control, treatments 1 and treatment 2. Figure 4C). In case of more than two sets or groups, and only the comparison to the one option is relevant, Dunnett's multiple comparison test was used. For example, Dunnett's multiple comparison test was used when various treatments were only compared to negative control and not to each other.

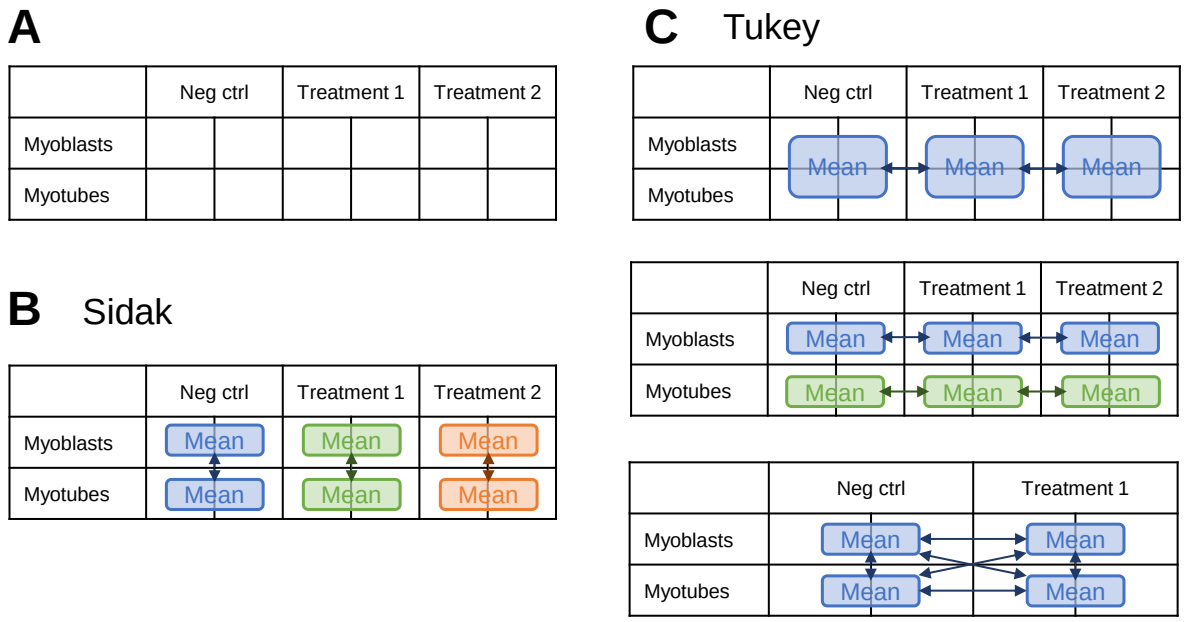

Figure 4. Options for multiple comparison in two-way ANOVA.
(A) Example of data formation in table. Sets in rows, groups in columns. (B-C) Schematic display of two-way ANOVA multiple comparison options. (B) Sidak's multiple comparison is used to compare sets within treatment groups, e.g. comparing myoblasts and myotubes both treated with negative control. (C) Tukey's multiple comparison test is used to compare different treatment groups to each other. It is applied for comparing the mean of all sets within one treatment group but also for comparing the individual means of sets within each treatment group to other treatment groups. Whenever all comparisons are only done in relation to a specific mean (e.g. negative control or myotubes), Dunnett's multiple comparisons test is performed.

3 Results

3.1 TGFβ1 persistently downregulates *PPARGC1A* transcript

Based on the reducing effects of TGFβ1 on insulin signaling and mitochondrial regulators and enzymes in differentiated human myotubes (Bohm et al., 2016a), we aimed to elucidate the mechanism behind these effects. Firstly, we studied the time course of this effect. We stimulated primary human skeletal muscle cells preconfluently with vehicle control, 1 ng/ml TGFβ1 or 10 µM Inhibitor (SB431542). Subsequently, we differentiated the cells for 5 days without TGFβ1. Strikingly, we still found PGC1α (gene name *PPARGC1A*) transcript expression downregulated in differentiated myotubes (Figure 5) 5 days after ending TGFβ1 stimulation. This effect was abrogated in the presence of TGFβ1 inhibitor.

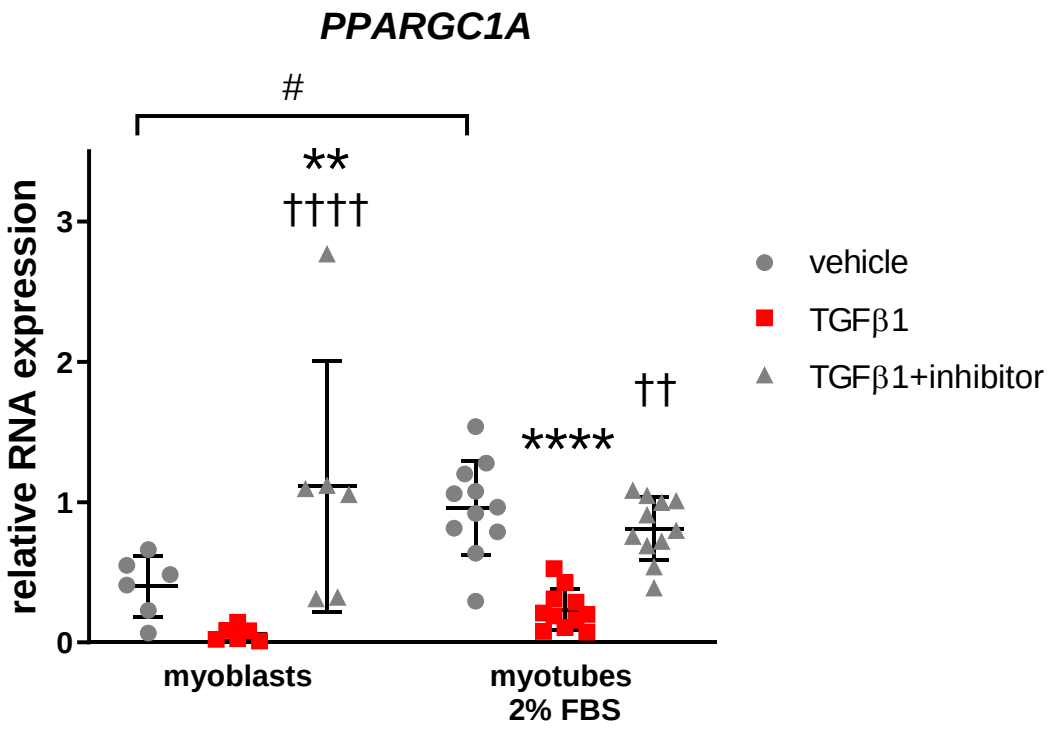

Figure 5. TGFβ1 treatment leads to persistent downregulation of *PPARGC1A* transcript. Undifferentiated human myoblasts were treated with 1 ng/ml TGFβ1, inhibitor (10 µM SB431542), or vehicle control for 48 h. Subsequently, myoblasts were differentiated in the presence of 2% FBS for 5 days to myotubes. Shown values were normalized to *TBP* as reference gene and to individual donors and are displayed as symbols for individual values with means ± SD (myoblasts n = 6, myotubes n = 11). Grey circles symbolize vehicle-treated samples; red squares TGFβ1-treated; grey triangles TGFβ1 and inhibitor-treated. Two-way ANOVA with Tukey's multiple comparisons test comparing all means was used. * p-value of the comparison to vehicle samples within the group of myoblasts or myotubes. † p-value of the comparison to TGFβ1 treated samples within the group of myoblasts or myotubes. # p-value of the comparison of vehicle samples in myoblasts and myotubes. One symbol $p < 0.05$; two symbols $p < 0.01$; four symbols $p < 0.0001$.

3.2 Effects of TGFβ1 on transcriptional level

To explore this prolonged effect of TGFβ1 on gene expression in an unbiased manner, we investigated long RNA expression after 5 days of myo-differentiation by RNA sequencing. In addition, we quantified the small RNAs by sequencing to analyze the TGFβ1-induced changes of these potential regulators of transcription and translation. We preconfluently stimulated primary skeletal muscle cells with 1 ng/ml TGFβ1, or 10 µM SB431542, a TGFβ1 inhibitor, or vehicle control for 48 h, and subsequently differentiated them in 2% FBS for 5 days (Figure 6). The isolated total RNA underwent long and small RNA sequencing.

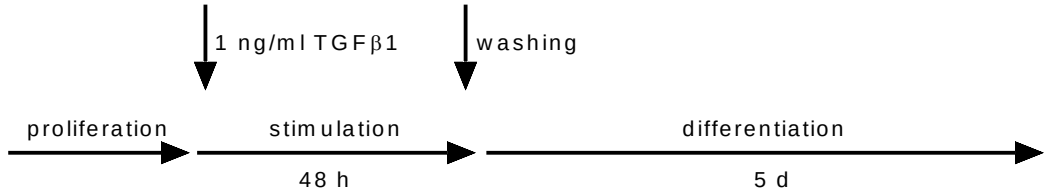

Figure 6. Timeline of TGFβ1 stimulation in myoblasts for RNA sequencing.
Primary human myoblasts were proliferated and preconfluently stimulated with 1 ng/ml TGFβ1 or vehicle control for 48 h before differentiation to myotubes for 5 days. Subsequently, total RNA was harvested.

In long RNA sequencing, we found 1116 transcripts differentially regulated ($p < 0.05$, $FC > |1.3|$) in TGFβ1-treated samples compared to vehicle-treated control samples. 682 of those transcripts showed an opposite regulation in samples treated with TGFβ1 and the inhibitor. In this condition, 1102 transcripts were differentially regulated compared to vehicle-treated samples (Figure 7A).

Small RNA sequencing data underwent two different analysis approaches as described in methods and shown in Figure 3. In the classical approach, the comparison of vehicle- and TGFβ1-treated cells led to 57 differentially regulated sncRNAs ($p < 0.05$, $FC > |1.3|$). Of these, 49 sncRNAs showed an opposite regulation in TGFβ1 and inhibitor treated cells, with a total number of 93 sncRNAs regulated in this group in comparison to control cells (Figure 7B). In contrast, the DEUS analysis readouts are unique sequences, which however share identical regions with other unique sequences. Consequently, several sequences can cover one annotated sncRNA. Thus, the DEUS analysis leads to higher numbers of differentially expressed hits. The comparison of vehicle- and TGFβ1-treated samples in the DEUS analysis gave 1168 differentially regulated unique sequences ($p < 0.05$, $FC > |1.3|$), the overlap with opposite regulated unique sequences in the TGFβ1- and inhibitor-treated condition was 991 unique sequences and the total number of differentially regulated unique sequences in this condition compared to control was 2423 (Figure 7C). About 60 % of unique sequences from DEUS analysis could be annotated.

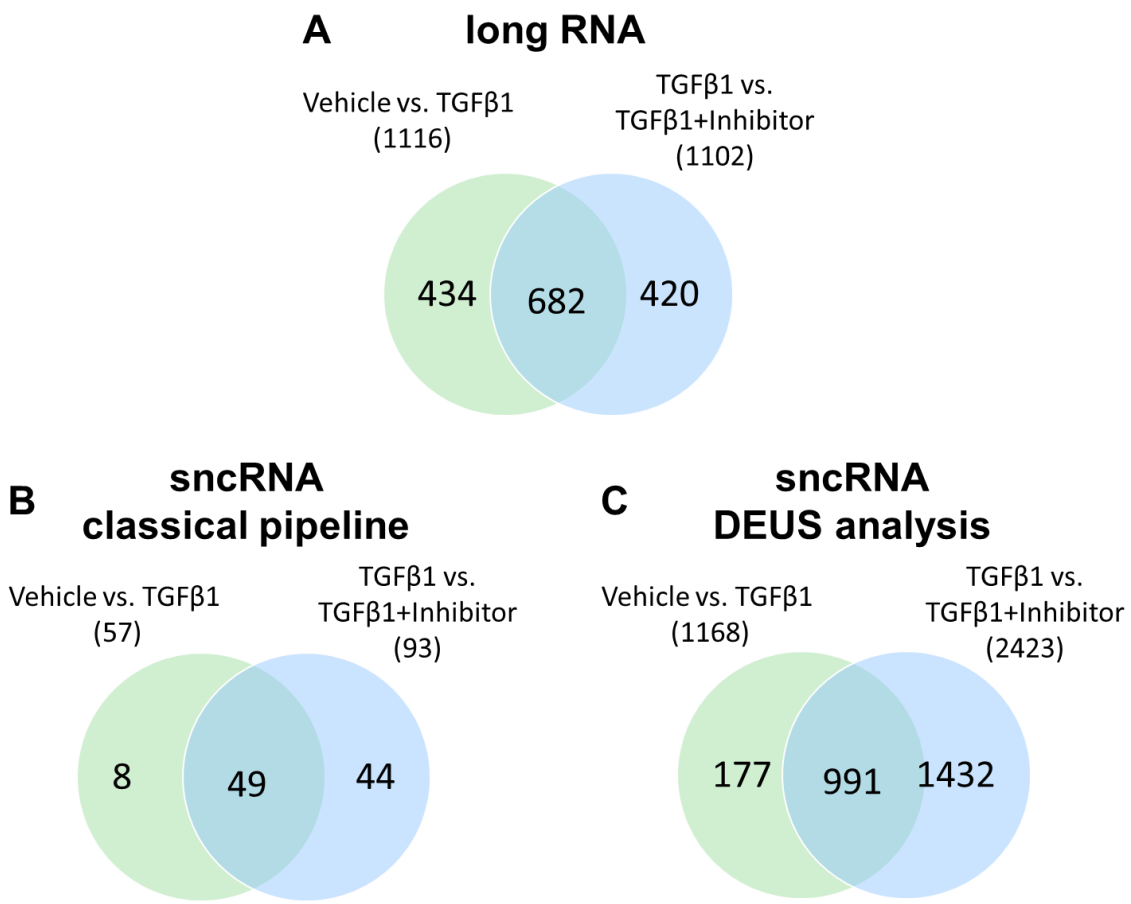

Figure 7. Overview of differentially regulated transcripts after TGFβ1 treatment.
Undifferentiated human myoblasts (n = 5) were treated with 1 ng/ml TGFβ1, inhibitor (10 µM SB431542), or vehicle control for 48 h. Subsequently, myoblasts were differentiated in the presence of 2% FBS for 5 days to myotubes. Shown are numbers of differentially regulated transcripts with p_{adj} < 0.05 and FC > |1.3|. (A) Differentially regulated long RNAs. (B-C) Differentially regulated sncRNAs after analysis using (B) the classical pipeline and (C) DEUS analysis as described in methods.

3.2.1 TGFβ1 represses mitochondrial proteins and regulators and mitochondrially encoded transcripts

For the analysis of long RNA sequencing, we had a closer look on the differentially regulated transcripts ($p < 0.05$ and FC > |1.3|), and generated an overlap list of the two comparisons TGFβ1 vs. vehicle (1116 differentially regulated transcripts) and TGFβ1 vs. TGFβ1 and inhibitor (1102 differentially regulated transcripts). This overlap list of 682 transcripts contained only oppositely regulated transcripts. By careful manual investigation of this list and results from Ingenuity pathway analysis, we encountered that the results of long RNA sequencing were in line with previous findings. TGFβ1 led to upregulation of extracellular matrix proteins, as well as downregulation of *PGC1α*, differentiation markers, and mitochondrial proteins and regulators (Figure 8). In specific, almost all mitochondrial encoded genes were downregulated (Figure 9).

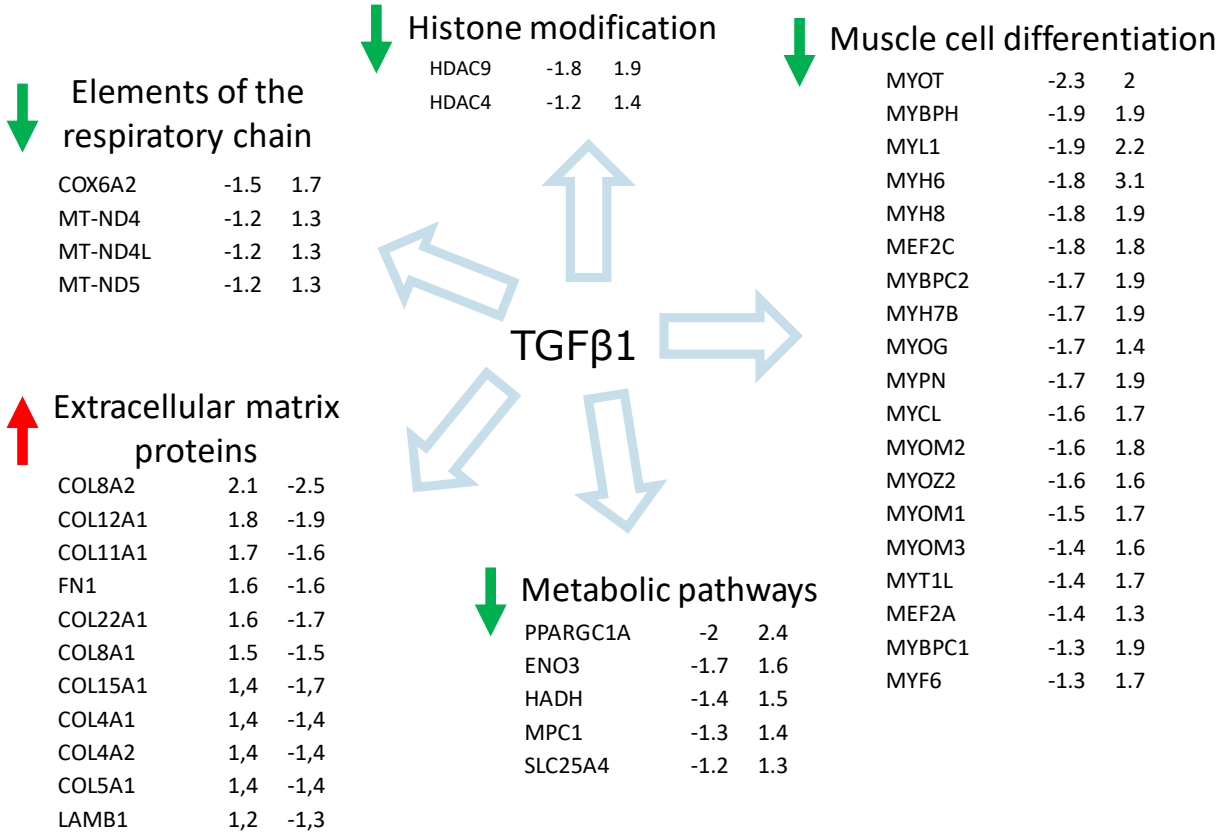

Figure 8. Groups of transcripts differentially regulated by TGFβ1 stimulation.
Myoblasts (n = 5) underwent 48 h of 1 ng/ml TGFβ1, 10 nM SB431542 (TGFβ1 inhibitor), or vehicle stimulation prior to 5 days of differentiation in the presence of 2% FBS. Tables were created by generating an overlap of the comparison of TGFβ1-treated vs. vehicle-treated samples with the comparison of TGFβ1-treated vs. TGFβ1 and inhibitor (SB431542) treated samples ($p_{adj} < 0.05$ and FC > |1.3|). From this overlap, long RNA transcripts that were enriched in specific pathways (based on manual annotation and Ingenuity pathway analysis) are shown. The first column shows the gene name, the second column the fold change of the comparison of vehicle vs. TGFβ1-treated samples, and the third column the fold change of the comparison of TGFβ1 vs. TGFβ1 and inhibitor (SB431542) treated samples. The opposite regulation in the second and third column shows the reversibility of TGFβ1's effect by addition of the inhibitor.

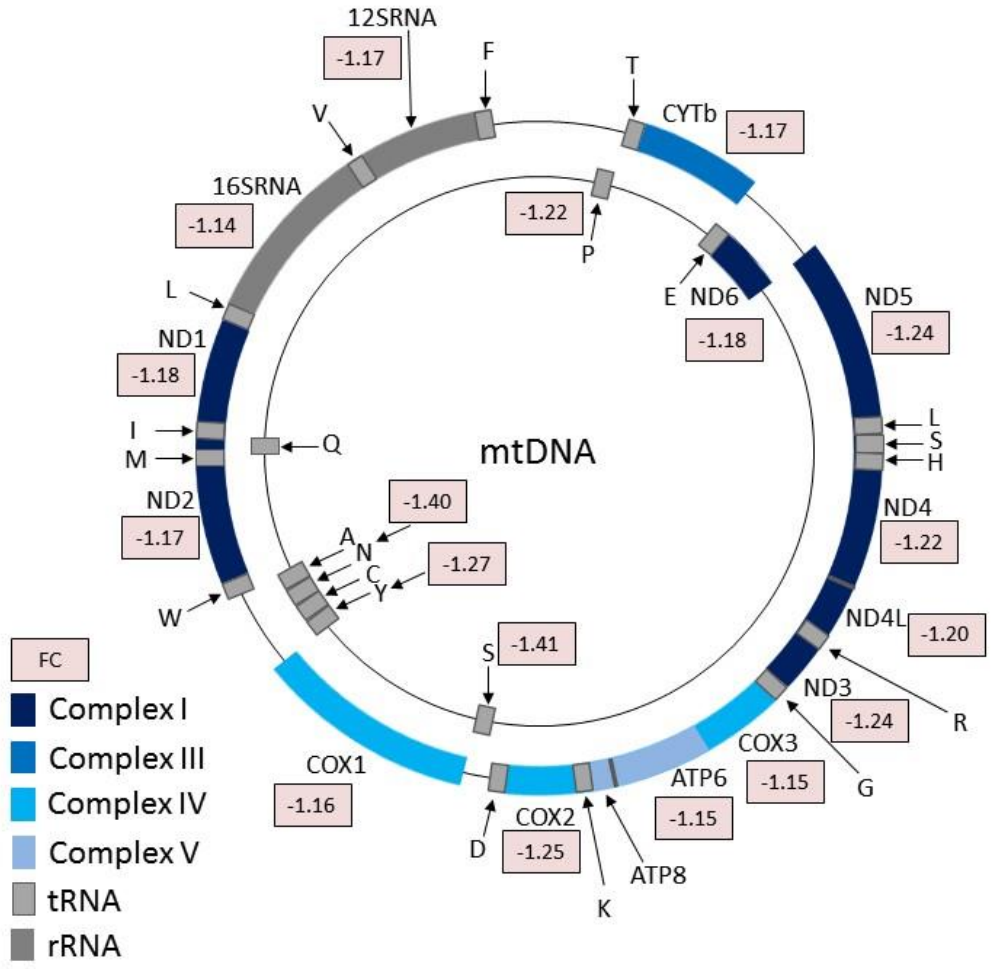

Figure 9. TGFβ1 treatment reduces mitochondrially encoded transcripts.
Scheme of mitochondrial DNA. Myoblasts (n = 5) were stimulated preconfluently for 48 h with 1 ng/ml TGFβ1 or vehicle control prior to 5 days of differentiation in the presence of 2% FBS. RNA of myotubes underwent RNA sequencing and bioinformatical analysis. Boxes next to genes show the linear fold change of TGFβ1-treated in comparison to vehicle control samples, $p < 0.05$.

When analyzing our dataset (1116 differentially regulated transcripts in the comparison of TGFβ1 and vehicle treated samples as shown in Figure 7A, FC > |1.3|, $p < 0.05$) with the Ingenuity pathway analysis software, TGFB1 was the top hit for potential upstream regulators, which confirms that our experiment worked (Figure 10A). Among the other activated upstream regulators received in the IPA analysis, as shown in Figure 10A, are known pathway members of TGFβ1, namely SMAD4 and SMAD2, as well as PI3K (Phosphoinositide 3-kinase) which is a well-known downstream target of TGFβ1 (Derynck and Zhang, 2003). Within the downregulated upstream regulators, we found components of extracellular matrix, FBN1 (fibrillin 1), COL18A1 (collagen type XVIII alpha 1 chain), and COL6A1 (collagen type VI alpha 1 chain). Reflecting the suppression of myo-differentiation by TGFβ1, several muscle specific transcription factors (MYOD1, MEF2C

(myocyte enhancer factor 2C), MYOG, PAX3 (paired box 3)) were also predicted as downregulated upstream regulators.

Amongst the most downregulated transcripts after TGFβ1 stimulation (Figure 10B), one was particularly interesting to us: *RRAGD*. Ras-related GTP-binding protein D (*RRAGD*) is an essential part of the activation of mTORC1 by amino acids (Sancak et al., 2008) and therefore highly relevant in the context of metabolic adaption to exercise. In the comparison of TGFβ1 and vehicle control, *RRAGD* had a fold change of -3.0 ($p_{adj} < 0.0001$). PGC1α was found on position 27 of the list of most downregulated transcripts with a fold change of -2.0 ($p_{adj} < 0.0001$) in the comparison vehicle and TGFβ1-treated. The most upregulated transcript was *LDLRAD4* (Low-Density Lipoprotein Receptor Class A Domain-Containing Protein 4, formerly C18ORF1). Interestingly, *LDLRAD4* was described to inhibit TGFβ signaling by competition for SMAD2/3 binding (Nakano et al., 2014).

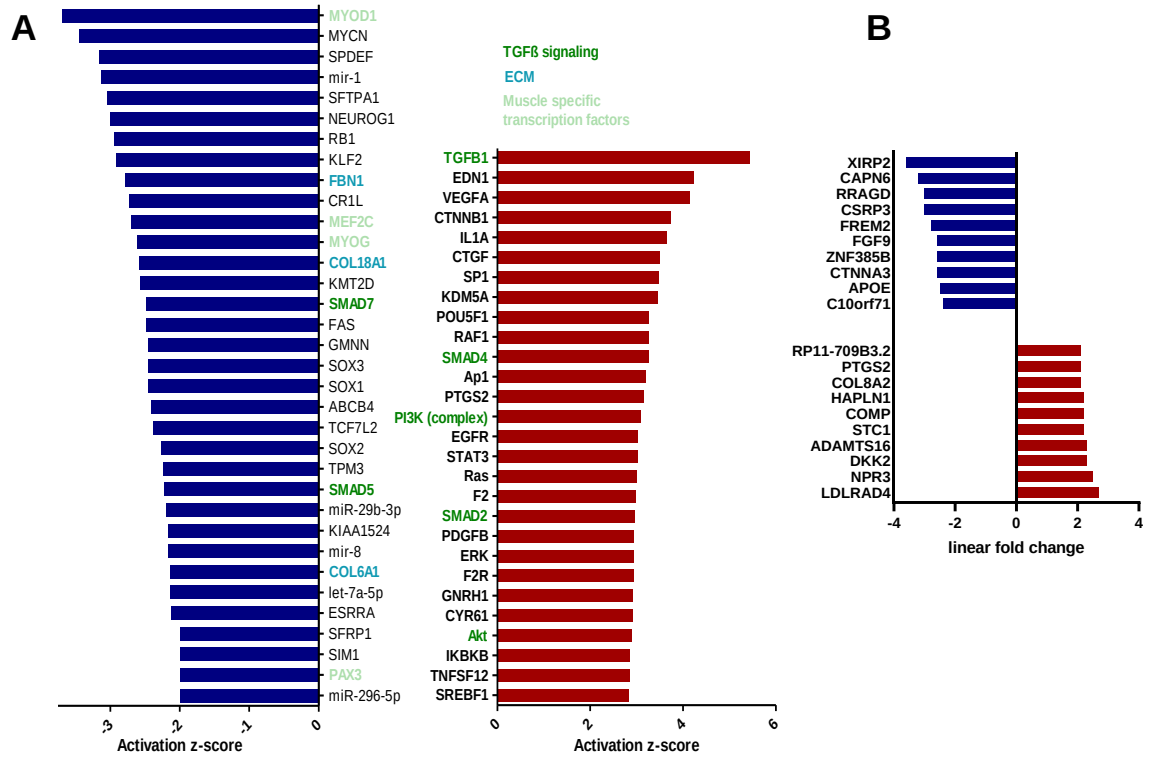

Figure 10. Upstream regulators from Ingenuity pathway analysis and top regulated transcripts. Primary human myoblasts (n = 5) were preconfluently stimulated for 48 h with 1 ng/ml TGFβ1 or vehicle control followed by 5 days of differentiation in the presence of 2% FBS. RNA samples underwent sequencing. (A) Long RNA transcripts with a FC > |1.3| ($p < 0.05$) were used for Ingenuity pathway analysis (input 1116 differentially regulated transcripts). From the IPA upstream regulator analysis, we removed chemicals and only kept biological molecules. Inhibited (blue, z-score < -2) and activated (red, z-score > 2.8) upstream regulators from Ingenuity pathway analysis software are shown. Related regulators are marked with the same color. (B) The 10 top up- and downregulated long RNA transcripts after TGFβ1 treatment, sorted by fold change.

3.2.2 TGFβ1 treatment in myoblasts leads to regulation of sncRNAs in myotubes

For the analysis of sncRNA sequencing, two different bioinformatical analyses were used as described in methods (Figure 3). The results of the classical pipeline which first annotates the detected sequences followed by comparing different treatments, are shown as a heatmap in Figure 11A. For the annotation in this pipeline, gene names were used. The heatmap shows all transcripts with a significant regulation by TGFβ1 vs. vehicle-treated samples ($p < 0.05$; no fold change cut off, all $FC < |1.14|$). Many miRNAs were downregulated by TGFβ1. Only a few miRNAs were upregulated by TGFβ1 treatment, the most upregulated being miR-1294 with a two-fold expression in TGFβ1 treated samples compared to vehicle control ($FC = 2.09$). In the samples treated with TGFβ1 and the TGFβ1 inhibitor SB431542, the effects induced by TGFβ1 were reversed to transcript levels of control samples.

To identify the most robust candidate miRNAs, we decided to focus on miRNAs for which the differential expression after TGFβ1 treatment was reversible with TGFβ1 inhibitor treatment. Therefore, we created an overlap of the differentially expressed small RNAs ($p < 0.05$, $FC < |1.3|$) in the comparison of vehicle control and TGFβ1 and the comparison of TGFβ1 and TGFβ1 and inhibitor for both, classical pipeline and DEUS analysis. To compare the results of DEUS analysis and the classical pipeline, we could only use miRNAs that were annotated in the DEUS analysis. As several sequences can be annotated to the same miRNA by the DEUS analysis, we calculated the average linear FC for each annotated miRNA in the overlap to only have a single FC for each differentially regulated miRNA (Figure 11B). For the annotation in the DEUS analysis, the nomenclature for mature miRNAs was used (Figure 11B).

Thus, Figure 11B shows the most robust results from sncRNA sequencing: all these miRNAs were detected by using both pipelines, and were found to be regulated by TGFβ1 treatment, and this effect was reversed when using the TGFβ1 inhibitor. The four miRNAs that are most upregulated by TGFβ1 treatment were miR-143, miR-181a2, miR-708, and miR-31. The most downregulated miRNAs by TGFβ1 treatment in both analyses were miR-499a, miR-208b, miR146b, and miR-139. As already seen in the heatmap (Figure 11A) for the classical analysis, the DEUS analysis also found more miRNAs downregulated than upregulated by TGFβ1 treatment.

For further experiments, we needed to decide which strand of mature miRNA we want to detect. We therefore checked the results of the DEUS analysis, giving us more detailed information about the regulated miRNAs. For all beforementioned miRNAs, the guide strand, meaning the more abundant strand, of miRNA was the one significantly regulated in our results, except for miR-181a2, here we technically investigated hsa-miR-181a2-3p, while hsa-miR-181a2-5p is the more abundant form.

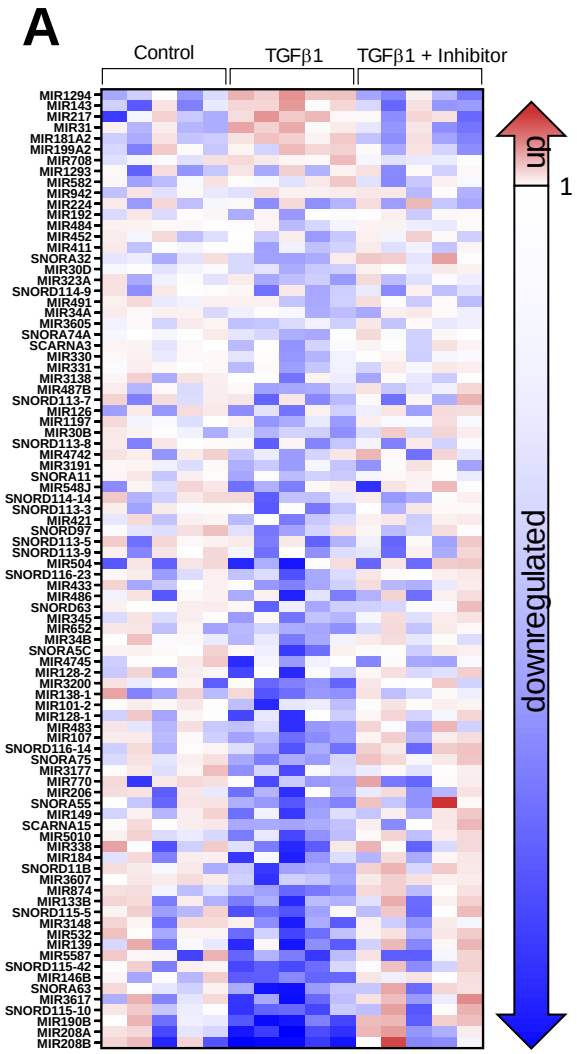

B

DEUS analysis	FC	classical pipeline	FC
hsa-miR-143	2,11	MIR143	1,99
hsa-miR-181a-2	1,89	MIR181A2	1,78
hsa-miR-708	1,85	MIR708	1,45
hsa-miR-31	1,82	MIR31	1,87
hsa-miR-145	1,81		
hsa-miR-21	1,49		
hsa-miR-199a-1	1,47	MIR199A2	1,47
hsa-miR-100	1,42	MIR100	1,34
hsa-miR-455	1,40	MIR455	1,35
hsa-miR-125a	1,38	MIR125A	1,34
hsa-miR-125b	1,33	MIR125B1	1,32
hsa-miR-191	-1,40		
hsa-miR-188	-1,47		
hsa-miR-486	-1,49		
hsa-miR-345	-1,51		
hsa-miR-107	-1,53	MIR107	-1,36
hsa-miR-149	-1,58	MIR149	-1,46
hsa-miR-675	-1,58		
hsa-miR-532	-1,68	MIR532	-1,49
hsa-miR-500a	-1,69		
hsa-miR-501	-1,81		
hsa-miR-874	-1,81	MIR874	-1,49
hsa-miR-133b	-1,84	MIR133B	-1,46
hsa-miR-182	-1,86		
hsa-miR-184	-1,88	MIR184	-1,56
hsa-miR-133a-2	-2,04		
hsa-miR-362	-2,04		
hsa-miR-502	-2,08		
hsa-miR-139	-2,13	MIR139	-1,80
hsa-miR-146b	-2,34	MIR146B	-1,67
hsa-miR-208b	-3,51	MIR208B	-2,59
hsa-miR-499a	-4,42	MIR499A	-3,06

Figure 11. Small RNAs differentially regulated 5 days after TGFβ1 treatment.
Primary human myoblasts (n = 5) were stimulated preconfluently for 48 h with 1 ng/ml TGFβ1, 10µM SB431542 (TGFβ1 inhibitor) or vehicle prior to differentiation with 2% FBS for 5 days. Harvested RNA underwent sequencing. Results of the bioinformatical analysis are shown here. Panel (A) shows a heatmap of results from the classical pipeline. The classical pipeline annotates sequences from analysis to the genome, followed by the comparison of different treatments. In this pipeline, the gene names of sncRNAs were used. The heatmap was created with Excel and GraphPad Prism using the t-test $p < 0.05$ from Excel as a cut off and sorting for fold change in the comparison TGFβ1 vs. vehicle. Colors represent log2 fold change with white being 1, blue downregulated and red upregulated. Panel (B): In the DEUS analysis, unique sequences are compared before annotation. This leads to several sequences annotated to the same miRNA. We created an overlap of the DEUS analysis results of control vs. TGFβ1 and TGFβ1 vs TGFβ1 + inhibitor. From this list, we calculated the average linear fold change (FC) for each annotated miRNA. The left side of Figure 11B shows the results from the DEUS analysis using the nomenclature for mature miRNAs. The right side of Figure 11B shows the miRNAs from the classical pipeline that match this list of differentially regulated miRNAs using the nomenclature for gene names. The colors are adapted to the colors of the heatmap in (A).

Additionally, in the DEUS analysis, one cluster of similar sequences with the same core sequence, which was downregulated in TGFβ1-treated samples, was notable. The cluster is comprised of 61 sequences, the core sequence is 17 bases long and the longest single sequence is 35 bases long (Figure 12). None of these sequences could be mapped to a known miRNA. The fragments origin from the

mitochondrially encoded tRNA glutamic acid and thus, Starscan software predicted a potential target site of these RNA sequences in the mitochondrial DNA. We therefore called it “mitosRNA” and took it to the list of potential interesting candidates.

Figure 12. MitosRNA: Cluster of 61 sequences from DEUS analysis.
In the DEUS analysis of sequencing data, this cluster of unique sequences was downregulated in TGFβ1-treated compared to vehicle-treated samples. The genetic code of the base sequence is displayed as letters, with the number of unique sequences containing the specific base at the same position in the sequence written below. Black letters symbolize the detected core sequence with 59 or more of the 61 unique sequences possessing the respective base at the corresponding position. Dark grey symbolizes between 30 and 58 base pairs and light grey less than 20 of the 61 unique sequences possessing this base at this position in the sequence.

3.3 Influence of differentiation and differentiation medium on the effects of TGFβ1 on miRNAs, regulators of metabolism and targets of TGFβ1

To validate the sequencing results, an additional experiment with the same setup was performed: Primary human myoblasts were stimulated for 48 h with 1 ng/ml TGFβ1, vehicle control or inhibitor (10µM SB431542) and subsequently differentiated to myotubes. Furthermore, cells were harvested at an earlier time point as myoblasts directly after the end of the 48 h-TGFβ1 stimulation, before the differentiation process began, to investigate the effect of myo-differentiation on miRNAs, regulators of metabolism and known targets of TGFβ1. Additionally, cells were differentiated with both 2% FBS as in the experiment for sequencing and with 0% FBS to investigate the effects of different differentiation media.

As potentially interesting miRNA candidates, we chose the top and bottom hits of the overlapping candidates shown in Figure 11. Additionally, we decided to investigate two more upregulated miRNAs from DEUS analysis, miR-145, miR-21, and the top hit of the classical pipeline miR-1294. To the list of downregulated miRNAs of interest, we added miR-133b and miR-206 because of their well described roles in skeletal muscle (Sempere et al., 2004) and appearance in our data. While miR-133b was found both classical pipeline and DEUS analysis Figure 11B), miR-206 was only differentially expressed in the comparison of TGFβ1-treated vs. vehicle but missed significance when comparing TGFβ1 vs. TGFβ1 and inhibitor-treated samples in both classical pipeline and DEUS analysis. All miRNAs were investigated using qPCR.

3.3.1 TGFβ1 regulates not all miRNAs already in myoblasts

When differentiating TGFβ1-stimulated myoblasts to myotubes, we found two groups of differentially regulated miRNAs. The first group is upregulated by TGFβ1 directly after treatment in myoblasts and still differentially expressed after differentiation in myotubes (Figure 13A-E) while the second group has very low expression levels in myoblasts and is downregulated by TGFβ1 only in myotubes (Figure 13F-K). For miR-708 and miR-1294, we could not confirm the sequencing results (Figure 13L-M). For the mitosRNA, we only observed a weak effect of TGFβ1 in myotubes and a small difference between mitosRNA levels in vehicle samples of myoblasts and differentiated myotubes (Figure 13N). The data shown in Figure 13 was generated from myotubes samples differentiated without FBS.

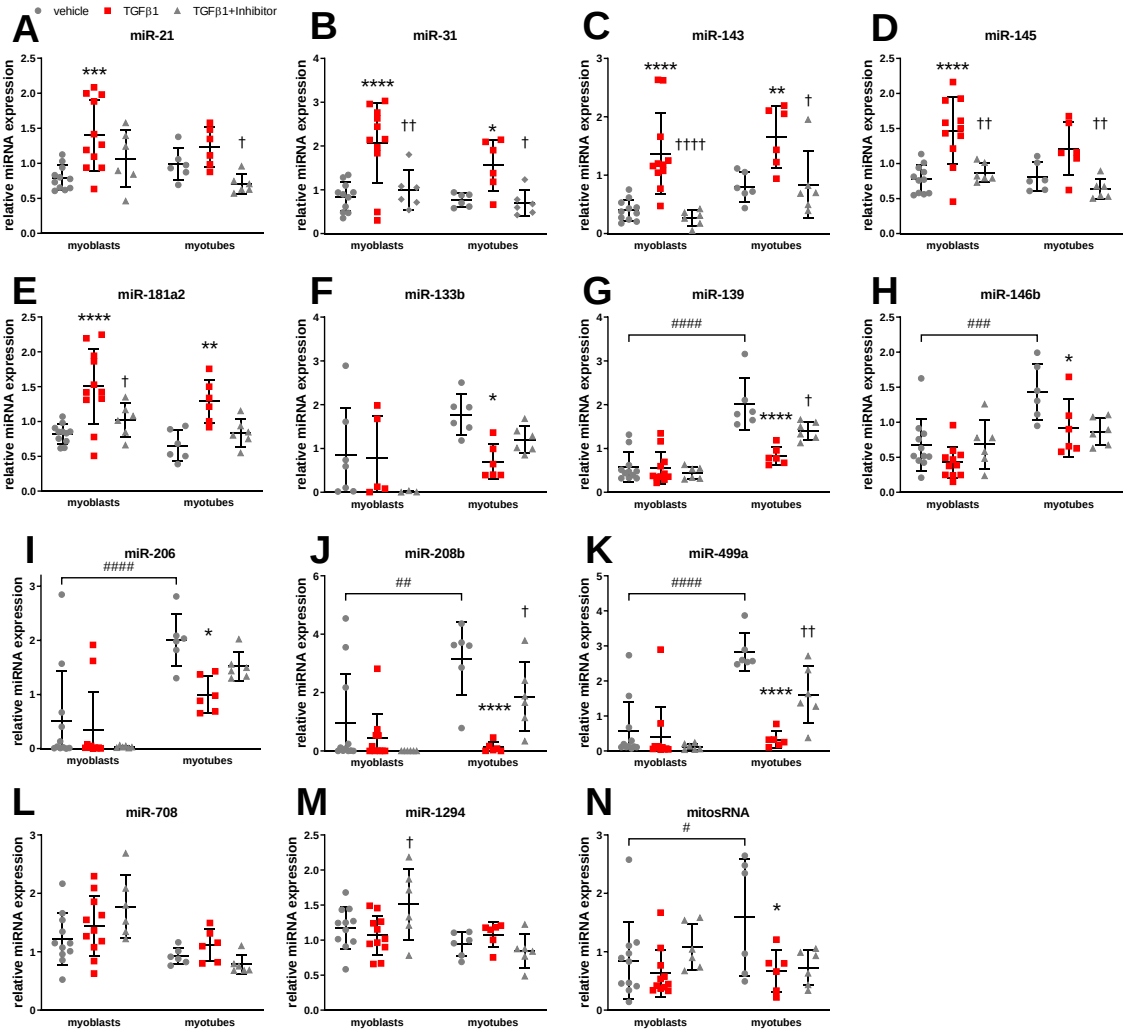

Figure 13. MicroRNAs differentially expressed after TGFβ1 treatment before and after differentiation.

Myoblasts were harvested directly after 48 h of 1 ng/ml TGFβ1 (red squares), vehicle control (grey circles) or Inhibitor (10 µM SB431542; grey triangles) treatment. Myotubes were differentiated for 5 days without FBS after the end of TGFβ1 treatment. All data are normalized to individual donor and endogenous controls RNU6 and miR-3615 and displayed as symbols for individual values with mean ± SD. All statistical analyses are two-way ANOVA. The comparison within myoblasts or myotubes was done with Tukey's multiple comparisons test, whereas the comparison of vehicle samples of myoblasts and myotubes was done with Sidak's multiple comparison test. * p-value of comparison vehicle and TGFβ1; † p-value of comparison of TGFβ1 + Inhibitor and TGFβ1. # p-value of the comparison of vehicle samples in myoblasts and myotubes. One symbol $p < 0.05$; two symbols $p < 0.01$; three symbols $p < 0.001$; four symbols $p < 0.0001$. (A-E) miR-21, miR-31, miR-143, miR-145 and miR-181a2 are upregulated in myoblasts and myotubes. (F-K) miR-133b, miR-139, miR-206, miR-208b and miR-499a are downregulated by TGFβ1 in myotubes and have low expression in myoblasts. (L-M) TGFβ1 has no effect on miR-708 or miR-1294. (N) mitosRNA was decreased by TGFβ1 treatment in myotubes.

3.3.2 Influence of used differentiation medium

Next, we compared the effect of TGFβ1 on myotubes differentiated in the presence of 2% FBS to myotubes differentiated in the absence of FBS. This protocol was shown to reduce the number of non-differentiated myocytes and to increase the abundance of muscle-specific proteins such as MYH1, 2, and 7 (Hoffmann et al., 2018). This improved differentiation medium is also supplemented with BSA-coupled fatty acids palmitate and oleate, and carnitine as described in methods.

When comparing transcript levels of samples differentiated with 0% FBS or 2% FBS, we found the most striking difference in PGC1α (Figure 14A) where vehicle treated myotubes differentiated without FBS showed more than double the expression of PGC1α transcript compared to myotubes differentiated with 2% FBS as previously described in (Hoffmann et al., 2018). For the other investigated transcripts, *RRAGD*, *COX6A2* (cytochrome c oxidase subunit 6A2), *MYH7*, *PRKAA2*, and *LDLRAD4* no significant differences of transcript expression in vehicle treated myotubes were detected. However, *RRAGD* showed a trend towards downregulation by TGFβ1 with both differentiation media. Some of the investigated TGFβ1 effects appeared to be more pronounced in the absence of FBS. For *LDLRAD4* transcript, we found a difference in TGFβ1-treated myotubes depending on the used differentiation medium.

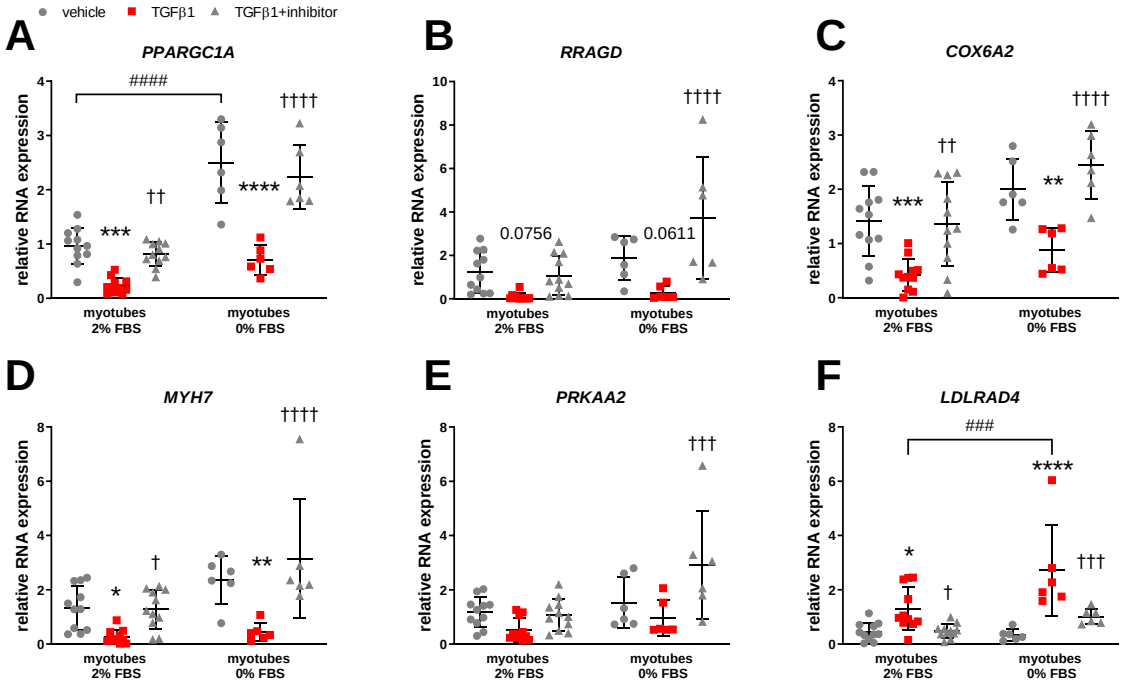

Figure 14. Effects of FBS content during myo-differentiation on regulators of metabolism and differentiation markers.
Myoblasts (n = 5-11) were treated with 1 ng/ml TGFβ1 or 10 µM TGFβ1 inhibitor SB431542 prior to differentiation. Two different media for differentiation were used: differentiation medium with 2% FBS or differentiation medium without FBS (0% FBS in graphs) supplemented with coupled fatty acids palmitate and oleate, and carnitine. All data are from qPCR, normalized to individual donors and endogenous control *TBP*. Data are displayed as symbols for individual values (grey circles: vehicle; red squares: TGFβ1; grey triangles: TGFβ1 and inhibitor) with mean ± SD. We used two-way ANOVA with Tukey's multiple comparison test to compare within groups of myoblasts and myotubes. Two-way ANOVA with Sidak's multiple comparisons test was used to compare within respective treatment among groups. * p-value of comparison of vehicle and TGFβ1; † p-value of the comparison of TGFβ1 + Inhibitor and TGFβ1. # p-value of the comparison of vehicle or TGFβ1-treated samples of myoblasts and myotubes as indicated. One symbol $p < 0.05$; two symbols $p < 0.01$; three symbols $p < 0.001$; four symbols $p < 0.0001$.

When looking at the expression of miRNAs, differences between vehicle-treated samples were found only in miRNAs with higher expression in myotubes than in myoblasts. Namely, miR-133b, miR-139, miR-208b and miR-499a showed significantly higher expression in vehicle-treated samples of myotubes differentiated without FBS compared to vehicle-treated samples of myotubes differentiated in the presence of 2% FBS (Figure 15F, G, J, K).

Furthermore, the reduction of transcript levels caused by TGFβ1 treatment appeared to be more pronounced in myotubes differentiated without FBS for miR-133b, miR-139, miR-206, miR-208b and miR-499a, which are all miRNAs with higher expression in myotubes than in myoblasts (Figure 15F, G, I, J, K). For miRNAs that do not increase expression during myo-differentiation (Figure 15A-E), miR-21, miR-31, miR-143, miR-145 and miR-181a2, the effects induced by TGFβ1 were unchanged.

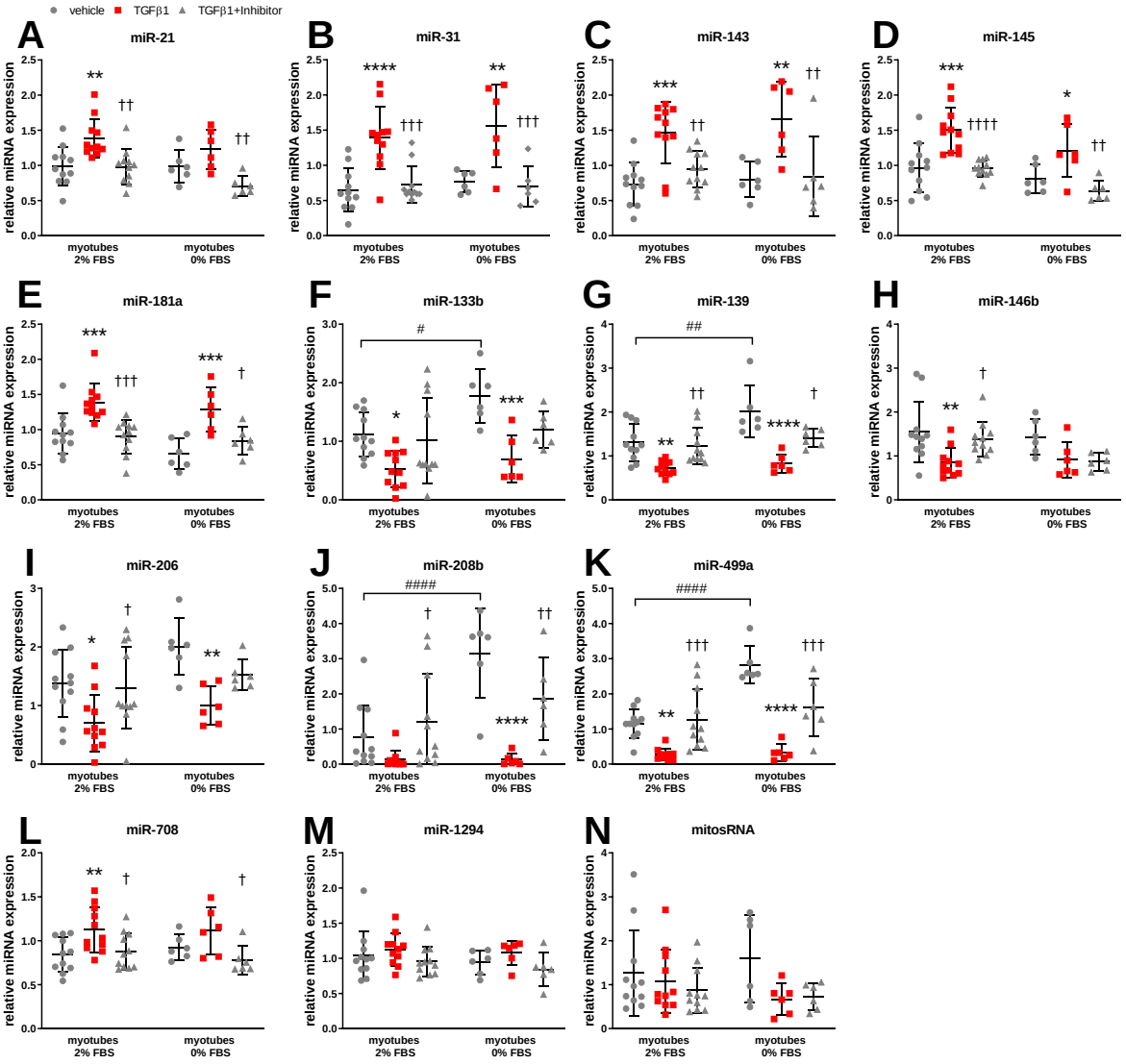

Figure 15. Effect of FBS concentration during myo-differentiation after TGFβ1 treatment on miRNAs.

Human myoblasts (n = 6-11) were treated with vehicle control, 1 ng/ml TGFβ1 or 10 µM TGFβ1 inhibitor SB431542 for 48 h and subsequently differentiated to myotubes either without FBS, supplemented with coupled fatty acids palmitate, oleate and carnitine or with 2% FBS. All data were normalized to donor and endogenous controls *RNU6* and miR-3615. Data are displayed as symbols for individual values (grey circles: vehicle; red squares: TGFβ1; grey triangles: TGFβ1 and inhibitor) with mean ± SD. Two-way ANOVA with Tukey's multiple comparison test was used to compare different treatments within groups of myotubes differentiated with or without 2% FBS. Two-way ANOVA with Sidak's multiple comparisons test was used to compare within respective treatment among groups. * p-value of the comparison of vehicle and TGFβ1; † p-value of comparison of TGFβ1 + Inhibitor and TGFβ1. # p-value of the comparison of vehicle-treated myoblasts and myotubes as indicated. One symbol $p < 0.05$; two symbols $p < 0.01$; three symbols $p < 0.001$; four symbols $p < 0.0001$.

3.4 Effect of myo-differentiation on miRNAs, regulators of metabolism and targets of TGFβ1

Since some of the investigated miRNAs and other TGFβ1 targets were upregulated after 5 days of differentiation and this might play a role in their response to TGFβ1 stimulation, we additionally studied the time course during myo-differentiation. Cells were cultured until confluency, subsequently differentiation was initiated by switching to the fusion medium without FBS (= day 0) as it resulted in higher degree of differentiation. Samples were taken on days 0, 1, 3 and 5 of differentiation. For protein samples, cells were additionally stimulated with 10 µM insulin for 10 minutes before harvesting.

3.4.1 MiRNAs during myo-differentiation

As expected from the results shown in Figure 13, the miRNAs already regulated by TGFβ1 in myoblasts, miR-21, miR-31, miR-143, miR-145, and miR-181a2, did not show higher expression with advanced differentiation (Figure 16A-E). The miRNAs not clearly changed by TGFβ1 treatment in Figure 13, miR-708, and miR-1294, also did not increase expression levels with advance differentiation (Figure 16F-G). Two of the mentioned miRNAs, miR-31 and miR-1294, even decreased throughout differentiation (Figure 16B and G). The regulation of miRNAs that increased expression with myo-differentiation (Figure 13) was confirmed: miR-133b, miR-139, miR-146b, miR-206, miR-208b, and miR-499a increased during differentiation (Figure 16H-M). Lastly, we did not observe changes in expression level during myo-differentiation for mitosRNA (Figure 16N), in contrast to the difference observed in Figure 13N in vehicle-treated samples.

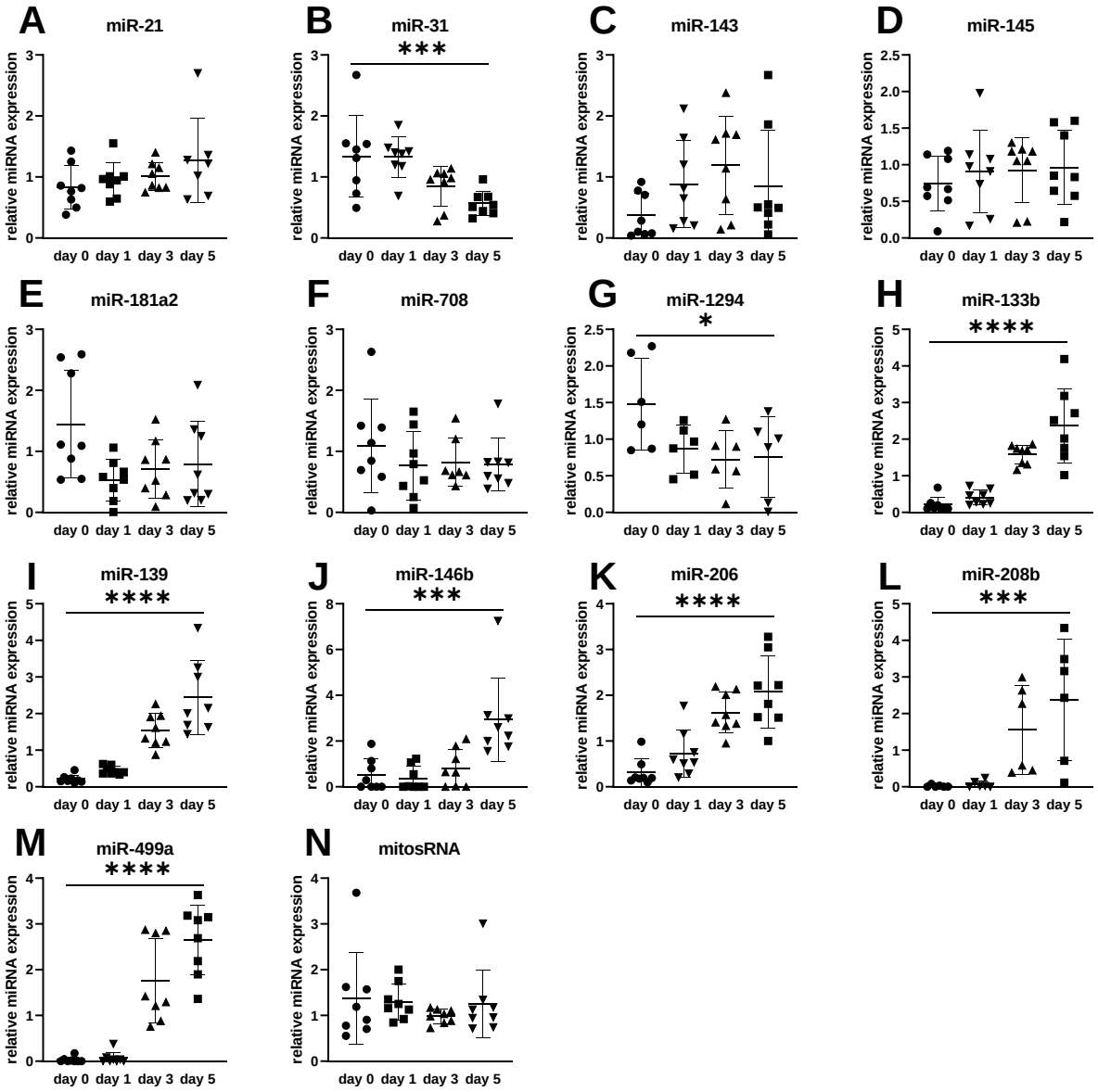

Figure 16. Differentiation of myoblasts increases some miRNAs but not all.
Myoblasts were differentiated without the presence of FBS after confluency. Day 0 equals the start of differentiation by serum withdrawal. Expression of mature miRNAs was detected in qPCR. All qPCR data were normalized to individual donors and reference sncRNAs *RNU6* and miR-3615. Data are displayed as symbols for individual values with mean ± SD. All data were analyzed using one-way ANOVA with test for trend. (A-G) miRNAs showing no upregulation during differentiation. (H-M) miRNAs increasing during differentiation. (N) mitosRNA does not change during differentiation. * $p < 0.05$; *** $p < 0.001$; **** $p < 0.0001$.

3.4.2 Regulators of metabolism and targets of TGFβ1 during myo-differentiation

Next, we analyzed mRNA levels of the regulators of metabolism that were influenced by TGFβ1 treatment as described in (Bohm et al., 2016a) and (Hoffmann et al., 2018). Additionally, we studied *RRAGD*, which was one of the top downregulated transcripts in the sequencing analysis (Figure 10B) and is a member of the mTOR (mammalian target of rapamycin) pathway.

We observed an increase in mRNA expression with differentiation for all investigated transcripts *CPT1B*, *RRAGD*, PGC1α, *MYH1*, and *MYH2* (Figure 17).

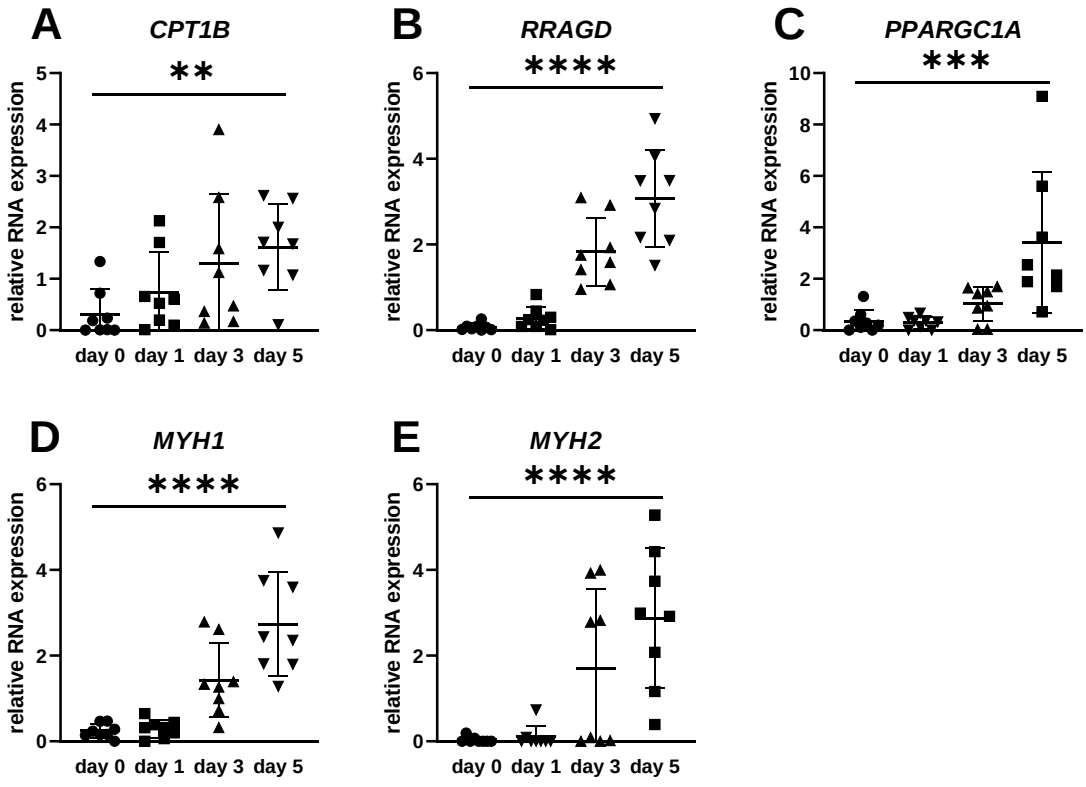

Figure 17. Myo-differentiation increased *CPT1B*, *RRAGD*, *PPARGC1A*, *MYH1,* and *MYH2* expression.
Myoblasts were differentiated without the presence of FBS after confluency. Day 0 equals the start of differentiation by serum withdrawal. Expression of transcripts was detected using qPCR. All qPCR data were normalized to the individual donor and reference genes *TBP* and *RPS13*. Data are displayed as symbols for individual values with mean ± SD. All data were analyzed using one-way ANOVA with test for trend. ** $p < 0.01$; *** $p < 0.001$; **** $p < 0.0001$.

On protein level, we observed an increase in the insulin-induced phosphorylation of serine-473 of AKT during myo-differentiation (Figure 18A). In non-insulin stimulated samples, we observed an increase with myo-differentiation in ATP5A (Figure 18B), but no change in AMPKα2 (Figure 18C) protein (test for trend p = 0.1361).

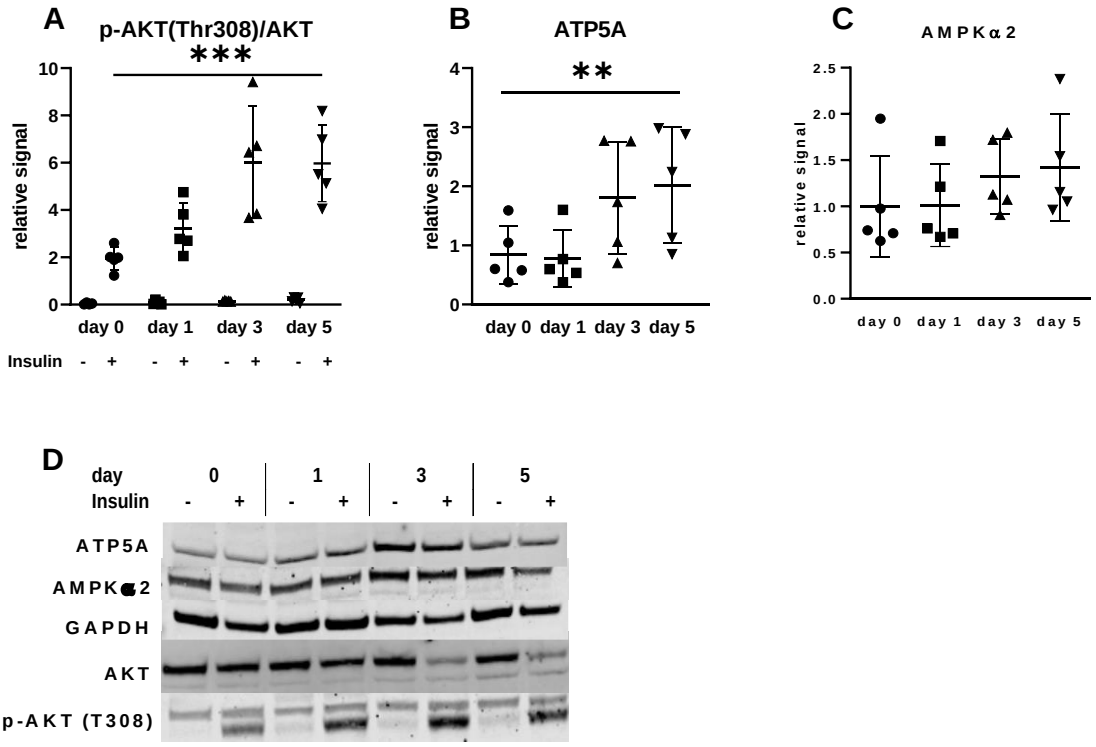

Figure 18. Differentiation of myoblasts increased phosphorylation of AKT and abundance of ATP5A protein.
(A-C) Quantification results of western blot data. All western blot data were normalized to donor. Data are displayed as symbols for individual values with mean ± SD. (A) Insulin-induced phosphorylation of threonine 308 of AKT relative to total AKT increased during differentiation. One-way ANOVA with test for trend only looking at insulin-stimulated samples. (B-C) Only data from non-insulin stimulated samples was used for quantification. Data normalized to endogenous control GAPDH. One-way ANOVA with test for trend. (B) ATP5A protein increased during differentiation. (C) AMPKα2 protein level did not increase during differentiation. (D) Representative western blots of ATP5A, AMPKα2, GAPDH, AKT, and p-AKT (Thr308). Only data of non-insulin stimulated cells are shown in quantification of ATP5A and AMPKα2.

3.5 Finding a model to overexpress or repress miRNAs

After the identification of TGFβ1-regulated miRNAs, we next wanted to look at functional application of these candidate miRNAs. We therefore needed a suitable model in which we could overexpress or repress miRNAs to see what functional role each miRNA has.

3.5.1 Transfecting miRNA mimics into primary human myotubes

To stay as close as possible to the human system, we wanted to continue working with primary human myotubes. We first settled for locked nucleic acid (LNA) stabilized miRNA mimics, which are also widely used to study miRNA functionality (Gottmann et al., 2018; Noguchi et al., 2013).

We decided to use viromer blue as transfection tool, as the group had previously used it successfully to transfect siRNA in primary human myoblasts and differentiated myotubes (Ingerslev et al., 2017; Klingler et al., 2016). In our establishing experiments, we saw the best results when leaving the cells for 24 h with the transfection solution. When using longer transfection times, we had no better transfection rate (data not shown).

3.5.1.1 Concentration of miRNA Mimics

A common issue with miRNA mimics is toxicity by RNA-overloading of the cells (Karbiener et al., 2014). We therefore wanted to use moderate amounts of miRNA mimics and first tested transfecting 1 nM and 10 nM miRNA mimics. With both concentrations, we clearly detected higher amounts of miRNA in qPCR (Figure 19). For single miRNA transfections, we therefore settled for 10 nM, to not loose effects when working with too low concentrations. For transfections of a mix of miRNAs, we used a total concentration of 5 nM assuming that synergistic effects will enhance effects.

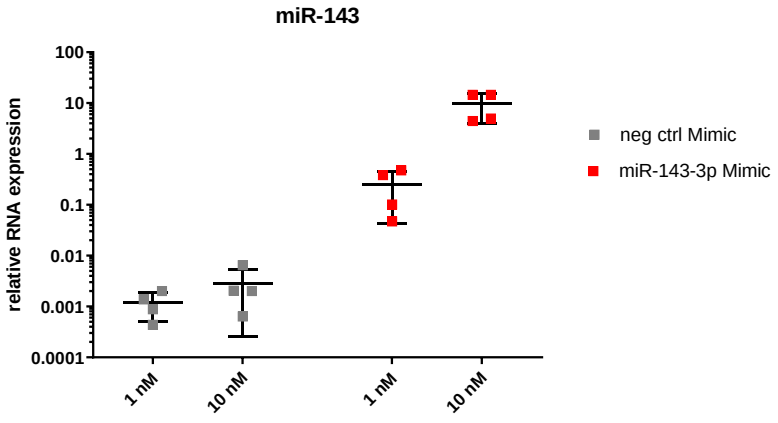

Figure 19. Establishing of used miRNA mimics concentrations.
Primary human myoblasts (n = 4) were preconfluently transfected with 1 nM or 10 nM LNA stabilized miRNA mimic miR-143-3p or with negative control mimic for 24 h prior to differentiation to myotubes for 5 days. Mature miRNA levels were quantified in qPCR. Data were normalized to donor and to reference gene *RNU6*. Graph is displayed with logarithmic y-axis. Data are displayed as symbols for individual values (grey: negative control mimic; red: miR-143 mimic) with mean ± SD.

3.5.1.2 Controls

Analog to a vehicle control for TGFβ1 or insulin stimulation, we used a negative control miRNA mimic, containing an RNA sequence that will not affect human cells but consists of a LNA stabilized RNA sequence like the used miRNA mimics. Additionally, we used an untreated medium-only control, and we introduced an optical positive control, a Cy3-tagged nonsense miRNA that can be imaged in life cells. Furthermore, we wanted to control for functionality of miRNA mimics. Therefore, we decided to use miR-122 mimic and looked at *ALDOA* (aldolase, fructose-bisphosphate A) transcript as readout as a positive control. MiR-122 has been described to decrease *ALDOA* transcript levels (Fabani and Gait, 2008) and is commercially sold as a positive control (Dharmacon, CP-004000-01).

Thus, our control workflow would be firstly, to check cell growth by bright field microscopy, and secondly control transfection efficiency by looking at Cy3 staining in cells in culture. After harvesting, we would control miRNA levels in qPCR, always comparing to untreated and negative mimic control. As a positive control, we would lastly check mRNA levels of ALDOA in miR-122 treated samples. In the graphs of this thesis, the untreated control is not shown, as the comparison to the negative control mimic is more relevant.

3.6 A mix of miRNA mimics fails to compensate TGFβ1 effects

To examine whether the suppression of miRNAs by TGFβ1 during differentiation leads to the observed inhibition of differentiation, *PPARGC1A* expression, ATP5A protein and phosphorylation of AKT, we treated cells with TGFβ1 as before but added a 5 nM miRNA mimics mix of miR-133b, miR-206, miR-208b, and miR-499a on day 1 of differentiation (Figure 20A) to compensate for the downregulation of these miRNAs. The choice of miRNAs was based on the top two regulated candidates, miR-499a and miR-208b, complemented with the well-described myo-miRNAs miR-133b and miR-206.

While the treatment with TGFβ1 reduced the endogenous expression level of these miRNA in myotubes on day 5 as expected, the abundance of the miRNAs in the transfected cells was strongly increased and not influenced by TGFβ1 (Figure 20B-E). Transfection efficiency was good as observed by the fluorescence signal of the Cy3-labeled miRNA mimic negative control. On day 5 of differentiation, which equals to 3 days after washing the cells after transfection, cells transfected with the respective mimic were still clearly showing Cy3 fluorescence (Figure 20F). In our positive control, we found a clear decrease of *ALDOA* transcript after transfection with miR-122 mimic in all independent experiments, but it was not statistically significant (Figure 20G).

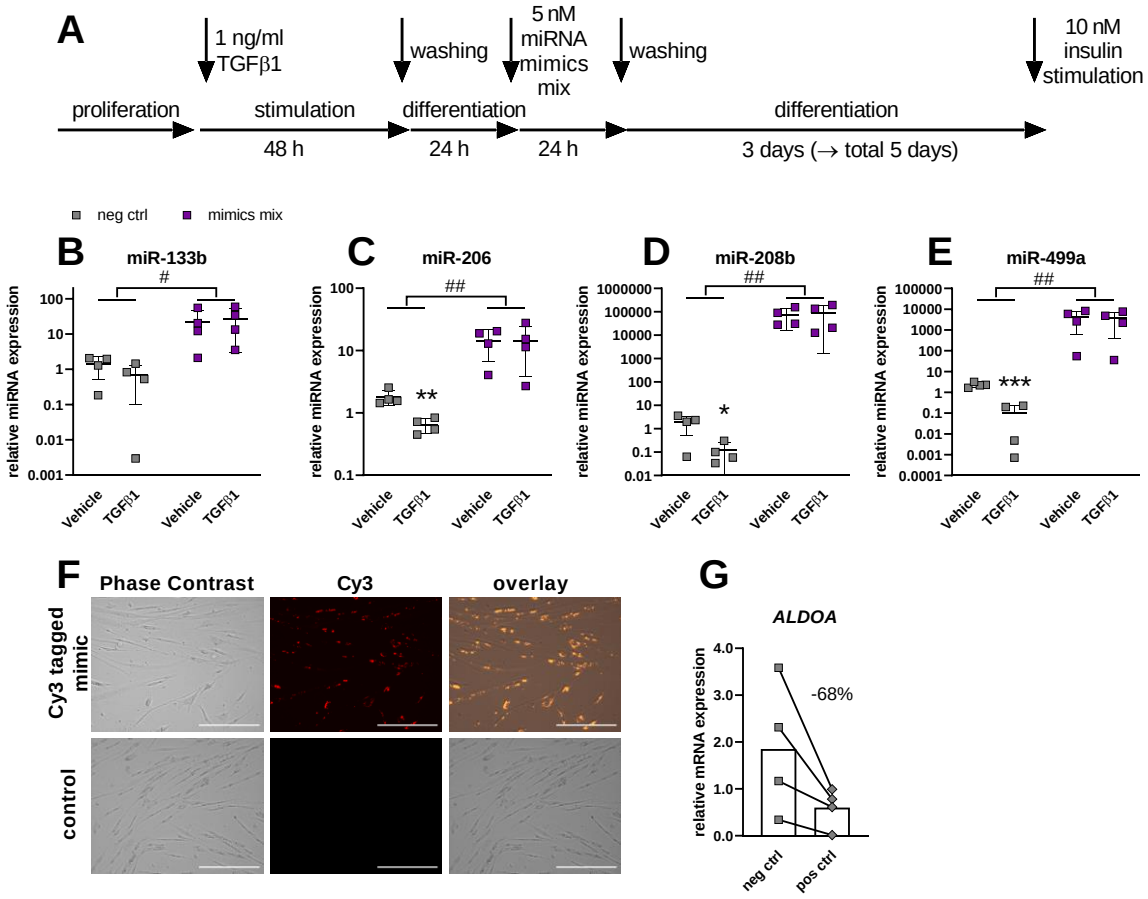

Figure 20. Transfection of miRNA mimics mix after TGFβ1 stimulation.
Primary human myoblasts (n = 4) were stimulated with vehicle control or 1 ng/ml TGFβ1 for 48h before confluence. Subsequently, differentiation without FBS was initiated. On day 1 of differentiation (approximately 24h after start of differentiation), a mix of 4 miRNA mimics (miR-133b, miR-206, miR-208b and miR-499a) at a total concentration of 5 nM (1.25 nM per miRNA) or 5 nM of controls (negative control, Cy3-tagged transfection control or positive control) were transfected into the cells. (A) Schematic display of the timing of the experiment. (B-E) Relative miRNA expression obtained using qPCR. All data were normalized to individual donor and endogenous controls *RNU6* and miR-3615. Data are displayed as symbols for individual values (grey: negative control mimic; purple: miRNA mimic mix) with mean ± SD. Y-axis is in logarithmic scale. * Unpaired, two-tailed t-test comparing negative control mimic to mimics mix transfected samples; # unpaired, two-tailed t-test comparing TGFβ1 and vehicle only in negative control mimic transfected samples. One symbol $p < 0.05$; two symbols $p < 0.01$; three symbols $p < 0.001$. (F) Microscope images of Cy3 control and negative control on day 5 of differentiation. Scale bars 200 µm. From left to right: Phase contrast in bright field; Cy3 fluorescence; merged image of phase contrast and Cy3 fluorescence. (G) Relative *ALDOA* expression from qPCR. Data normalized to donor and to endogenous controls *TBP* and *RPS13*. Statistically not significant in t-test or Welch's test. Indicated decrease shows difference between means (bars).

As additional positive control, also controlling for functional activity of the transfected miRNA mimics, we further tested *MEOX2* (mesenchyme homeobox 2) transcript as it is described to be regulated by miR-206 in the C2C12 skeletal muscle cell line (Goljanek-Whysall et al., 2012) and it showed a slight upregulation in our sequencing results (vehicle vs. TGFβ1-treated fold change of 1.6 with $p_{adj} = 0.0079$). However, in cells treated with miRNA mimic mix containing 1.25 nM miR-206 mimic, we could not detect a reduction of *MEOX2* transcript compared to negative control (Figure

20H). On the other hand, TGFβ1 treatment increased *MEOX2* expression in vehicle-treated samples but not in samples treated with miRNA mimic mix. Thus, the addition of miR-206 mimic (1.25 nM in the miRNA mimics mix) might compensate for the inhibition of miR-206 due to TGFβ1 treatment when looking at *MEOX2* expression. Additionally, we tested samples from a different experiment, where 1 nM or 10 nM miR-206 mimic was transfected preconfluently and alone instead of in a mix of miRNA mimics. In those samples, there is a trend of a reduction of *MEOX2* transcript in 10 nM miR-206 mimic treated samples compared to 10 nM negative control treated samples. In samples treated with only 1 nM miR-206 mimic we could not see this trend (Figure 20I).

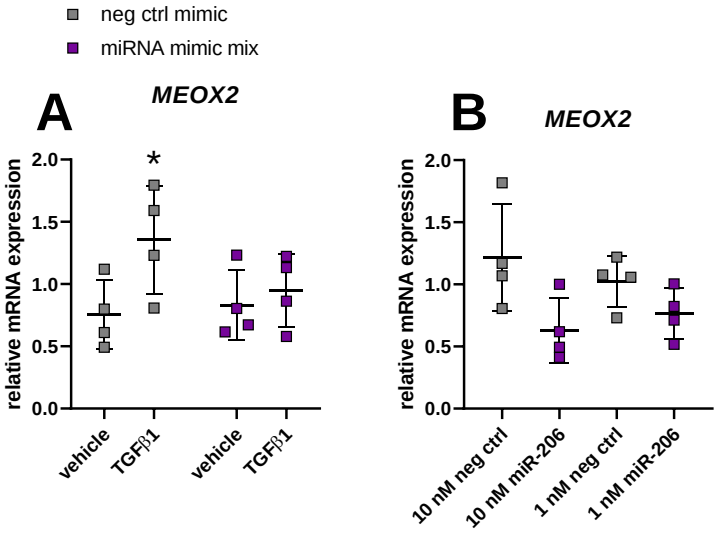

Figure 21. *MEOX2* expression levels as functional control for transfection of miR-206 mimic. Relative mRNA concentration of *MEOX2* from qPCR. Data normalized to donor and to endogenous controls *TBP* and *RPS13*. Data are displayed as symbols for individual values (grey: negative control mimic; purple: miRNA mimic mix or miR-206 mimic) with mean ± SD. (A) Primary human myoblasts (n = 4) were stimulated with vehicle control or 1 ng/ml TGFβ1 for 48h before confluence. Subsequently, differentiation without FBS was initiated. On day 1 of differentiation (approximately 24h after start of differentiation), a mix of 4 miRNA mimics (miR-133b, miR-206, miR-208b and miR-499a) at a total concentration of 5 nM (1.25 nM per miRNA) or 5 nM of negative control mimic were transfected into the cells. Two-way ANOVA with Sidak's multiple comparisons test comparing vehicle-treated samples and TGFβ1-treated samples. * $p < 0.05$ (B) In a different experiment without TGFβ1 stimulation, myoblasts were transfected with 1 nM or 10 nM miR-206 mimic or negative control mimic preconfluently for 24 h and subsequently differentiated for 5 days. No statistically significant differences between controls and miR-206 mimic (unpaired t-test 10 nM neg ctrl vs. 10 nM miR-206 $p = 0.059$).

Despite the high levels of miRNA mimics in our transfected cells and at least partially successful positive controls, we could not observe a compensation of the effects of TGFβ1 on the investigated parameters by the miRNA mimics mix. All observed differences persisted after treatment with miRNA mimics mix (Figure 23). TGFβ1 treated cells showed the same level of *PPARGC1A*, *MYH1*, and *MYH2* transcript with or without miRNA mimics mix (Figure 23A-C).

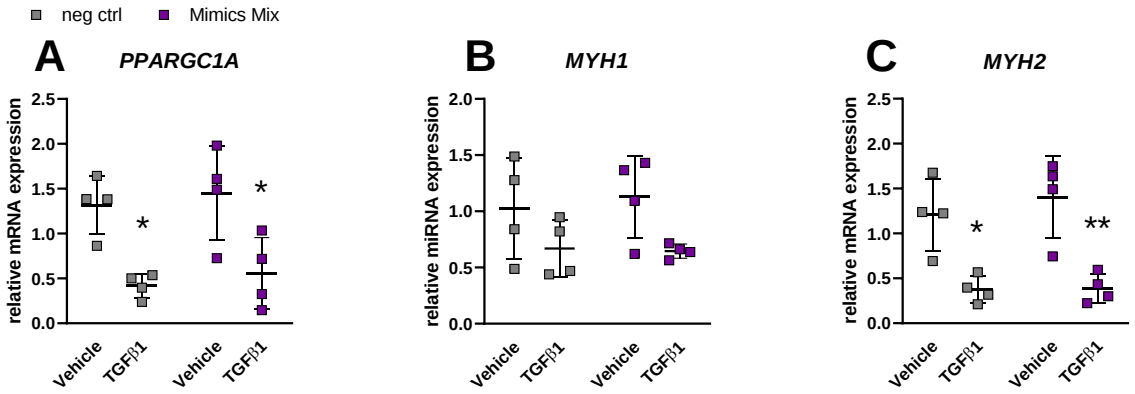

Figure 22. miRNA mimics mix did not compensate TGFβ1 effects on mRNA level.
Primary human myoblasts (n = 4) were stimulated with vehicle control or 1 ng/ml TGFβ1 for 48h before confluence. Subsequently, differentiation without FBS was initiated. On day 1 of differentiation (approximately 24h after start of differentiation), a mix of 4 miRNA mimics (miR-133b, miR-206, miR-208b and miR-499a) at a total concentration of 5 nM (1.25 nM per miRNA) or 5 nM of negative control mimic were transfected into the cells. Relative mRNA expression data from qPCR. Data normalized to donor and endogenous control *GAPDH*. Data are displayed as symbols for individual values (grey: negative control mimic; purple: miRNA mimic mix) with mean ± SD. Two-way ANOVA with Tukey's multiple comparisons test comparing all groups to each other. * $p < 0.05$; ** $p < 0.01$. (A) *PPARGC1A*, (B) *MYH1* and (C) *MYH2*.

On protein level, miRNA mimics mix also failed to change levels of ATP5A, AMPKα2, phosphorylation of AKT or MYH1/2 in TGFβ1 treated samples (Figure 23). Concluding these results, the downregulation of differentiation-dependent miRNAs was maybe not key for the observed effects of TGFβ1 on PGC1α, phosphorylation of AKT and ATP5A.

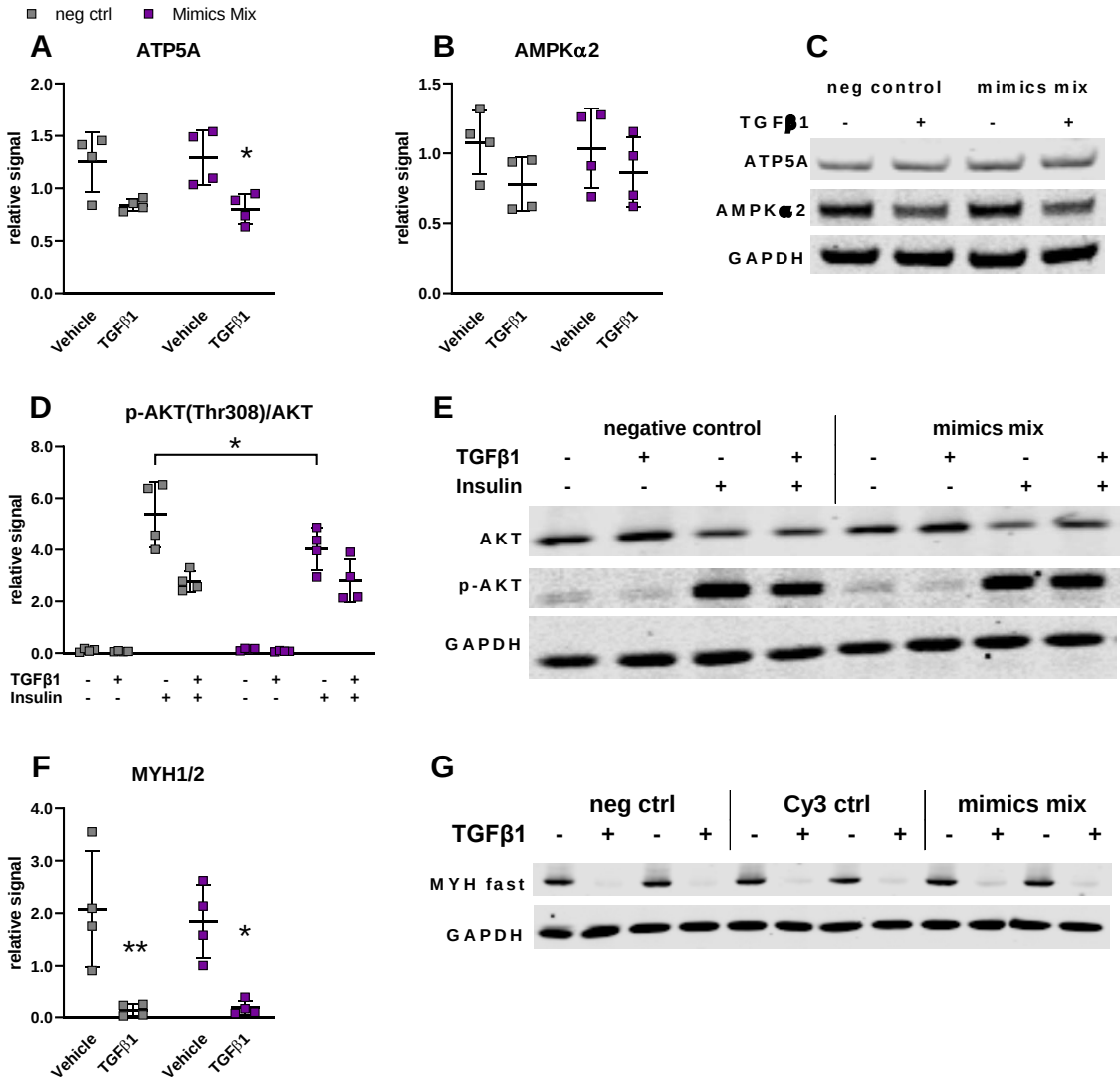

Figure 23. miRNA mimics mix did not compensate TGFβ1 effects on protein level.
Primary human myoblasts (n = 4) were stimulated with vehicle control or 1 ng/ml TGFβ1 for 48h before confluence. Subsequently, differentiation without FBS was initiated. On day 1 of differentiation (approximately 24h after start of differentiation), a mix of 4 miRNA mimics (miR-133b, miR-206, miR-208b and miR-499a) at a total concentration of 5 nM (1.25 nM per miRNA) or 5 nM of negative control mimic were transfected into the cells. Cells for protein samples were stimulated with 10 µM insulin or control prior to harvesting. Data are displayed as symbols for individual values (grey: negative control mimic; purple: miRNA mimic mix) with mean ± SD. (A) ATP5A and (B) AMPKα2 quantification of protein expression. Data were normalized to individual donor and loading control GAPDH. Two-way ANOVA Tukey's multiple comparisons test comparing all cell means. (C) Representative blot of ATP5A and AMPKα2 protein expression as well as loading control GAPDH. (D) Quantification phosphorylation of threonine 308 of AKT relative to total AKT protein. Two-way ANOVA with Sidak's multiple comparisons test comparing negative control and mimics mix for each treatment. (E) Representative blot of AKT, p-AKT (Thr308) and loading control GAPDH. (F) Quantification of MYH1/2 protein expression. Data normalized to individual donor and endogenous control GAPDH. Two-way ANOVA with Tukey's multiple comparisons test comparing all cell means. (G) Representative blot of MYH1/2 and GAPDH. Values of Cy3 control transfected cells were not used for quantification in F. * $p < 0.05$; ** $p < 0.01$.

3.7 Effect of single miRNAs upregulated by TGFβ1

As we could not compensate the effects of TGFβ1 by supplementing with TGFβ1-reduced miRNAs, the miRNAs independent of myo-differentiation became increasingly interesting. In order to investigate if any of the differentiation-independent upregulated miRNAs alone could induce the same effects on regulators of metabolism as TGFβ1, we treated cells preconfluently with 10 nM miRNA mimics. Subsequently, differentiation was initiated, and cells were harvested on day 5 of differentiation (Figure 25A). We decided to focus on miR-31, miR-143, and miR-145, because miR-31 and miR-143 showed very clear upregulation by TGFβ1 and have been described to have roles in insulin signaling (Gottmann et al., 2018; Jordan et al., 2011) or glucose homeostasis (Fang et al., 2012). We added miR-145 because it is in the same miRNA cluster as miR-143 and they are co-expressed, originating from the same host gene *CARMN* (cardiac mesoderm enhancer-associated non-coding RNA, also *MIR143HG*, miR-143 host gene).

All miRNA expression levels were clearly increased after transfection with the respective miRNA mimics (Figure 24B-D). The Cy3-tagged miRNA mimic control showed good transfection efficiency in the optical control (Figure 24G). However, the positive control miR-122 did not clearly reduce *ALDOA* transcript (Figure 24E). As an additional positive control, we investigated *IGFBP5* (insulin like growth factor binding protein 5) transcript, since miR-143 is described to reduce *IGFBP5* mRNA and protein abundance in muscle (Soriano-Arroquia et al., 2016). On transcript level, we could not find a difference in *IGFBP5* levels after transfection of miR-143 (Figure 24F).

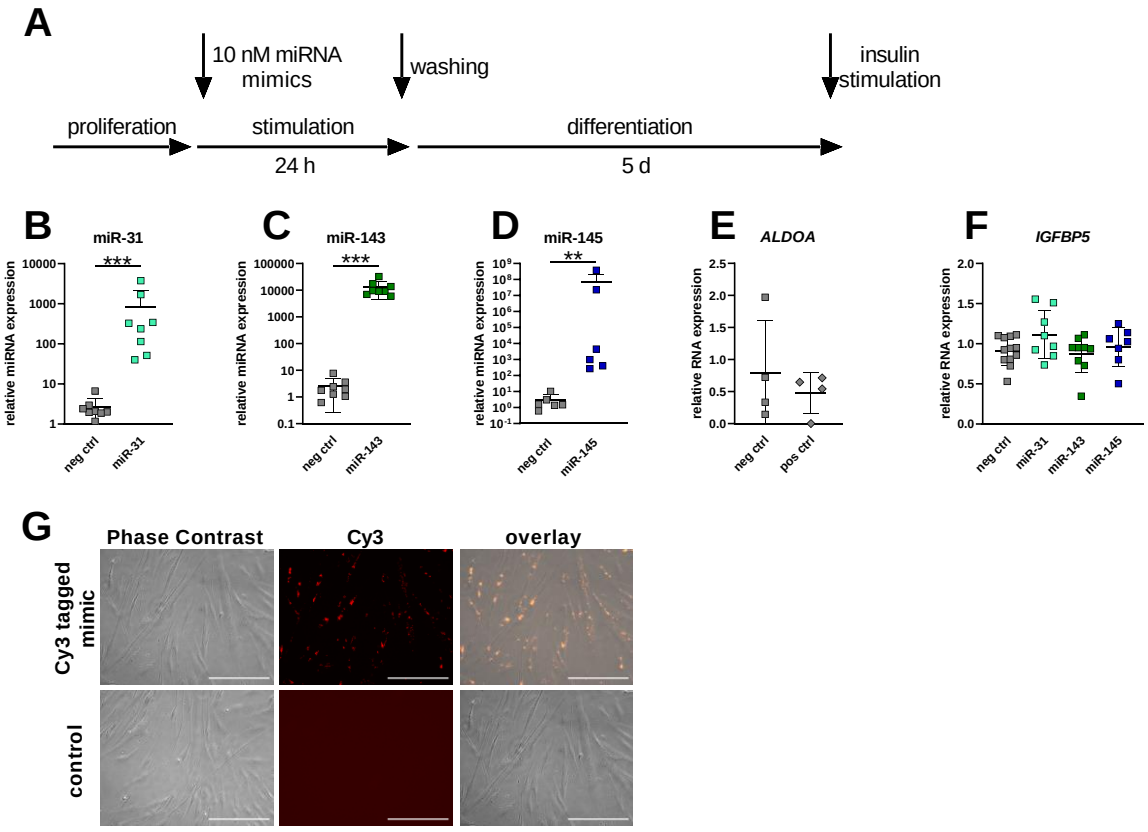

Figure 24. Transfection of miRNA mimics miR-31, miR-143, and miR-145.
Primary human myoblasts (n = 4-8) were transfected with 10 nM miR-31, miR-143, miR-145 or control mimics (negative control, positive control, and Cy3-tagged control) for 24 h before confluence and subsequently differentiated for 5 days. Cells for protein samples were stimulated with 10 µM insulin or control prior to harvesting (results in Figure 25). (A) Schematic plan of experiment. (B-F) Quantification of qPCR results after differentiation. Data are displayed as symbols for individual values with mean ± SD. (B-D) Levels of mature miRNAs. MiRNA data were normalized to individual donor and RNU6 as endogenous control. Results of Mann-Whitney test are indicated in graphs. ** $p < 0.01$; *** $p < 0.001$. (E) Positive control *ALDOA*. qPCR data normalized to individual donor and reference genes *TBP* and *RPS13*. (F) *IGFBP5* normalized to donor and endogenous controls *TBP* and *RPS13*. (G) Microscope images of Cy3 control and negative control on day 5 of differentiation. Scale bars 200 µm. From left to right: Phase contrast in bright field; Cy3 fluorescence; merged image of phase contrast and Cy3 fluorescence.

MYH1 and *MYH2* as markers of differentiation were not suppressed by miR-31, miR-143 or miR-145 mimic treatment, however, we observed a slight increase in *MYH2* by miR-143 mimic (Figure 25A-B) in comparison to the negative control mimic. *PPARGC1A* transcript was not reduced by miRNA mimic treatment, in contrary, we found miR-31 mimic to upregulate *PPARGC1A* expression compared to control mimic (Figure 25C). Insulin-stimulated phosphorylation of AKT as a marker for insulin signaling in skeletal muscle was decreased by miR-31 mimic treatment, but not by transfection of miR-143 or miR-145 (Figure 25D-E).

Jordan et al. described a mechanism of miR-143 suppressing phosphorylation of AKT via ORP8 (Jordan et al., 2011). We did not find effects on ORP8 protein by miR-143 mimic or other

investigated miRNA mimics (Figure 25M-P). We further did not observe effects of the transfected miRNA mimics on MYH1/2 protein levels (Figure 25H-I).

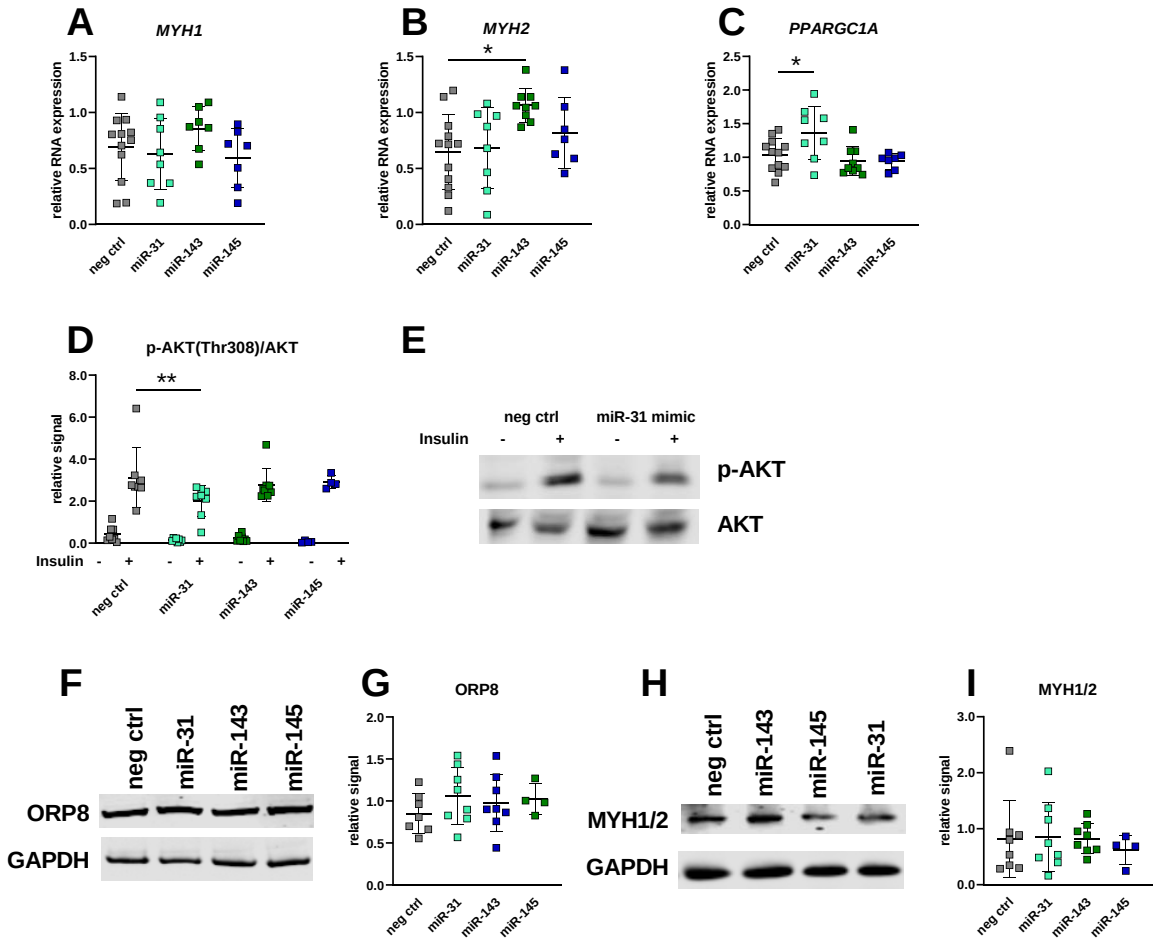

Figure 25. Effects of miR-31, miR-143, and miR-145 mimics on markers of differentiation and regulators of metabolism.
Primary human myoblasts (n = 4-8) were transfected with 10 nM miR-31, miR-143, miR-145 or control mimics for 24 h before confluence and subsequently differentiated for 5 days. Cells for protein samples were stimulated with 10 µM insulin or control prior to harvesting. (A-C) miR-31, miR-145, and miR-143 mimic do not suppress *MYH1* (A), *MYH2* (B) or *PPARGC1A* (C) transcript. All mRNA data normalized to donor and reference genes *TBP* and *RPS13*. One-way ANOVA with Dunnett's multiple comparisons test comparing to negative control mimic. (E) Representative western blot of p-AKT (Thr308) and AKT. (D, G, I) Quantification of western blot analysis shown in E, F, and H. (D) Insulin induced phosphorylation of threonine 308 of AKT compared to total AKT. Two-way ANOVA with Dunnett's multiple comparisons test comparing to negative control mimic within the insulin or control-stimulated group. (F) Representative western blot of ORP8 and GAPDH. (G) ORP8 protein level normalized to donor and GAPDH as loading control. (H) Representative western blot of MYH1/2 and GAPDH. (I) MYH1/2 protein level normalized to donor and endogenous control GAPDH. For all * $p < 0.05$; ** $p < 0.01$.

3.8 TGFβ1 did not lead to the same effects in C2C12 cells

Since we detected only minor effects of transfected miRNA mimics in the human skeletal muscle cells and we did not observe the reported regulation of ORP8 and *IGFBP5* by miR-143, we decided to use an alternative model to study the effect of our miRNA candidates. We assume that transfecting mimics into primary myoblasts could not adequately model the *in vivo* situation. Jin et al. showed that transfection of vectors containing the miRNA stem loop are superior to transfecting mature miRNAs like the mimics we used in primary myoblasts (Jin et al., 2015). In order to be able to transfect vectors without viral transduction, we changed the model system to the most common skeletal muscle cell line, C2C12, a murine immortalized cell line.

To be able to compare the results to our results from human myoblasts, we repeated the TGFβ1 stimulation experiment on the C2C12 cell line to see if the miRNAs are naturally regulated the same way in C2C12 cells as in primary human myoblasts. Thus, we stimulated C2C12 cells preconfluently for 48h with 1 ng/ml TGFβ1 or vehicle control before initiating differentiation by switching to differentiation medium for C2C12 cells. Additionally, we stimulated cells with 1 ng/ml TGFβ1 or vehicle control at a later time point, on day 3 of differentiation, for the last 48h before harvesting in order to be able to see acute effects.

Surprisingly, we did not see the effects observed in primary human myoblasts. We could not detect a difference in *Ppargc1a* transcript (Figure 26A) which is a highly constant and reproducible result we consistently see in primary human myoblasts. We also did not find a measurable reduction of differentiation markers *Myh2* or *Myh7*. Transforming growth factor beta induced (*Tgfbi*) was not increased in TGFβ1 stimulated samples. Further, we did not observe effects on any of our miRNA candidates (Figure 26B-L). Some of the miRNAs that are only expressed with differentiation in human myoblasts showed a trend to a reduction by TGFβ1 but none of them was statistically significant (e.g. Figure 26J).

Thus, using transient transfection of vectors in C2C12 cells does not appear to be a comparable model to investigate overexpression of TGFβ1-regulated miRNAs.

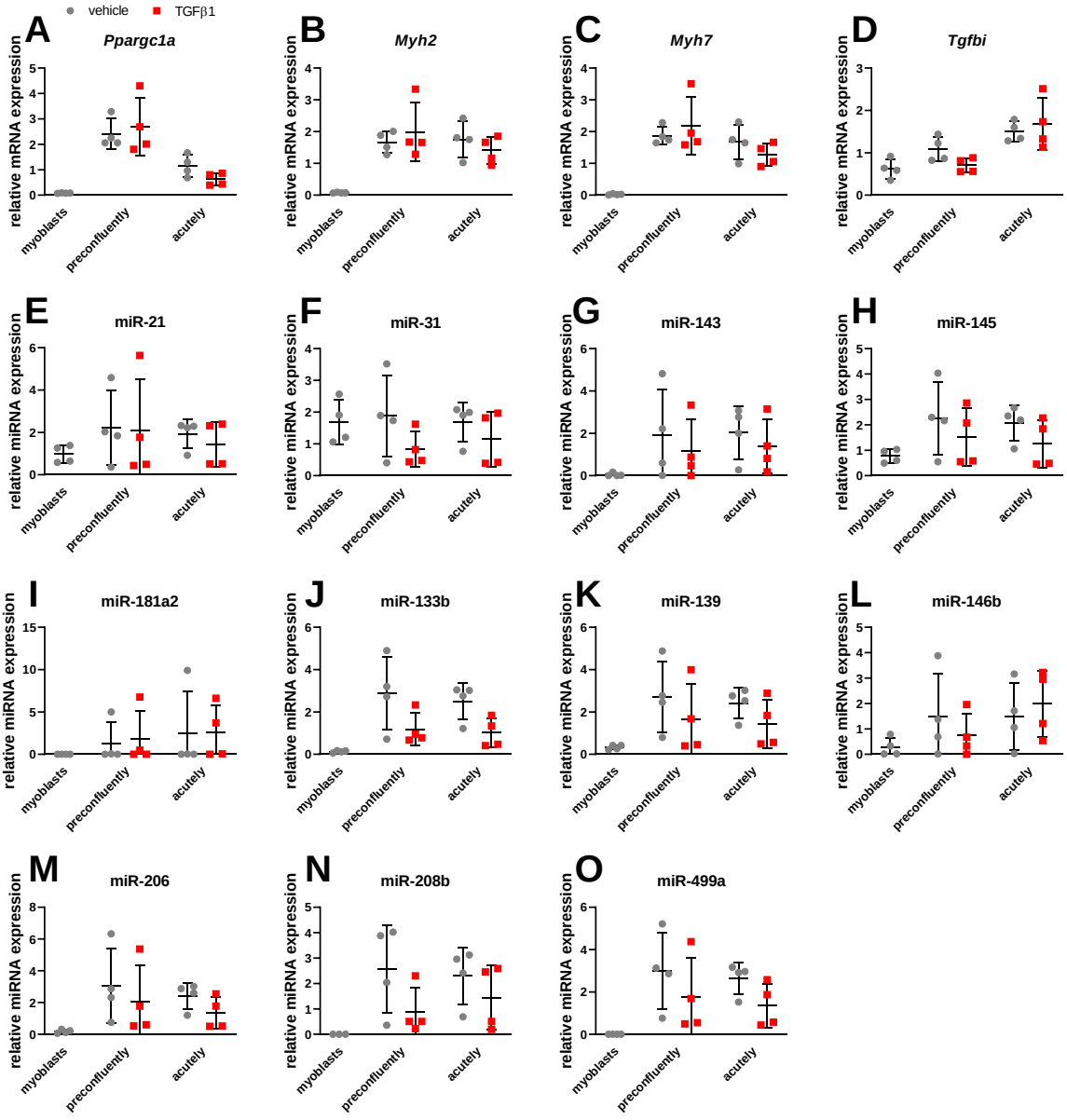

Figure 26. TGFβ1 effects in C2C12 cells.
C2C12 cells were stimulated either preconfluently or acutely (starting on day 3 of differentiation) for 48h with 1 ng/ml TGFβ1 or vehicle control and differentiated upon confluency for 5 days. All shown data were obtained by qPCR and normalized to batch. Data are displayed as symbols for individual values (grey: vehicle-treated; red: TGFβ1-treated) with mean ± SD. Two-way ANOVA with Sidak's multiple comparison test comparing within preconfluently or acutely stimulated samples did not find significant differences. Statistical comparison to myoblasts was not performed. (A-D) *Ppargc1a*, *Myh2*, *Myh1* and *Tgfbi* transcript normalized to endogenous control *TBP*. (B-L) microRNAs normalized to endogenous controls RNU6 and miR-3615.

3.9 *PPARGC1A* promoter methylation was not affected by TGFβ1 stimulation

Another possible explanation for the prolonged effect of TGFβ1 on PGC1α expression, apart from miRNAs, could be a methylation of the PGC1α promoter after TGFβ1 stimulation. We therefore teamed up with Jennifer Kriebel from the Institute of Epidemiology at the Helmholtz Zentrum München who used DNA from my experiment for analyses of the *PPARGC1A* promoter.

There are four known promoters for the *PPARGC1A* gene, two of them are used for gene expression in skeletal muscle (Popov et al., 2015). In the following, the classical, canonical promoter is called canonical promoter, the second promoter commonly expressed in skeletal muscle is called alternative promoter, and the two other promoters are called liver promoter and brain promoter named after the tissues they are described to be specific for (Felder et al., 2011; Soyal et al., 2012).

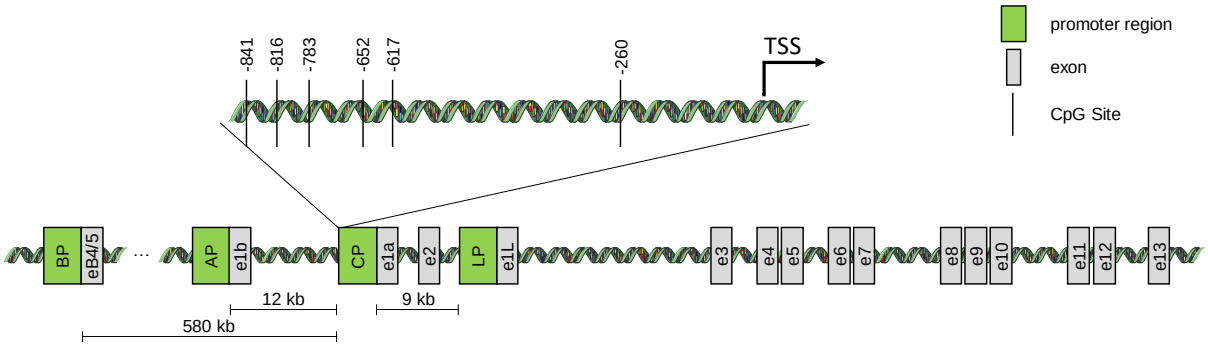

Figure 27. *PPARGC1A* promoters.
Schematic display of the *PPARGC1A* gene, its promoters, and 6 published CpG sites. The PPARGC1A gene has four described promoters, marked as green boxes: the canonical promoter (CP), the alternative promoter (AP), the liver promoter (LP), and the brain promoter (BP). Exons are displayed as grey boxes. Six described CpG sites, upstream of the transcription start site (TSS) of the canonical promoter are schematically displayed in the zoom-in. Part of this figure is based on the figure of (Martinez-Redondo et al., 2015) showing PPARGC1A promoters.

We analyzed 294 CpG sites in total using 37 primer pairs. Of these CpG sites, 54 CpG sites were located in the canonical promoter, 16 in the alternative promoter, 25 in the liver promoter, and 199 in the brain promoter. TGFβ1 did not affect promoter methylation at any *PPARGC1A* promoter, not acutely and not after 5 days of differentiation (Figure 28). After applying stricter quality control measures (all CpG sites with values of 0.7 or less methylation in the positive controls excluded), there were still 48 CpG sites included for the canonical promoter, 8 in the alternative promoter, 18 in the liver promoter, and 132 in the alternative promoter. When calculating the mean of all CpG sites for each promoter (using the cut-off of 0.7 in the positive control and not distinguishing treatments), we can compare the grades of methylation of each promoter. Interestingly, the lowest grades of methylation (less than 10%) were found for the canonical promoter and the brain promoter, while alternative promoter and liver promoter were methylated around 20% and 40% respectively.

The most investigated CpG sites of the *PPARGC1A* promoter are all located in the canonical promoter. Using the TSS 23,891,700 on chromosome 4 they namely are -841, -816, -783, -652, -617

and -260 (Brons et al., 2010; Gillberg et al., 2013; Ling et al., 2008; Xie et al., 2015). None of these CpG sites was differentially methylated after TGFβ1 treatment or differentiation to myotubes in our samples (data not shown).

As we did not see any differences in region averages or individual methylation sites, we concluded that methylation of the PGC1α promoter is not the cause for the effects we observed.

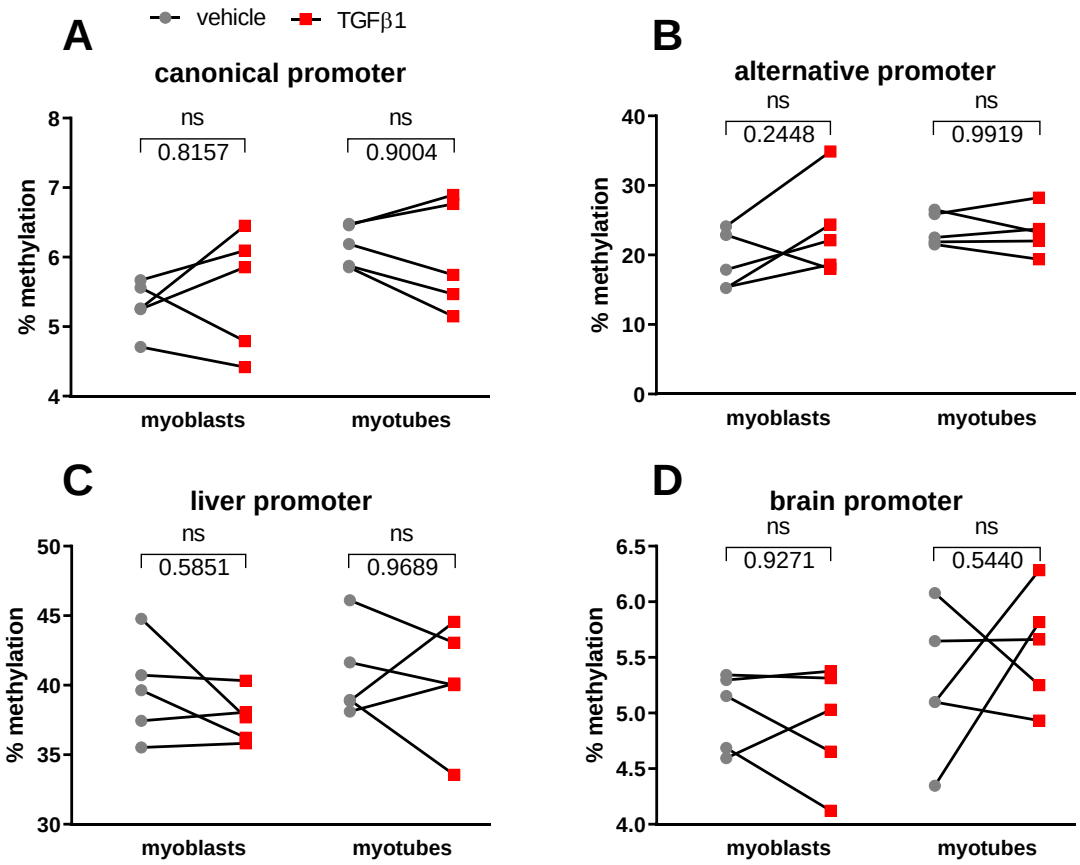

Figure 28. Analysis of the methylation of different promoters of PPARGC1A.
Human myoblasts (n = 5) were stimulated with 1 ng/ml TGFβ1 or vehicle control for 48 h before confluency and either directly harvested as myoblasts or differentiated without FBS to myotubes for 5 days. The graphs show percent methylation in the specific promoter regions: (A) canonical *PPARGC1A* promoter, (B) alternative *PPARGC1A* promoter, (C) liver *PPARGC1A* promoter, and (D) brain *PPARGC1A* promoter. (A-D) Two-way ANOVA with Sidak's multiple comparison test comparing within groups was used. Grey circles: treated with vehicle-control; red squares: treated with TGFβ1.

4 Discussion

To understand the role of TGFβ1 in the metabolic adaption to exercise, the mechanisms by which TGFβ1 influences metabolic regulators and insulin signaling need to be elucidated. We aimed to identify TGFβ1-regulated genes and regulating RNAs to uncover the underlying mechanisms of TGFβ1 in skeletal muscle. Based on our finding that the transcript of PGC1α, an important metabolic regulator, is persistently downregulated when stimulating myoblasts with 1 ng/ml TGFβ1 before differentiation for 5 days without TGFβ1, we investigated the molecular mechanism of this prolonged effect. We aimed to identify miRNAs that are regulated by TGFβ1 5 days after stimulation by sequencing and to investigate their role in the effects of TGFβ1 on metabolic regulators and insulin signaling.

4.1 TGFβ1-regulated miRNAs in human skeletal muscle and other organs

Since we observed a prolonged effect of TGFβ1 on PGC1α 5 days after end of treatment, which can be mediated by epigenetic regulation via miRNAs, sequencing of sncRNAs as potential regulators for this extended impact was performed. For the analysis of sncRNA sequencing data, two different approaches were used as described in methods (Figure 3). The main advantage of the DEUS analysis is the direct use of unique sequences. In the case of our dataset, about 60% of the unique sequences could be annotated to known sncRNAs. Consequently, the information on 40% of our unique sequences would have been lost when only using the classical pipeline. However, we only made use of this advantage for the mitosRNA cluster of unique sequences, which we could not confirm consistently regulated by TGFβ1 in further experiments. Nevertheless, the use of two pipelines and subsequent analysis with a combination of both results, validated our results. Two qPCR-confirmed regulated miRNAs, miR-21 and miR-145, were only found by DEUS analysis.

All miRNAs we found most upregulated after TGFβ1 treatment, namely miR-21, miR-31, miR-143, miR-145, and miR-181a2, have been described to be regulated by TGFβ1 in other tissues (see Table 13 for references). The miRNAs we found downregulated by TGFβ1, miR-133b, miR-139, miR-146b, miR-206, miR-208b, and miR-499a, all have been described in skeletal muscle differentiation or development (see Table 13 for references).

On the other hand, miRNAs and the miRNA machinery have been described to influence TGFβ signaling (Mishra et al., 2014; Suzuki, 2018; Yu et al., 2012). Out of our list of TGFβ1 regulated candidates, miR-21 has been shown to downregulate TGFβR2 in colon cancer and prostate cancer cells (Mishra et al., 2014; Yu et al., 2012). Hence, a negative feedback loop of miR-21 on TGFβ signaling is likely. However, in our samples, *TGFβR2* transcript was not statistically significantly regulated 5 days after the end of TGFβ1 stimulation.

Furthermore, some of the miRNAs we found regulated originate from host genes which were also regulated by TGFβ1 treatment. The first example is miR-21 which is located within *VMP1* (vacuole membrane protein 1). *VMP1* showed a trend for upregulation in TGFβ1 treated samples (FC = 1.3, p_{adj} = 0.0753), while miR-21 was clearly upregulated (Figure 11). The second example is miR-139, located within *PDE2A* (phosphodiesterase 2A), both downregulated after TGFβ1 treatment (*PDE2A* FC = -1.5, p_{adj} = 0.0094). The origin of two other intragenic miRNAs lies in *MYH* genes: miR-208b is located within *MYH7* and miR-499a in *MYH7B*. In TGFβ1-treated samples, both miRNAs were downregulated, the regulation of *MYH7* was not significant (FC = -1.5, p_{adj} = 0.1084) in the comparison TGFβ1-treated vs. vehicle-treated but reached clear significance in the comparison of TGFβ1 with TGFβ1 inhibitor compared to TGFβ1 alone (FC = 1.9, p_{adj} = 0.0011), and *MYH7B* was also downregulated (FC = -1.7, p_{adj} = 0.0029). It is not uncommon to find intragenic miRNAs, they are usually expressed with their host gene (Rodriguez et al., 2004) and can work supporting or antagonizing their host gene (Liu et al., 2018). In mice, it was shown that intragenic myosin miRNAs miR-208b and miR-499a are co-expressed and control myosin expression and muscle fiber type by repressing a variety of transcriptional repressors for slow myofiber genes (van Rooij et al., 2009). Thus, the fact that a miRNA is not expressed independently does not mean that it has no distinct function.

Additionally, there are miRNAs that are co-expressed with other miRNAs, in our case for example miR-206 and miR-133b. Located in an intergenic region the two miRNAs are separated by 4.5k bp, they are most likely co-expressed (Nohata et al., 2012). Another cluster of miRNAs, relevant in this thesis, is the cluster covering miR-143 and miR-145. Their locations in the genome are only separated by approximately 1500 bp and they lie within the same long non-coding RNA *MIR143HG* (microRNA-143 host gene) and are co-transcribed (Vacante et al., 2019). Synergistic effects of miR-143 and miR-145 were described in bladder cancer looking at the repression of PI3K/AKT and MAPK pathways (Noguchi et al., 2013). On the other hand, it has been shown in liver of mice that miR-143 and miR-145 don't have the same regulatory functions, as miR-143 inhibits insulin stimulated AKT activation but miR-145 does not (Jordan et al., 2011). In the case of the miR-143/145 cluster, a tissue specific function is likely.

Table 13. Overview of miRNAs regulated by TGFβ1 in different experiments.
Myoblasts underwent 1 ng/ml TGFβ1 stimulation for 48 h prior to differentiation for 5 days with 0% or 2% FBS to myotubes. Right column: Publications of other groups of the respective miRNA. ↑/↓ significantly up-/downregulated by TGFβ1 treatment, (↑)/(↓) trend for regulation, ↔ no regulation by TGFβ1.

miRNA	**Sequencing**	**qPCR**			
		Myoblasts	**Myotubes (0%FBS)**	**Myotubes (2%FBS)**	
miRNAs regulated in myoblasts and myotubes					**Regulated by TGFβ1 in other tissues**
miR-21	↑	↑	(↑)	↑	(Ong et al., 2017) human, lung fibroblasts
miR-31	↑	↑	↑	↑	(Hu et al., 2015) rat, liver cells
miR-143	↑	↑	↑	↑	(Cheng et al., 2014; Long and Miano, 2011)
					Human, lung cancer cell line; human, smooth muscle cells
miR-145	↑	↑	(↑)	↑	(Long and Miano, 2011) human, smooth muscle cells
miR-181a2	↑	↑	↑	↑	(Wang et al., 2011) human, breast cancer cell lines
miRNAs regulated only in myotubes (low expression level in myoblasts)					**Described function in skeletal muscle**
miR-133b	↓	↔	↓	↓	(Chen et al., 2006) C2C12 and Xenopus laevis embryo
miR-139	↓	↔	↓	↓	(Zhou et al., 2018) cattle
miR-146b	↓	↔	↓	↓	(Khanna et al., 2014) mouse
miR-206	↓	↔	↓	↓	(Goljanek-Whysall et al., 2012; Kim et al., 2006; Winbanks et al., 2011)
					C2C12; C2C12; C2C12 and primary mouse skeletal muscle cells
miR-208b	↓	↔	↓	(↓)	(Drummond et al., 2009; McCarthy et al., 2009) human; rat
miR-499a	↓	↔	↓	↓	(Liu et al., 2016; McCarthy et al., 2009) mouse; rat
miRNAs not confirmed in qPCR					
miR-708	↑	↔	↔	↑	-
miR-1294	↑	↔	↔	↔	-
mitosRNA	↓	↔	↓	↔	-

4.2 Influence of differentiation and differentiation medium on the effects of TGFβ1 on miRNAs, regulators of metabolism and targets of TGFβ1

As we used samples from myoblasts and differentiated myotubes for confirmation of sequencing data, we quickly realized, that myo-differentiation has an impact on some of the observed effects of TGFβ1. To thoroughly investigate the influence of differentiation on TGFβ1 effects, we additionally tested two differentiation media, with 2% FBS and without FBS.

4.2.1 Differentiation-dependent and -independent regulation of miRNAs by TGFβ1

When comparing the effect of TGFβ1 on miRNAs in myoblasts and myotubes differentiated without FBS, the investigated miRNAs can be divided into three groups (Table 13): miRNAs regulated directly in myoblasts and persistently regulated in myotubes; miRNAs with low expression levels in myoblasts are repressed by TGFβ1 in myotubes; and miRNAs of which we could not confirm regulation by TGFβ1 in qPCR. We did not find miR-708 and miR-1294 regulated in myoblasts or myotubes. For the mitosRNA, we saw a slight downregulation in myotubes differentiated without FBS, but not with 2% FBS, and the levels of samples treated with TGFβ1 and inhibitor did not differ from those treated with TGFβ1 alone. This left us with two groups of miRNAs regulated by TGFβ1: the differentiation-independent miRNAs miR-21, miR-31, miR-143, miR-145, and miR-181a2 which were upregulated by TGFβ1; and the differentiation-dependent miRNAs miR-133b, miR-139, miR-146b, miR-206, miR-208b, and miR-499a which are downregulated in myotubes after TGFβ1 treatment in myoblasts.

To gain a clear picture of differentiation effects on regulated miRNAs and other targets of TGFβ1, we investigated the time course of differentiation without treatment with TGFβ1. Differentiation-independent miRNAs were confirmed to not increase during differentiation (Figure 16A-E). In contrary, miR-31 showed a decrease throughout differentiation (Figure 16B). Differentiation-dependent miRNAs were confirmed to increase expression throughout differentiation (Figure 16H-M).

Interestingly, all differentiation-independent miRNAs have been described to be upregulated by TGFβ1 in other tissues, while all differentiation-dependent miRNAs have described roles in skeletal muscle development or differentiation (reference in Table 13).

4.2.2 Effects of myo-differentiation

Differentiation of myoblasts and fusion to myotubes is a highly regulated process, as e.g. reviewed in (Abmayr and Pavlath, 2012; Rochlin et al., 2010). It leads to an increase in myosins, e.g. *MYH1* and *MYH2* as shown in Figure 17, which can thus be used as transcriptional markers to follow the degree of differentiation.

Not only miRNAs, but also regulators of metabolism and targets of TGFβ1 showed clear changes during myo-differentiation. *PGC1α*, *CPT1B*, and *RRAGD* increased with the differentiation markers *MYH1* and *MYH2* (Figure 17). It has been shown that PGC1α expression is increased in differentiated myotubes in C2C12 cells (Fortini et al., 2016; Remels et al., 2010; Sin et al., 2016) and primary human myoblasts (Hoffmann et al., 2018). Since it is known, that mitochondrial capacity and activity increase during myo-differentiation (Fortini et al., 2016; Hoffmann et al., 2018; Sin et al., 2016) and PGC1α is a regulator of mitochondrial biogenesis, it is likely, that PGC1α is regulating increasing mitochondrial function during myo-differentiation (Duguez et al., 2002; Remels et al., 2010; Sin et al., 2016). PGC1α has further been shown to co-activate *Cpt1b* promoter in skeletal muscle of mice (Lau et al., 2004). Upregulation of *CPT1B* in myo-differentiation, supported by *PGC1α*, contributes to increasing mitochondrial substrate oxidation as *CPT1B* is an essential enzyme in β oxidation of fatty acids. *RRAGD* plays a critical role in the activation of mTOR1 by amino acids (Sancak et al., 2008). An increase of *RRAGD* thus could mean an increase in mTOR1 signaling which is needed for myoblast fusion (Kikani et al., 2019).

On protein level, we observed an increase of insulin-induced phosphorylation of threonine 308 of AKT relative to total AKT, as well as an increase in ATP5A with differentiation. In line with these results, it was shown that constitutive activation of AKT increases muscle mass in mice (Lai et al., 2004). Further, AKT has been shown necessary for skeletal muscle differentiation *in vitro* (Fujio et al., 1999; Rotwein and Wilson, 2009; Tureckova et al., 2001). The observed increase in ATP5A expression in differentiated myotubes is a measure of increased mitochondrial capacity, which is, as already mentioned above, also increasing during myo-differentiation (Fortini et al., 2016; Hoffmann et al., 2018; Sin et al., 2016).

Overall, an upregulation of AKT and mTOR pathways is in line with literature, as the IGF-AKT-mTOR pathway is known to positively regulate protein synthesis (Schiaffino et al., 2013), and protein synthesis is needed in restructuring differentiating cells towards contractile myotubes (Devlin and Emerson, 1978).

4.2.3 TGFβ1 and myo-differentiation

The inhibition of myo-differentiation by TGFβ1 was first described in 1986 (Massague et al., 1986; Olson et al., 1986). Since then, several mechanistic aspects of this inhibition have been elucidated. Vaidya et. al described reduced levels of *MyoD1* transcript, and demonstrated, that the loss of MyoD1 is not the sole cause for inhibition of differentiation, as constitutive *MyoD1* expression could not compensate the effects (Vaidya et al., 1989). Later this finding was confirmed, showing that the TGFβ1 effector SMAD3 directly represses *MyoD1* expression by DNA binding (Liu et al., 2001). In contrast, it was shown that TGFβ receptors are necessary for successful differentiation, independent of SMAD2 and SMAD3 molecules (Droguett et al., 2010). On the other hand, it was shown that

TGFβR2 misfunction also inhibits myo-differentiation (Filvaroff et al., 1994) and TGFβ1 is needed in high mitogen environment to induce differentiation (Zentella and Massague, 1992). Zentella and Massague used very low concentrations of TGFβ1 (0.06 ng/ml (5 pM) in contrast to 1 – 5 ng/ml used in all other mentioned studies), thus a dose-dependence as demonstrated in (Olson et al., 1986) where creatine kinase activity was higher in the lowest TGFβ1 concentration (0.125 ng/ml estimated from graph) than in control cells, is very plausible. In this case, the half-maximal repression of TGFβ1 was reported at 0.5 ng/ml and the maximal repression at 1 ng/ml (Olson et al., 1986). Hence, low concentrations of TGFβ1 might be necessary for myo-differentiation, however, high concentrations of TGFβ1 (1 ng/ml and higher) inhibit differentiation in murine, porcine, and human myoblasts.

An increase in MyoD degradation and decrease of myogenin expression was shown by Schabort et al. who further showed that TGFβ treatment prevents cell cycle exit and thus blocks myoblast differentiation (Schabort et al., 2009). Another study concerning the inhibition of cell cycle arrest has shown continued expression of TWIST2 after TGFβ1 treatment (Murakami et al., 2008). In our samples *TWIST2* expression was not significantly different in TGFβ1 treated samples.

Another described mechanism is the upregulation of myostatin (*MSTN*) by TGFβ1 (Budasz-Rwiderska et al., 2005) which in turn leads to downregulation of MyoD and inhibits differentiation (Langley et al., 2002). In our experiments, *MSTN* transcript was upregulated (FC = 1.5, $p_{adj} = 0.0016$) 5 days after end of TGFβ1 stimulation. Myostatin is a profound inhibitor of muscle growth (McPherron et al., 1997).

Lastly, Winbanks et al. showed, that TGFβ1 inhibits myo-differentiation via miR-206 and miR-29 both also downregulating HDAC4 independent of TGFβ1 (Winbanks et al., 2011). *HDAC4* transcript was slightly decreased in TGFβ1-treated samples in our experiments, 5 days after end of TGFβ1 stimulation (Figure 8). As TGFβ1 seems to lead to a broad range of differentially regulated transcripts potentially responsible for the inhibition of myo-differentiation, the regulation is most likely very complex and depends on many variables. In contrast to most studies, we investigated the effects of TGFβ1 5 days after induction of myo-differentiation, which, however, still leads to clearly reduced expression of differentiation markers (Figure 7).

4.2.4 TGFβ1-regulated miRNAs and myo-differentiation

As described before, differentiation-dependent miRNAs are all described skeletal muscle miRNAs (references in Table 13). Thus, we hypothesized, that TGFβ1 suppresses differentiation-dependent miRNAs that are necessary for myo-differentiation. In this case, supplementing TGFβ1-treated myoblasts with the missing miRNAs during differentiation can potentially compensate the effects if they are caused by inhibited differentiation.

To test if the effects of TGFβ1 on regulators or metabolism are regulated via the downregulation of differentiation-mediated miRNAs, we transfected miRNA mimics on day 1 of differentiation to simulate the endogenous increase during myo-differentiation (Figure 16) and give enough time for miRNA mimics to act. However, we could not recover any of the effects induced by TGFβ1 by supplementation with a mix of miRNA mimics (Figure 22, Figure 23).

As discussed above, miR-206, one of the miRNAs used in the miRNA mimics mix, has been shown to be downregulated by TGFβ1 (Winbanks et al., 2011) and the inhibition of myo-differentiation caused by TGFβ1 stimulation could be counteracted by supplementing with miR-206 mimics by Winbanks et al.. The study investigated acute effects, while we investigated effects on day 5 of differentiation. Furthermore, experimental conditions, such as the concentration of used miRNA mimics and the use of controls, differed from our investigations. This will be discussed in more detail in chapter 4.4.1 Importance of controls.

On the other hand, inhibition of myo-differentiation could be caused by miRNAs upregulated by TGFβ1. Elevation of miR-31 by miRNA mimics has been shown to inhibit differentiation in C2C12 cells (Liu et al., 2017). This is in line with decreasing miR-31 expression throughout myo-differentiation in our results. Thus, the effects of TGFβ1 on differentiation could also be regulated via miR-31. In this case, transfection of miR-31 mimics would lead to the same effects as TGFβ1 stimulation regardless of direct effect of miR-31 on regulators of metabolism or an indirect effect due to decreased differentiation.

However, when transfecting miRNA mimics preconfluently, before differentiating for 5 days, we did not find inhibitory effects of miR-31, miR-143 or miR-145 on differentiation (measured by *MYH1* and *MYH2* transcript and protein levels). These findings are in contrast to (Liu et al., 2017), who showed inhibition of differentiation by miR-31 mimics in C2C12 cells. Then again, Liu at al. investigated effects 48 h after transfection with miR-143 mimics while we looked at cells after 5 days of differentiation. We cannot exclude that we would have seen an inhibition of differentiation by miR-31 mimics 48 h after transfection.

Summarizing, we did not find an influence of any of the used miRNA mimics on myo-differentiation, not by compensation of TGFβ1-downregulated miRNAs, nor by transfection of TGFβ1-upregulated miRNAs.

4.2.5 Influence of used differentiation medium

As described in (Hoffmann et al., 2018), differentiation without FBS reduces the number of non-differentiated myocytes and increases the abundance of muscle-specific proteins such as MYH1, 2, and 7 more efficiently than differentiation with 2% FBS. Thus, differentiation without FBS lead to a

cleaner culture than differentiation with 2% FBS, containing nearly no undifferentiated cells (Hoffmann et al., 2018).

When comparing the expression of miRNAs in myotubes differentiated with 2% FBS or without FBS, differentiation-independent miRNAs did not differ in their response to TGFβ1. Whereas the differentiation-dependent miRNAs showed more pronounced downregulation by TGFβ1 (smaller p-value TGFβ1 vs. vehicle-treated) with the FBS-free medium (Figure 15). With the exception of miR-146b (Figure 15H), it seems, that the cause for the changes in p-value when differentiating with or without 2% FBS depend on changes of expression levels of the miRNAs during myo-differentiation. The miRNAs miR-133b, miR-139, miR-208b, and miR-499b were more abundant after differentiation without FBS (Figure 14). This is well in accordance with the cleaner differentiation observed when differentiating without FBS as published in (Hoffmann et al., 2018).

In conclusion, the RNA expression pattern comparing the two differentiation media (Figure 14, Figure 15) confirmed the published improved differentiation method from (Hoffmann et al., 2018).

4.3 Regulation of PGC1α and other metabolic regulators by TGFβ1

4.3.1 Is the effect of TGFβ1 mediated by miRNAs?

If the effects of TGFβ1 on regulators of metabolism are regulated via the upregulation of miRNAs, transfecting these miRNAs alone should induce the same effects on regulators of metabolism as TGFβ1. To test this hypothesis, we transfected cells preconfluently with 10 nM miRNA mimics of miR-31, miR-143, and miR-145, which were all upregulated by TGFβ1 treatment. Subsequently, myoblasts were differentiated to myotubes for 5 days. We saw clear Cy3 expression in cells transfected with Cy3 control and detected strongly (>> 100x) increased miRNA levels in transfected cells. However, the positive control miR-122 did not lead to a reduction in *ALDOA* transcript levels, neither did we find a reduction of *IGFBP5* by miR-143 (Figure 24) as described in (Soriano-Arroquia et al., 2016). The most described pathway of miRNA action involves degradation of mRNA and thereby preventing translation (Jonas and Izaurralde, 2015). It is thus possible, that the effects of the investigated miRNAs mainly affect translation and the effects are therefore not visible on transcriptional level. We tested three commercially available antibodies against IGFBP5 without a clear signal corresponding success and were therefore not yet able to test the effects of miR-143 on IGFBP5 on protein level.

We did not find inhibitory effects of miR-31, miR-143 or miR-145 on PGC1α transcript or ORP8 protein. As clear effects of overexpression of miR-143 on insulin-induced phosphorylation (Thr308 and Ser473) of AKT were demonstrated in liver cells of mice (Jordan et al., 2011), and vascular smooth muscle cells (Blumensatt et al., 2014), and a mechanism via ORP8 was described (Blumensatt et al., 2014; Jordan et al., 2011), we were surprised to not find effects of miR-143 mimic on ORP8 or

p-AKT(Thr308). In our experiment, ORP8 protein levels were very stable. In contrast to (Jordan et al., 2011), who found nearly no expression of ORP8 in skeletal muscle in mice, ORP8 was clearly expressed in primary human myotubes in our experiments.

In contrast to the negative results using miR-143 mimics, we found a significant reduction of insulin-induced phosphorylation of threonine 308 of AKT in cells transfected with miR-31 mimic. As demonstrated in (Gottmann et al., 2018), miR-31 mimic decreases expression of transcripts of insulin signaling, e.g. *IRS1* (insulin receptor substrate 1) and *GLUT4* in human adipocytes. This is in line with our finding of a decrease in insulin-induced phosphorylation of AKT (Thr308) in myotubes transfected with miR-31 mimics. In their experiments, (Gottmann et al., 2018) used 20 nM, while we used 10 nM miR-31 mimics for transfection. It is possible, that the effect would be clearer if we increased the concentration of transfected miRNA mimics.

10 µM insulin was used to stimulate cells in all experiments, a concentration above the physiological concentration, which is expected to maximally stimulate insulin receptor-mediated downstream signaling events (Sarabia et al., 1992). It is possible, that the used concentration was too high to detect sensitive differences between samples. Further experiments will compare lower insulin concentrations in the submaximal range. Nevertheless, we did not find ORP8 regulated, thus, the pathway suggested by (Jordan et al., 2011) is, as discussed above, not affected in our experiments, independent of the used insulin concentration. With regard to the effects of other tested miRNA mimics on the insulin-dependent phosphorylation of AKT, it is possible that we might have missed some effects.

4.3.2 Regulation of PGC1α and other metabolic regulators by TGFβ1

When looking at the results of long RNA sequencing, mitochondrial proteins and regulators, as well as mitochondrially encoded transcripts were decreased in TGFβ1-treated cells. The effects were reversible by additional introduction of the TGFβ1 inhibitor SB431542 (10 nM). These results are in line with previous publications of our group (Bohm et al., 2016a) where TGFβ1 stimulation decreased *PGC1α* expression and expression of other regulators of metabolism such as *HADHA (*hydroxyacyl-CoA dehydrogenase trifunctional multienzyme complex subunit alpha), *CTP1B*, *TFAM* (transcription factor A, mitochondrial) or *PRKAA2*. Here we showed that the effects on *PGC1α* expression persist 5 days after the end of TGFβ1 stimulation.

Additionally, we found all transcripts of mitochondrially encoded subunits of the respiratory chain downregulated in TGFβ1 treated cells. In (Bohm et al., 2016a), it was shown that TGFβ1 suppresses mitochondrial regulators and enzymes such as ATP5A. Moreover, published in (Hoffmann et al., 2018), we showed that TGFβ1 leads to a lower mitochondrial content in myoblasts and possibly more important, that myo-differentiation increases mitochondrial content. Thus, by inhibiting differentiation, TGFβ1 will inhibit the increase of mitochondrial content accordingly, additional to the direct reduction of mitochondrial content due to TGFβ1 treatment of myotubes.

These results are in line with studies by other groups, all investigating acute effects of TGFβ1 on different cells, tissues, or organisms. In the comparison of cells from various tissues of murine and human origin, It was shown that the KEGG pathway “metabolic pathways” is commonly downregulated by TGFβ1 (Abnaof et al., 2014). The necessity of mitochondrial regulation for fibrotic effects of TGFβ1 has been discussed in (Jain et al., 2013), showing that reactive oxygen species (ROS) generated from complex III of the mitochondrial respiratory chain are needed for TGFβ1-induced gene expression in fibroblasts.

Tiano et al. demonstrated a mechanism of TGFβ1 to inhibit PGC1α via SMAD3 in myotubes (Tiano et al., 2015). SMAD3 directly occupies promoter regions of *PGC1α* and the irisin precursor *FNDC5* (fibronectin type III domain containing 5). In their experiments, they either examined acute effects of TGFβ1 in C2C12 cells differentiated for 3 days before initiating 48 h of TGFβ1 stimulation or continuous stimulation during differentiation for 4 days (Tiano et al., 2015). In contrast, we investigated effects when only stimulating in undifferentiated myoblasts prior to differentiation for 5 days and used primary human skeletal muscle cells. Since binding of SMAD3 to the promoter regions of PGC1α requires the TGFβ1-dependent phosphorylation of SMAD3, which is an acutely regulated transient mechanism, this might not explain the observed effects in our study, but only the shorter-term effects of TGFβ1 after 24 – 48 h.

4.3.3 *PPARGC1A* promoter methylation is not affected by TGFβ1 stimulation

Most CpG sites in the mammalian genome are methylated except for CpG islands, which are usually localized upstream of transcription start sites of genes. When CpG islands of promoter regions are methylated, transcription can be suppressed (Weber et al., 2007). Therefore, we investigated promoter methylation of the *PPARGC1A* gene in TGFβ1-treated myotubes, to examine whether the prolonged effect of TGFβ1 on PGC1α was due to hypermethylation of the PGC1α promoter.

We studied 229 CpG sites in four different promoter regions of the *PPARGC1A* promoter. Methylation sites of the *PPARGC1A* promoter that are frequently discussed to be regulated und to influence transcription of the gene are all located in the canonical promoter as described in results. They were all unchanged by TGFβ1 treatment in our samples.

We detected a low methylation grade in the canonical and brain promoter (5.7% and 5.2% respectively) and a higher overall percentage of methylation in alternative (22.4%) and liver promoter (39.6%). This is surprising, since a low grade of methylation generally equals to a high use of the respective promoter for transcription, and the brain promoter is not described to be commonly used in skeletal muscle cells (Popov et al., 2015). Furthermore, while the canonical promoter is continuously active in skeletal muscle, the alternative promoter is the promoter described to be most influenced in skeletal muscle, e.g. by acute exercise, (Popov et al., 2015) and showed a methylation grade of about 22% in our samples, unaffected of TGFβ1 treatment.

Changes in promoter methylation of the canonical *PPARGC1A* promoter in skeletal muscle in humans have been described in several conditions, e.g. acute exercise (Barres et al., 2012), in high fat feeding in humans with normal birth weight compared to low birth weight (Brons et al., 2010), and in first degree relatives of type 2 diabetics (Gillberg et al., 2013). However, Brons et al. and Gillberg et al. (Brons et al., 2010; Gillberg et al., 2013) both did not find a correlation of *PPARGC1A* transcript expression and *PPARGC1A* promoter methylation in skeletal muscle of humans, allowing the speculation, that *PPARGC1A* promoter methylation is not as central in the regulation of mRNA expression *in vivo* as others have suggested. (Popov et al., 2015) describe a constant "basal" expression by the canonical promoter and a variable expression, e.g. induced by acute exercise, by the alternative promoter, not looking at methylation but only at expressed isoforms of PGC1α.

As we could not find differences in methylation status in our samples, we conclude that the observed prolonged effect of TGFβ1 on PGC1α is not transmitted by *PPARGC1A* promoter methylation in our experiments.

4.4 Experimental consideration about transfecting miRNA mimic into skeletal muscle cells

4.4.1 Importance of controls

In the positive control *MEOX2*, which is described to be regulated by miR-206, we saw a decrease of expression level in TGFβ1-treated cells in negative control mimic-treated but not in miRNA mimic mix treated cells (Figure 21). When transfecting only miR-206, the concentration seemed pivotal: 1 nM miR-206 had no effect on *MEOX2*, 10 nM miR-206 showed a trend of reduction of *MEOX2*. The 5 nM mimics mix contained 1.25 nM miR-206 mimic, thus, possibly not enough to reduce *MEOX2* expression directly, but enough to compensate the negative effect of TGFβ1 on *MEOX2*. It is therefore likely, that the used concentration of miRNA mimics mix was too low to detect effects on the investigated transcripts and proteins. (Winbanks et al., 2011) successfully compensated effects of TGFβ1 on HDAC4 by substituting with miR-206 mimic. They used a concentration of 200 nM miRNA mimic and stimulated primary murine cells or C2C12 cells with 5 ng/ml TGFβ1. However, they did not investigate prolonged effects and found differences only on protein level. One major drawback of their study is the lack of negative control mimics, all reported data are compared to untreated controls. It is likely, that a treatment with 200 nM miRNA mimic, regardless of the specific sequence, will lead to changes in cells including cell death (Jin et al., 2015) or influence myo-differentiation. As shown in Figure 29, transfecting 10 nM miRNA mimics or negative control miRNA reduces the abundance of *MYH1* irrespective of the used miRNA.

We used a mix of miRNA mimics as we wanted to compensate for the broad suppression of miRNAs by TGFβ1. The choice of miRNAs was based on the two top downregulated miRNAs, miR-499a (FC = -4.42 in DEUS analysis) and miR-208b (FC = -3.51 in DEUS analysis), plus the two miRNAs well

described in skeletal muscle and regulated by TGFβ1 treatment, miR-133b (FC = -1.84 in DEUS analysis) and miR-206 (FC = -1.38 in DEUS analysis). Alternatively, or additionally, we could have used more top downregulated miRNAs, e.g. the next two in the list, miR-146b (FC = -2.34 in DEUS analysis) and miR-139 (FC = -2.13 in DEUS analysis). The complex regulations of myo-differentiation, and especially the involvement of regulatory miRNA networks, are not fully uncovered. However, using the most regulated miRNAs and supplementing with two miRNAs that were also regulated and have essential roles in development and regeneration of skeletal muscle, is likely to include relevant miRNAs. In the future, experiments with a miRNA mimics mix containing six miRNAs, the four we used here, plus miR-146b and miR-139, will be investigated. Furthermore, a higher concentration of miRNA mimic mix will be evaluated, of course carefully keeping unspecific effects in mind and always in comparison to the same load of negative control mimic.

4.4.2 C2C12 vs. human skeletal muscle cells: TGFβ1 does not lead to the same effects

Overall, the results of our experiments transfecting miRNA mimics into primary cells were not as clear as hoped for. Several effects of investigated miRNAs were described by other groups, but we could not reproduce them in primary skeletal muscle cells as discussed above. As another approach, we aimed to use a pre-miRNA-containing vector to circumvent potential limitations of transfecting high concentrations of miRNAs. For transfection of vectors without the need to use viral transduction, we decided to change model system to the most common skeletal muscle cell line, C2C12, a murine immortalized cell line.

To investigate, whether C2C12 cells express the same miRNAs and if TGFβ1 will lead to a regulation of these miRNAs, we stimulated C2C12 cells with TGFβ1. We expected effects on *Ppargc1a* and differentiation markers *Myh2* and *Myh7*, like the reduction we observed in human primary myotubes and expected similar effects on miRNAs. However, we did not find a clear regulation. *Ppargc1a*, *Myh2* or *Myh7* expression levels did not significantly differ between TGFβ1 and vehicle-treated samples. *Tgfbi* was not increased by TGFβ1 stimulation. The lack of increasing *Tgfbi* levels in C2C12 cells was observed in our lab before by other investigators (unpublished data). Nevertheless, we saw increases of PGC1α transcript, *Myh2*, *Myh7* with myo-differentiation as expected. Furthermore, all differentiation-dependent miRNAs showed very low expression in myoblasts (Figure 26).

We used human TGFβ1, as the mature protein shares 99% identity with murine Tgfβ1. Recombinant human TGFβ1 has been used in stimulation studies in C2C12 cells or murine primary cells (Figueroa and Hayman, 2004; Murakami et al., 2008; Winbanks et al., 2011) and it is unlikely that the use of human recombinant TGFβ1 is the reason for a lack of observed effects in our experiment.

Other groups that have stimulated C2C12 cells with TGFβ1 and found an inhibition of differentiation markers like the one we observed in primary human cells. For example, (Figueroa and Hayman, 2004)

stimulated C2C12 cells with 1 ng/ml TGβ1 and saw a clear reduction in MYH1/2 protein. However, they simultaneously changed to differentiation medium and started TGFβ1 stimulation, while we either first stimulated with TGFβ1 before differentiation start or only started TGFβ1 stimulation on day 3 of differentiation, when most cells are already fused to myotubes. In a similar experiment, (Winbanks et al., 2011) also induced differentiation at the same time as TGFβ1 treatment. They stimulated C2C12 cells for 48 h with 5 ng/ml TGFβ1, compared to 1 ng/ml in our experiments. They showed decreased levels of miR-206 and miR-133b in TGFβ1-treated compared to control-treated cells, in line with our observations in primary human myotubes (Figure 13F, I). Tiano et al. stimulated C2C12 cells as myotubes after 3 days of differentiation with TGFβ1 for 24 h and showed a clear reduction of *PGC1α* transcript in TGFβ1 treated cells (Tiano et al., 2015). Their experiment is comparable to ours, we also differentiated C2C12 cells for 3 days before stimulating them with 1 ng/ml TGFβ1 for 48 h, but we observed only a trend for less *PGC1α* transcript in TGFβ1-treated samples (Figure 26A).

We currently have no explanation why C2C12 cells do not show prolonged effects on PGC1α as expected. First transfection experiments using vectors containing pre-miRNAs did not show effects on the investigated transcripts and proteins and were not pursued further after identifying the lack of prolonged inhibition of PGC1α transcript in C2C12 cells to TGFβ1 treatment.

4.4.3 miRNA mimics - opportunities and weaknesses

As explained earlier, we wanted to transfect primary human myoblasts with miRNAs without using viral transduction of vectors. Thus, we used miRNA mimics, which possess the sequence of the respective mature miRNA.

To circumvent overload with RNA species, we aimed to use low miRNA concentrations. In the manufacturer's protocol, 50 nM miRNA mimics are recommended (Qiagen). Using 5 nM and 10 nM miRNA mimics, we assumed to work well under the limit for toxic side effects, as many groups use higher concentrations, and we still detected plain increases of miRNA levels in cells (Figure 19).

The use of miRNA mimics has been criticized to lead to unspecific effects, meaning miRNA mimics with a random sequence could also cause effects, and the use of lentiviral transduction of pre-miRNA-containing plasmids was shown to affect targets at much lower measurable concentrations of mature miRNA (Jin et al., 2015). The main difference between the two systems is the maturity state of the delivered miRNA. In lentiviral transductions pre-miRNAs, in the form of stem loop miRNAs, are used, while miRNA mimics are built of the mature miRNA sequence complemented by a passenger strand that is usually chemically stabilized. The processing of stem loop miRNAs to functional mature miRNAs involves several steps and enzymes as reviewed in (Creugny et al., 2018). It is thus possible, that the processing of miRNAs already plays a role for their effects and the transfection of mature miRNAs, like miRNA mimics, would bypass parts of the miRNA machinery.

Furthermore, passenger strands of miRNA mimics accumulate in the cells and potentially lead to unspecific effects (Jin et al., 2015; Sokilde et al., 2015). Additionally, biologically inactive miRNA mimics could explain the lack of clear effects, expected from a robust biological activity of the transfected miRNA mimics. It is possible, that big parts of miRNA mimics are not active in the cytoplasm but packed into cellular vesicles and thereby inactivated (Thomson et al., 2013). To exclude unspecific effects, all our results were studied in relation to control miRNA mimic and not untreated control. Comparing to untreated control would often have led to misleading effects as shown in Figure 29.

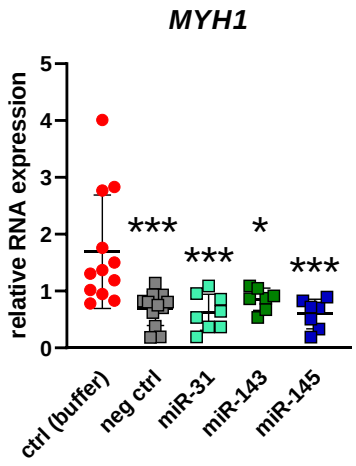

Figure 29. Transfection of miRNA mimics leads to unspecific effects.
This is the same graph as shown in Figure 25A but with the additional dataset of untreated control (buffer). Primary human myoblasts (n = 8-12) were transfected with miR-31, miR-143, miR-145 or negative control mimics for 24 h before confluence and subsequently differentiated for 5 days. Quantification of qPCR results. Data are displayed as symbols for individual values with mean ± SD. miR-31, miR-143, miR-145 mimic, and negative control mimic suppress *MYH1* transcript when comparing to untreated control. All mRNA data normalized to donor and reference genes *TBP* and *RPS13*. One-way ANOVA with Dunnett's multiple comparisons test comparing to untreated control.

Taking this together with the results of the transfection with miRNA mimics mix discussed above, the concentration of miRNA mimics we used might have been too low to induce significant effects. It could therefore be worthwhile to try higher miRNA mimic concentrations, e.g. 20 nM as used in (Gottmann et al., 2018), or even 50 nM as recommended by Qiagen. It was our aim to use as little miRNA mimic as possible, and we did find strongly increased levels of miRNAs in our cells. On the other hand, if the bulk of miRNA mimics is inactivated inside vesicles, a higher concentration might lead to more active miRNA in the cell. It would be useful to test higher concentrations, always cautiously comparing to cells treated with negative control mimics.

4.5 Outlook and conclusion

Interestingly, many of the miRNAs we found regulated by TGFβ1 have been described to be affected by exercise, including differentiation-independent and differentiation-dependent miRNAs. Described circulating microRNAs in exercise that were regulated by TGFβ1 in our experiments are miR-21, miR-133b, miR-143, miR-145, miR-146, miR-206, and miR-499 (Sapp et al., 2017). However, the evidence is contradictory, underlining the complexity of the issue. For example, circulating miR-21 levels in blood of healthy males with low aerobic fitness (measured as VO_{2peak}) were increased compared to healthy males with high aerobic fitness (Bye et al., 2013). On the other hand, circulating miR-21 was shown to increase after acute bouts of exercise (Baggish et al., 2011; Xu et al., 2016), but be decreased 30 minutes after the end of exercise (Kilian et al., 2016). Furthermore, increases in circulating miR-21 after an acute bout of exercise were shown to be higher in obese subjects than in lean controls (Bao et al., 2018). Looking at the differentiation-dependent miR-133b as an example, a study comparing uphill (concentric) and downhill (eccentric) running found circulating miR-133b upregulated only in early recovery of downhill running (Banzet et al., 2013). Contrasting, circulating miR-133b was shown decreased after high intensity cycling (Cui et al., 2015) and increased after high intensity running (Cui et al., 2016).

We do not know the origin of the published circulating miRNAs, but there is a possibility that they origin from muscle tissue, maybe induced by TGFβ1. The fact that these miRNAs circulate in the blood stream opens new possibilities for the mechanism how TGFβ1 inhibits insulin sensitivity in non-responders. Possibly, circulating miRNAs influence other tissues, for example liver or adipose tissue. It has been shown, that miR-143 impairs insulin signaling in liver, more precisely the phosphorylation of AKT after insulin stimulation (Jordan et al., 2011), and in fat, miR-31 mimics suppressed important transcripts of insulin signaling *IRS1* and *GLUT4* (Gottmann et al., 2018). Thus, one very speculative hypothesis is that impaired response in insulin sensitivity after a training intervention is the result of an interplay between organs, caused by circulating miRNAs which possibly originate from dysregulated TGFβ1 signaling in skeletal muscle after exercise. In smooth muscle, the role of TGFβ1 seems to be very different. TGFβ1 is needed for differentiation of smooth muscle cells (Coletta et al., 2018; Valcourt et al., 2005) and this process involves miR-143 and miR-145 (Avalle et al., 2017). This could be part of a beneficial TGFβ1 response after exercise, since training improves cardiac output (Ellison et al., 2012), possibly supported by TGFβ1 induced cardiomyocyte differentiation. Thus, complete inhibition of TGFβ1 signaling would not be a perfect solution as it might have side effects, e.g. inhibited cardiomyocyte differentiation.

Another angle is to look at investigated animal models. Amongst full body miRNA mouse knock-out models of the miRNAs we found regulated by TGFβ1, only miR-143 has a published phenotype. Homozygous miR-143 knock-out was lethal while heterozygous mice did not show a significant

phenotype in any of the screened parameters (International Mouse Phenotyping Consortium, 2020). Thus, one intact allele most likely can compensate the loss in heterozygous mice.

To name another animal study, in pigs, comparing animals with high lean mass to animals with lower lean mass within three different breeds, several differentiation-dependent miRNAs were detected differentially regulated, namely miR-146b, miR-206, and miR-499a. Furthermore, TGFβ1 signaling was deregulated in the comparison (Ropka-Molik et al., 2018). This is in line with our hypothesis that dysregulated TGFβ1 signaling affects muscle tissue negatively, and likely contributing to non-response in exercise.

To summarize, TGFβ1 regulates miRNAs in skeletal muscle and their role in regulating metabolism is possible but the mechanisms remain unknown. Based on research from other fields and laboratories, a role of miRNAs in non-response to exercise is possible. With our results of TGFβ1-induced miR-31 suppressing phosphorylation threonine 308 of AKT, we contribute another small part to the understanding of this complex regulation.

5 References

Abmayr, S.M., and Pavlath, G.K. (2012). Myoblast fusion: lessons from flies and mice. Development *139*, 641-656.

Abnaof, K., Mallela, N., Walenda, G., Meurer, S.K., Sere, K., Lin, Q., Smeets, B., Hoffmann, K., Wagner, W., Zenke, M., *et al.* (2014). TGF-beta stimulation in human and murine cells reveals commonly affected biological processes and pathways at transcription level. BMC Syst Biol *8*, 55.

AbouAssi, H., Slentz, C.A., Mikus, C.R., Tanner, C.J., Bateman, L.A., Willis, L.H., Shields, A.T., Piner, L.W., Penry, L.E., Kraus, E.A., *et al.* (2015). The effects of aerobic, resistance, and combination training on insulin sensitivity and secretion in overweight adults from STRRIDE AT/RT: a randomized trial. Journal of applied physiology (Bethesda, Md : 1985) *118*, 1474-1482.

Abrigo, J., Simon, F., Cabrera, D., Cordova, G., Trollet, C., and Cabello-Verrugio, C. (2018). Central Role of Transforming Growth Factor Type Beta 1 in Skeletal Muscle Dysfunctions: An Update on Therapeutic Strategies. Curr Protein Pept Sci *19*, 1189-1200.

Ahlborg, B., Bergström, J., Ekelund, L.-G., and Hultman, E. (1967). Muscle Glycogen and Muscle Electrolytes during Prolonged Physical Exercise1. Acta Physiologica Scandinavica *70*, 129-142.

Allen, R.E., and Boxhorn, L.K. (1987). Inhibition of skeletal muscle satellite cell differentiation by transforming growth factor-beta. J Cell Physiol *133*, 567-572.

Allen, R.E., and Boxhorn, L.K. (1989). Regulation of skeletal muscle satellite cell proliferation and differentiation by transforming growth factor-beta, insulin-like growth factor I, and fibroblast growth factor. J Cell Physiol *138*, 311-315.

Ambros, V. (2004). The functions of animal microRNAs. Nature *431*, 350-355.

American Diabetes Association (2014). Diagnosis and Classification of Diabetes Mellitus (American Diabetes Association), pp. S81-S90.

Avalle, L., Incarnato, D., Savino, A., Gai, M., Marino, F., Pensa, S., Barbieri, I., Stadler, M.B., Provero, P., Oliviero, S., *et al.* (2017). MicroRNAs-143 and -145 induce epithelial to mesenchymal transition and modulate the expression of junction proteins. Cell Death Differ *24*, 1750-1760.

Baggish, A.L., Hale, A., Weiner, R.B., Lewis, G.D., Systrom, D., Wang, F., Wang, T.J., and Chan, S.Y. (2011). Dynamic regulation of circulating microRNA during acute exhaustive exercise and sustained aerobic exercise training. The Journal of Physiology *589*, 3983-3994.

Bajpeyi, S., Tanner, C.J., Slentz, C.A., Duscha, B.D., McCartney, J.S., Hickner, R.C., Kraus, W.E., and Houmard, J.A. (2009). Effect of exercise intensity and volume on persistence of insulin sensitivity during training cessation. Journal of applied physiology (Bethesda, Md : 1985) *106*, 1079-1085.

Banzet, S., Chennaoui, M., Girard, O., Racinais, S., Drogou, C., Chalabi, H., and Koulmann, N. (2013). Changes in circulating microRNAs levels with exercise modality. J Appl Physiol *115*, 1237-1244.

Bao, F., Slusher, A.L., Whitehurst, M., and Huang, C.J. (2018). Circulating microRNAs are upregulated following acute aerobic exercise in obese individuals. Physiol Behav *197*, 15-21.

Barash, I.A., Mathew, L., Ryan, A.F., Chen, J., and Lieber, R.L. (2004). Rapid muscle-specific gene expression changes after a single bout of eccentric contractions in the mouse. Am J Physiol Cell Physiol *286*, C355-364.

Barres, R., Yan, J., Egan, B., Treebak, J.T., Rasmussen, M., Fritz, T., Caidahl, K., Krook, A., O'Gorman, D.J., and Zierath, J.R. (2012). Acute exercise remodels promoter methylation in human skeletal muscle. Cell Metab *15*, 405-411.

Barres, R., and Zierath, J.R. (2016). The role of diet and exercise in the transgenerational epigenetic landscape of T2DM. Nature reviews Endocrinology *12*, 441-451.

Bartel, D.P. (2004). MicroRNAs: genomics, biogenesis, mechanism, and function. Cell *116*, 281-297.

Bergstrom, J., Hultman, E., and Roch-Norlund, A.E. (1972). Muscle glycogen synthetase in normal subjects. Basal values, effect of glycogen depletion by exercise and of a carbohydrate-rich diet following exercise. Scand J Clin Lab Invest *29*, 231-236.

Bernasconi, P., Di Blasi, C., Mora, M., Morandi, L., Galbiati, S., Confalonieri, P., Cornelio, F., and Mantegazza, R. (1999). Transforming growth factor-beta1 and fibrosis in congenital muscular dystrophies. Neuromuscul Disord *9*, 28-33.

Birnbaum, M.J. (1989). Identification of a novel gene encoding an insulin-responsive glucose transporter protein. Cell *57*, 305-315.

Bjorntorp, P. (1990). "Portal" adipose tissue as a generator of risk factors for cardiovascular disease and diabetes. Arteriosclerosis *10*, 493-496.

Bjorntorp, P., Fahlen, M., Grimby, G., Gustafson, A., Holm, J., Renstrom, P., and Schersten, T. (1972). Carbohydrate and lipid metabolism in middle-aged, physically well-trained men. Metabolism *21*, 1037-1044.

Blau, H.M., and Webster, C. (1981). Isolation and characterization of human muscle cells. Proc Natl Acad Sci U S A *78*, 5623-5627.

Blumensatt, M., Wronkowitz, N., Wiza, C., Cramer, A., Mueller, H., Rabelink, M.J., Hoeben, R.C., Eckel, J., Sell, H., and Ouwens, D.M. (2014). Adipocyte-derived factors impair insulin signaling in differentiated human vascular smooth muscle cells via the upregulation of miR-143. Biochim Biophys Acta *1842*, 275-283.

Bohm, A., Hoffmann, C., Irmler, M., Schneeweiss, P., Schnauder, G., Sailer, C., Schmid, V., Hudemann, J., Machann, J., Schick, F., *et al.* (2016a). TGF-beta Contributes to Impaired Exercise Response by Suppression of Mitochondrial Key Regulators in Skeletal Muscle. Diabetes *65*, 2849-2861.

Bohm, A., Weigert, C., Staiger, H., and Haring, H.U. (2016b). Exercise and diabetes: relevance and causes for response variability. Endocrine *51*, 390-401.

Borel, A.L., Nazare, J.A., Smith, J., Almeras, N., Tremblay, A., Bergeron, J., Poirier, P., and Despres, J.P. (2012). Improvement in insulin sensitivity following a 1-year lifestyle intervention program in viscerally obese men: contribution of abdominal adiposity. Metabolism *61*, 262-272.

Bouchard, C., Blair, S.N., Church, T.S., Earnest, C.P., Hagberg, J.M., Hakkinen, K., Jenkins, N.T., Karavirta, L., Kraus, W.E., Leon, A.S., *et al.* (2012). Adverse metabolic response to regular exercise: is it a rare or common occurrence? PloS one *7*, e37887.

Boule, N.G., Weisnagel, S.J., Lakka, T.A., Tremblay, A., Bergman, R.N., Rankinen, T., Leon, A.S., Skinner, J.S., Wilmore, J.H., Rao, D.C., *et al.* (2005). Effects of exercise training on glucose homeostasis: the HERITAGE Family Study. Diabetes care *28*, 108-114.

Brennan, T.J., Edmondson, D.G., Li, L., and Olson, E.N. (1991). Transforming growth factor beta represses the actions of myogenin through a mechanism independent of DNA binding. Proc Natl Acad Sci U S A *88*, 3822-3826.

Brons, C., Jacobsen, S., Nilsson, E., Ronn, T., Jensen, C.B., Storgaard, H., Poulsen, P., Groop, L., Ling, C., Astrup, A., *et al.* (2010). Deoxyribonucleic acid methylation and gene expression of PPARGC1A in human muscle is influenced by high-fat overfeeding in a birth-weight-dependent manner. J Clin Endocrinol Metab *95*, 3048-3056.

Budasz-Rwiderska, M., Jank, M., and Motyl, T. (2005). Transforming growth factor-beta1 upregulates myostatin expression in mouse C2C12 myoblasts. J Physiol Pharmacol *56 Suppl 3*, 195-214.

Bye, A., Røsjø, H., Aspenes, S.T., Condorelli, G., Omland, T., and Wisløff, U. (2013). Circulating MicroRNAs and Aerobic Fitness – The HUNT-Study. PloS one *8*, e57496.

Chait, A., and den Hartigh, L.J. (2020). Adipose Tissue Distribution, Inflammation and Its Metabolic Consequences, Including Diabetes and Cardiovascular Disease. Front Cardiovasc Med *7*, 22.

Chal, J., and Pourquie, O. (2017). Making muscle: skeletal myogenesis in vivo and in vitro. Development *144*, 2104-2122.

Chen, J.F., Mandel, E.M., Thomson, J.M., Wu, Q., Callis, T.E., Hammond, S.M., Conlon, F.L., and Wang, D.Z. (2006). The role of microRNA-1 and microRNA-133 in skeletal muscle proliferation and differentiation. Nature genetics *38*, 228-233.

Cheng, T., Hu, C., Yang, H., Cao, L., and An, J. (2014). Transforming growth factor-beta-induced miR143 expression in regulation of non-small cell lung cancer cell viability and invasion capacity in vitro and in vivo. Int J Oncol *45*, 1977-1988.

Chiang, H.R., Schoenfeld, L.W., Ruby, J.G., Auyeung, V.C., Spies, N., Baek, D., Johnston, W.K., Russ, C., Luo, S., Babiarz, J.E., *et al.* (2010). Mammalian microRNAs: experimental evaluation of novel and previously annotated genes. Genes Dev *24*, 992-1009.

Church, T.S., Blair, S.N., Cocreham, S., Johannsen, N., Johnson, W., Kramer, K., Mikus, C.R., Myers, V., Nauta, M., Rodarte, R.Q., *et al.* (2010). Effects of aerobic and resistance training on hemoglobin A1c levels in patients with type 2 diabetes: a randomized controlled trial. Jama *304*, 2253-2262.

Climent, M., Quintavalle, M., Miragoli, M., Chen, J., Condorelli, G., and Elia, L. (2015). TGFbeta Triggers miR-143/145 Transfer From Smooth Muscle Cells to Endothelial Cells, Thereby Modulating Vessel Stabilization. Circ Res *116*, 1753-1764.

Coletta, R., Roberts, N.A., Randles, M.J., Morabito, A., and Woolf, A.S. (2018). Exogenous transforming growth factor-beta1 enhances smooth muscle differentiation in embryonic mouse jejunal explants. J Tissue Eng Regen Med *12*, 252-264.

Coyle, E.F. (1995). Substrate utilization during exercise in active people. Am J Clin Nutr *61*, 968S-979S.

Cozzone, D., Frojdo, S., Disse, E., Debard, C., Laville, M., Pirola, L., and Vidal, H. (2008). Isoform-specific defects of insulin stimulation of Akt/protein kinase B (PKB) in skeletal muscle cells from type 2 diabetic patients. Diabetologia *51*, 512-521.

Creugny, A., Fender, A., and Pfeffer, S. (2018). Regulation of primary microRNA processing. FEBS Lett *592*, 1980-1996.

Cui, S.F., Li, W., Niu, J., Zhang, C.Y., Chen, X., and Ma, J.Z. (2015). Acute responses of circulating microRNAs to low-volume sprint interval cycling. Frontiers in Physiology *6*.

Cui, S.F., Wang, C., Yin, X., Tian, D., Lu, Q.J., Zhang, C.Y., Chen, X., and Ma, J.Z. (2016). Similar Responses of Circulating MicroRNAs to Acute High-Intensity Interval Exercise and Vigorous-Intensity Continuous Exercise. Frontiers in Physiology *7*.

Czarkowska-Paczek, B., Zendzian-Piotrowska, M., Bartlomiejczyk, I., Przybylski, J., and Gorski, J. (2009). The effect of acute and prolonged endurance exercise on transforming growth factor-beta1 generation in rat skeletal and heart muscle. J Physiol Pharmacol *60*, 157-162.

Davidson, L.E., Hudson, R., Kilpatrick, K., Kuk, J.L., McMillan, K., Janiszewski, P.M., Lee, S., Lam, M., and Ross, R. (2009). Effects of exercise modality on insulin resistance and functional limitation in older adults: a randomized controlled trial. Arch Intern Med *169*, 122-131.

Davis, B.N., Hilyard, A.C., Lagna, G., and Hata, A. (2008). SMAD proteins control DROSHA-mediated microRNA maturation. Nature *454*, 56-61.

Davis, B.N., Hilyard, A.C., Nguyen, P.H., Lagna, G., and Hata, A. (2010). Smad proteins bind a conserved RNA sequence to promote microRNA maturation by Drosha. Mol Cell *39*, 373-384.

DeFronzo, R.A., Jacot, E., Jequier, E., Maeder, E., Wahren, J., and Felber, J.P. (1981). The effect of insulin on the disposal of intravenous glucose. Results from indirect calorimetry and hepatic and femoral venous catheterization. Diabetes *30*, 1000-1007.

Dela, F., Ingersen, A., Andersen, N.B., Nielsen, M.B., Petersen, H.H.H., Hansen, C.N., Larsen, S., Wojtaszewski, J., and Helge, J.W. (2019). Effects of one-legged high-intensity interval training on insulin-mediated skeletal muscle glucose homeostasis in patients with type 2 diabetes. Acta Physiol (Oxf) *226*, e13245.

Derynck, R., and Zhang, Y.E. (2003). Smad-dependent and Smad-independent pathways in TGF-beta family signalling. Nature *425*, 577-584.

Desvignes, T., Batzel, P., Berezikov, E., Eilbeck, K., Eppig, J.T., McAndrews, M.S., Singer, A., and Postlethwait, J.H. (2015). miRNA Nomenclature: A View Incorporating Genetic Origins, Biosynthetic Pathways, and Sequence Variants. Trends Genet *31*, 613-626.

Devlin, R.B., and Emerson, C.P., Jr. (1978). Coordinate regulation of contractile protein synthesis during myoblast differentiation. Cell *13*, 599-611.

Droguett, R., Cabello-Verrugio, C., Santander, C., and Brandan, E. (2010). TGF-beta receptors, in a Smad-independent manner, are required for terminal skeletal muscle differentiation. Experimental cell research *316*, 2487-2503.

Drummond, M.J., Glynn, E.L., Fry, C.S., Dhanani, S., Volpi, E., and Rasmussen, B.B. (2009). Essential amino acids increase microRNA-499, -208b, and -23a and downregulate myostatin and myocyte enhancer factor 2C mRNA expression in human skeletal muscle. J Nutr *139*, 2279-2284.

Duguez, S., Feasson, L., Denis, C., and Freyssenet, D. (2002). Mitochondrial biogenesis during skeletal muscle regeneration. Am J Physiol Endocrinol Metab *282*, E802-809.

Dulloo, A.G., Jacquet, J., Solinas, G., Montani, J.P., and Schutz, Y. (2010). Body composition phenotypes in pathways to obesity and the metabolic syndrome. Int J Obes (Lond) *34 Suppl 2*, S4-17.

Elbashir, S.M., Harborth, J., Lendeckel, W., Yalcin, A., Weber, K., and Tuschl, T. (2001). Duplexes of 21-nucleotide RNAs mediate RNA interference in cultured mammalian cells. Nature *411*, 494-498.

Ellison, G.M., Waring, C.D., Vicinanza, C., and Torella, D. (2012). Physiological cardiac remodelling in response to endurance exercise training: cellular and molecular mechanisms. Heart *98*, 5-10.

Esau, C., Kang, X., Peralta, E., Hanson, E., Marcusson, E.G., Ravichandran, L.V., Sun, Y., Koo, S., Perera, R.J., Jain, R., *et al.* (2004). MicroRNA-143 regulates adipocyte differentiation. J Biol Chem *279*, 52361-52365.

Fabani, M.M., and Gait, M.J. (2008). miR-122 targeting with LNA/2'-O-methyl oligonucleotide mixmers, peptide nucleic acids (PNA), and PNA-peptide conjugates. RNA (New York, NY) *14*, 336-346.

Fang, R., Xiao, T., Fang, Z., Sun, Y., Li, F., Gao, Y., Feng, Y., Li, L., Wang, Y., Liu, X., *et al.* (2012). MicroRNA-143 (miR-143) regulates cancer glycolysis via targeting hexokinase 2 gene. J Biol Chem *287*, 23227-23235.

Felder, T.K., Soyal, S.M., Oberkofler, H., Hahne, P., Auer, S., Weiss, R., Gadermaier, G., Miller, K., Krempler, F., Esterbauer, H., *et al.* (2011). Characterization of novel peroxisome proliferator-activated receptor gamma coactivator-1alpha (PGC-1alpha) isoform in human liver. J Biol Chem *286*, 42923-42936.

Figueroa, J.D., and Hayman, M.J. (2004). Differential effects of the Ski-interacting protein (SKIP) on differentiation induced by transforming growth factor-beta1 and bone morphogenetic protein-2 in C2C12 cells. Experimental cell research *296*, 163-172.

Filvaroff, E.H., Ebner, R., and Derynck, R. (1994). Inhibition of myogenic differentiation in myoblasts expressing a truncated type II TGF-beta receptor. Development *120*, 1085-1095.

Fortini, P., Iorio, E., Dogliotti, E., and Isidoro, C. (2016). Coordinated Metabolic Changes and Modulation of Autophagy during Myogenesis. Front Physiol *7*, 237.

Fujio, Y., Guo, K., Mano, T., Mitsuuchi, Y., Testa, J.R., and Walsh, K. (1999). Cell cycle withdrawal promotes myogenic induction of Akt, a positive modulator of myocyte survival. Mol Cell Biol *19*, 5073-5082.

Gaster, M., Kristensen, S.R., Beck-Nielsen, H., and Schroder, H.D. (2001). A cellular model system of differentiated human myotubes. APMIS *109*, 735-744.

Gillberg, L., Jacobsen, S.C., Ribel-Madsen, R., Gjesing, A.P., Boesgaard, T.W., Ling, C., Pedersen, O., Hansen, T., and Vaag, A. (2013). Does DNA methylation of PPARGC1A influence insulin action in first degree relatives of patients with type 2 diabetes? PloS one *8*, e58384.

Goedecke, J.H., and Micklesfield, L.K. (2014). The effect of exercise on obesity, body fat distribution and risk for type 2 diabetes. Med Sport Sci *60*, 82-93.

Golabi, P., Locklear, C.T., Austin, P., Afdhal, S., Byrns, M., Gerber, L., and Younossi, Z.M. (2016). Effectiveness of exercise in hepatic fat mobilization in non-alcoholic fatty liver disease: Systematic review. World journal of gastroenterology *22*, 6318-6327.

Goljanek-Whysall, K., Pais, H., Rathjen, T., Sweetman, D., Dalmay, T., and Munsterberg, A. (2012). Regulation of multiple target genes by miR-1 and miR-206 is pivotal for C2C12 myoblast differentiation. J Cell Sci *125*, 3590-3600.

Gollnick, P.D., Armstrong, R.B., Saltin, B., Saubert, C.W.t., Sembrowich, W.L., and Shepherd, R.E. (1973). Effect of training on enzyme activity and fiber composition of human skeletal muscle. J Appl Physiol *34*, 107-111.

Goodyear, L.J., Hirshman, M.F., Valyou, P.M., and Horton, E.S. (1992). Glucose transporter number, function, and subcellular distribution in rat skeletal muscle after exercise training. Diabetes *41*, 1091-1099.

Gosselin, L.E., Williams, J.E., Deering, M., Brazeau, D., Koury, S., and Martinez, D.A. (2004). Localization and early time course of TGF-beta 1 mRNA expression in dystrophic muscle. Muscle Nerve *30*, 645-653.

Gottmann, P., Ouni, M., Saussenthaler, S., Roos, J., Stirm, L., Jahnert, M., Kamitz, A., Hallahan, N., Jonas, W., Fritsche, A., *et al.* (2018). A computational biology approach of a genome-wide screen connected miRNAs to obesity and type 2 diabetes. Mol Metab *11*, 145-159.

Gregory, P.A., Bracken, C.P., Smith, E., Bert, A.G., Wright, J.A., Roslan, S., Morris, M., Wyatt, L., Farshid, G., Lim, Y.Y., *et al.* (2011). An autocrine TGF-beta/ZEB/miR-200 signaling network regulates establishment and maintenance of epithelial-mesenchymal transition. Mol Biol Cell *22*, 1686-1698.

Grishok, A., Pasquinelli, A.E., Conte, D., Li, N., Parrish, S., Ha, I., Baillie, D.L., Fire, A., Ruvkun, G., and Mello, C.C. (2001). Genes and Mechanisms Related to RNA Interference Regulate Expression of the Small Temporal RNAs that Control C. elegans Developmental Timing. Cell *106*, 23-34.

Hagberg, J.M., Jenkins, N.T., and Spangenburg, E. (2012). Exercise training, genetics and type 2 diabetes-related phenotypes. Acta Physiol (Oxf) *205*, 456-471.

Hamada, K., Vannier, E., Sacheck, J.M., Witsell, A.L., and Roubenoff, R. (2005). Senescence of human skeletal muscle impairs the local inflammatory cytokine response to acute eccentric exercise. FASEB journal : official publication of the Federation of American Societies for Experimental Biology *19*, 264-266.

Handschin, C., Chin, S., Li, P., Liu, F., Maratos-Flier, E., Lebrasseur, N.K., Yan, Z., and Spiegelman, B.M. (2007). Skeletal muscle fiber-type switching, exercise intolerance, and myopathy in PGC-1alpha muscle-specific knock-out animals. J Biol Chem *282*, 30014-30021.

Hawley, J.A. (2004). Exercise as a therapeutic intervention for the prevention and treatment of insulin resistance. Diabetes/metabolism research and reviews *20*, 383-393.

He, L., and Hannon, G.J. (2004). MicroRNAs: small RNAs with a big role in gene regulation. Nat Rev Genet *5*, 522-531.

Heinemeier, K.M., Bjerrum, S.S., Schjerling, P., and Kjaer, M. (2013). Expression of extracellular matrix components and related growth factors in human tendon and muscle after acute exercise. Scandinavian journal of medicine & science in sports *23*, e150-161.

Henry, R.R., Abrams, L., Nikoulina, S., and Ciaraldi, T.P. (1995). Insulin action and glucose metabolism in nondiabetic control and NIDDM subjects. Comparison using human skeletal muscle cell cultures. Diabetes *44*, 936-946.

Hoffmann, C., Hockele, S., Kappler, L., Hrabe de Angelis, M., Haring, H.U., and Weigert, C. (2018). The effect of differentiation and TGFbeta on mitochondrial respiration and mitochondrial enzyme abundance in cultured primary human skeletal muscle cells. Scientific reports *8*, 737.

Holloszy, J.O. (1967). Biochemical adaptations in muscle. Effects of exercise on mitochondrial oxygen uptake and respiratory enzyme activity in skeletal muscle. J Biol Chem *242*, 2278-2282.

Holmquist, P., and Torffvit, O. (2009). Urinary transforming growth factor-beta(1), collagen IV and the effect of insulin in children at diagnosis of diabetes mellitus. Scand J Urol Nephrol *43*, 142-147.

Horak, M., Novak, J., and Bienertova-Vasku, J. (2016). Muscle-specific microRNAs in skeletal muscle development. Dev Biol *410*, 1-13.

Hu, J., Chen, C., Liu, Q., Liu, B., Song, C., Zhu, S., Wu, C., Liu, S., Yu, H., Yao, D., *et al.* (2015). The role of the miR-31/FIH1 pathway in TGF-beta-induced liver fibrosis. Clin Sci (Lond) *129*, 305-317.

Hutvagner, G., McLachlan, J., Pasquinelli, A.E., Balint, E., Tuschl, T., and Zamore, P.D. (2001). A cellular function for the RNA-interference enzyme Dicer in the maturation of the let-7 small temporal RNA. Science *293*, 834-838.

Ingerslev, B., Hansen, J.S., Hoffmann, C., Clemmesen, J.O., Secher, N.H., Scheler, M., Hrabe de Angelis, M., Haring, H.U., Pedersen, B.K., Weigert, C., *et al.* (2017). Angiopoietin-like protein 4 is an exercise-induced hepatokine in humans, regulated by glucagon and cAMP. Mol Metab *6*, 1286-1295.

Ingjer, F. (1979). Capillary supply and mitochondrial content of different skeletal muscle fiber types in untrained and endurance-trained men. A histochemical and ultrastructural study. Eur J Appl Physiol Occup Physiol *40*, 197-209.

International Diabetes Federation (2017). IDF Diabetes Atlas, 8th edn. (Brussels, Belgium: International Diabetes Federation).

International Mouse Phenotyping Consortium (2020). MGI:2676828.

Ishitobi, M., Haginoya, K., Zhao, Y., Ohnuma, A., Minato, J., Yanagisawa, T., Tanabu, M., Kikuchi, M., and Iinuma, K. (2000). Elevated plasma levels of transforming growth factor beta1 in patients with muscular dystrophy. Neuroreport *11*, 4033-4035.

Ismail, I., Keating, S.E., Baker, M.K., and Johnson, N.A. (2012). A systematic review and meta-analysis of the effect of aerobic vs. resistance exercise training on visceral fat. Obesity reviews : an official journal of the International Association for the Study of Obesity *13*, 68-91.

Iwasaki, S., Kobayashi, M., Yoda, M., Sakaguchi, Y., Katsuma, S., Suzuki, T., and Tomari, Y. (2010). Hsc70/Hsp90 chaperone machinery mediates ATP-dependent RISC loading of small RNA duplexes. Mol Cell *39*, 292-299.

Jain, M., Rivera, S., Monclus, E.A., Synenki, L., Zirk, A., Eisenbart, J., Feghali-Bostwick, C., Mutlu, G.M., Budinger, G.R., and Chandel, N.S. (2013). Mitochondrial reactive oxygen species regulate transforming growth factor-beta signaling. J Biol Chem *288*, 770-777.

James, D.E., Kraegen, E.W., and Chisholm, D.J. (1985). Effects of exercise training on in vivo insulin action in individual tissues of the rat. The Journal of clinical investigation *76*, 657-666.

James, D.E., Strube, M., and Mueckler, M. (1989). Molecular cloning and characterization of an insulin-regulatable glucose transporter. Nature *338*, 83-87.

Jeske, T., Huypens, P., Stirm, L., Hockele, S., Wurmser, C.M., Bohm, A., Weigert, C., Staiger, H., Klein, C., Beckers, J., *et al.* (2019). DEUS: an R package for accurate small RNA profiling based on differential expression of unique sequences. Bioinformatics (Oxford, England) *35*, 4834-4836.

Jin, H.Y., Gonzalez-Martin, A., Miletic, A.V., Lai, M., Knight, S., Sabouri-Ghomi, M., Head, S.R., Macauley, M.S., Rickert, R.C., and Xiao, C. (2015). Transfection of microRNA Mimics Should Be Used with Caution. Front Genet *6*, 340.

Jonas, S., and Izaurralde, E. (2015). Towards a molecular understanding of microRNA-mediated gene silencing. Nat Rev Genet *16*, 421-433.

Jordan, S.D., Kruger, M., Willmes, D.M., Redemann, N., Wunderlich, F.T., Bronneke, H.S., Merkwirth, C., Kashkar, H., Olkkonen, V.M., Bottger, T., *et al.* (2011). Obesity-induced overexpression of miRNA-143 inhibits insulin-stimulated AKT activation and impairs glucose metabolism. Nat Cell Biol *13*, 434-446.

Karbiener, M., Glantschnig, C., and Scheideler, M. (2014). Hunting the needle in the haystack: a guide to obtain biologically meaningful microRNA targets. Int J Mol Sci *15*, 20266-20289.

Khanna, N., Ge, Y., and Chen, J. (2014). MicroRNA-146b promotes myogenic differentiation and modulates multiple gene targets in muscle cells. PloS one *9*, e100657.

Kikani, C.K., Wu, X., Fogarty, S., Kang, S.A.W., Dephoure, N., Gygi, S.P., Sabatini, D.M., and Rutter, J. (2019). Activation of PASK by mTORC1 is required for the onset of the terminal differentiation program. Proc Natl Acad Sci U S A *116*, 10382-10391.

Kilian, Y., Wehmeier, U.F., Wahl, P., Mester, J., Hilberg, T., and Sperlich, B. (2016). Acute Response of Circulating Vascular Regulating MicroRNAs during and after High-Intensity and High-Volume Cycling in Children. Frontiers in Physiology *7*.

Kim, H.K., Lee, Y.S., Sivaprasad, U., Malhotra, A., and Dutta, A. (2006). Muscle-specific microRNA miR-206 promotes muscle differentiation. J Cell Biol *174*, 677-687.

Klingler, C., Zhao, X., Adhikary, T., Li, J., Xu, G., Haring, H.U., Schleicher, E., Lehmann, R., and Weigert, C. (2016). Lysophosphatidylcholines activate PPARdelta and protect human skeletal muscle cells from lipotoxicity. Biochim Biophys Acta *1861*, 1980-1992.

Klip, A., McGraw, T.E., and James, D.E. (2019). Thirty sweet years of GLUT4. J Biol Chem *294*, 11369-11381.

Knowler, W.C., Barrett-Connor, E., Fowler, S.E., Hamman, R.F., Lachin, J.M., Walker, E.A., Nathan, D.M., and Diabetes Prevention Program Research, G. (2002). Reduction in the incidence of type 2 diabetes with lifestyle intervention or metformin. The New England journal of medicine *346*, 393-403.

Kriska, A.M., Saremi, A., Hanson, R.L., Bennett, P.H., Kobes, S., Williams, D.E., and Knowler, W.C. (2003). Physical activity, obesity, and the incidence of type 2 diabetes in a high-risk population. Am J Epidemiol *158*, 669-675.

Kuwahara, K., Honda, T., Nakagawa, T., Yamamoto, S., Hayashi, T., and Mizoue, T. (2017). Body mass index trajectory patterns and changes in visceral fat and glucose metabolism before the onset of type 2 diabetes. Scientific reports *7*, 43521.

Lai, E.C. (2003). microRNAs: runts of the genome assert themselves. Curr Biol *13*, R925-936.

Lai, K.M., Gonzalez, M., Poueymirou, W.T., Kline, W.O., Na, E., Zlotchenko, E., Stitt, T.N., Economides, A.N., Yancopoulos, G.D., and Glass, D.J. (2004). Conditional activation of akt in adult skeletal muscle induces rapid hypertrophy. Mol Cell Biol *24*, 9295-9304.

Lakka, T.A., Rankinen, T., Weisnagel, S.J., Chagnon, Y.C., Rice, T., Leon, A.S., Skinner, J.S., Wilmore, J.H., Rao, D.C., Bouchard, C., *et al.* (2003). A quantitative trait locus on 7q31 for the changes in plasma insulin in response to exercise training: the HERITAGE Family Study. Diabetes *52*, 1583-1587.

Langley, B., Thomas, M., Bishop, A., Sharma, M., Gilmour, S., and Kambadur, R. (2002). Myostatin inhibits myoblast differentiation by down-regulating MyoD expression. J Biol Chem *277*, 49831-49840.

Lau, P., Nixon, S.J., Parton, R.G., and Muscat, G.E. (2004). RORalpha regulates the expression of genes involved in lipid homeostasis in skeletal muscle cells: caveolin-3 and CPT-1 are direct targets of ROR. J Biol Chem *279*, 36828-36840.

Lauritzen, H.P., Galbo, H., Brandauer, J., Goodyear, L.J., and Ploug, T. (2008). Large GLUT4 vesicles are stationary while locally and reversibly depleted during transient insulin stimulation of skeletal muscle of living mice: imaging analysis of GLUT4-enhanced green fluorescent protein vesicle dynamics. Diabetes *57*, 315-324.

Lauritzen, H.P., Galbo, H., Toyoda, T., and Goodyear, L.J. (2010). Kinetics of contraction-induced GLUT4 translocation in skeletal muscle fibers from living mice. Diabetes *59*, 2134-2144.

Lee, R.C., Feinbaum, R.L., and Ambros, V. (1993). The C. elegans heterochronic gene lin-4 encodes small RNAs with antisense complementarity to lin-14. Cell *75*, 843-854.

Lee, S., Kuk, J.L., Davidson, L.E., Hudson, R., Kilpatrick, K., Graham, T.E., and Ross, R. (2005). Exercise without weight loss is an effective strategy for obesity reduction in obese individuals with and without Type 2 diabetes. Journal of applied physiology (Bethesda, Md : 1985) *99*, 1220-1225.

Lee, Y., Ahn, C., Han, J., Choi, H., Kim, J., Yim, J., Lee, J., Provost, P., Radmark, O., Kim, S., *et al.* (2003). The nuclear RNase III Drosha initiates microRNA processing. Nature *425*, 415-419.

Lee, Y., Jeon, K., Lee, J.T., Kim, S., and Kim, V.N. (2002). MicroRNA maturation: stepwise processing and subcellular localization. EMBO J *21*, 4663-4670.

Li, B., Fan, J., and Chen, N. (2018). A Novel Regulator of Type II Diabetes: MicroRNA-143. Trends in endocrinology and metabolism: TEM *29*, 380-388.

Ling, C., Del Guerra, S., Lupi, R., Ronn, T., Granhall, C., Luthman, H., Masiello, P., Marchetti, P., Groop, L., and Del Prato, S. (2008). Epigenetic regulation of PPARGC1A in human type 2 diabetic islets and effect on insulin secretion. Diabetologia *51*, 615-622.

Liu, B., Liu, C., Cong, W., Li, N., Zhou, N., Tang, Y., Wei, C., Bai, H., Zhang, Y., and Xiao, J. (2017). Retinoid acid-induced microRNA-31-5p suppresses myogenic proliferation and differentiation by targeting CamkIIdelta. Skelet Muscle *7*, 8.

Liu, B., Shyr, Y., Cai, J., and Liu, Q. (2018). Interplay between miRNAs and host genes and their role in cancer. Brief Funct Genomics *18*, 255-266.

Liu, D., Black, B.L., and Derynck, R. (2001). TGF-beta inhibits muscle differentiation through functional repression of myogenic transcription factors by Smad3. Genes Dev *15*, 2950-2966.

Liu, J., Liang, X., Zhou, D., Lai, L., Xiao, L., Liu, L., Fu, T., Kong, Y., Zhou, Q., Vega, R.B., *et al.* (2016). Coupling of mitochondrial function and skeletal muscle fiber type by a miR-499/Fnip1/AMPK circuit. EMBO Mol Med *8*, 1212-1228.

Long, X., and Miano, J.M. (2011). Transforming growth factor-beta1 (TGF-beta1) utilizes distinct pathways for the transcriptional activation of microRNA 143/145 in human coronary artery smooth muscle cells. J Biol Chem *286*, 30119-30129.

Lund, J., Helle, S.A., Li, Y., Løvsletten, N.G., Stadheim, H.K., Jensen, J., Kase, E.T., Thoresen, G.H., and Rustan, A.C. (2018). Higher lipid turnover and oxidation in cultured human myotubes from athletic versus sedentary young male subjects. Scientific reports *8*, 17549.

Martin, J.F., Li, L., and Olson, E.N. (1992). Repression of myogenin function by TGF-beta 1 is targeted at the basic helix-loop-helix motif and is independent of E2A products. Journal of Biological Chemistry *267*, 10956-10960.

Martinez-Redondo, V., Pettersson, A.T., and Ruas, J.L. (2015). The hitchhiker's guide to PGC-1alpha isoform structure and biological functions. Diabetologia *58*, 1969-1977.

Massague, J., Cheifetz, S., Endo, T., and Nadal-Ginard, B. (1986). Type beta transforming growth factor is an inhibitor of myogenic differentiation. Proc Natl Acad Sci U S A *83*, 8206-8210.

McCarthy, J.J., Esser, K.A., Peterson, C.A., and Dupont-Versteegden, E.E. (2009). Evidence of MyomiR network regulation of beta-myosin heavy chain gene expression during skeletal muscle atrophy. Physiol Genomics *39*, 219-226.

McIntyre, E.A., Halse, R., Yeaman, S.J., and Walker, M. (2004). Cultured Muscle Cells from Insulin-Resistant Type 2 Diabetes Patients Have Impaired Insulin, but Normal 5-Amino-4-Imidazolecarboxamide Riboside-Stimulated, Glucose Uptake. The Journal of Clinical Endocrinology & Metabolism *89*, 3440-3448.

McPherron, A.C., Lawler, A.M., and Lee, S.J. (1997). Regulation of skeletal muscle mass in mice by a new TGF-beta superfamily member. Nature *387*, 83-90.

Mikines, K.J., Sonne, B., Farrell, P.A., Tronier, B., and Galbo, H. (1988). Effect of physical exercise on sensitivity and responsiveness to insulin in humans. Am J Physiol *254*, E248-259.

Mishra, S., Deng, J.J., Gowda, P.S., Rao, M.K., Lin, C.L., Chen, C.L., Huang, T., and Sun, L.Z. (2014). Androgen receptor and microRNA-21 axis downregulates transforming growth factor beta receptor II (TGFBR2) expression in prostate cancer. Oncogene *33*, 4097-4106.

Montero, D., and Lundby, C. (2017). Refuting the myth of non-response to exercise training: 'non-responders' do respond to higher dose of training. J Physiol *595*, 3377-3387.

Murakami, M., Ohkuma, M., and Nakamura, M. (2008). Molecular mechanism of transforming growth factor-beta-mediated inhibition of growth arrest and differentiation in a myoblast cell line. Dev Growth Differ *50*, 121-130.

Muralimanoharan, S., Maloyan, A., and Myatt, L. (2016). Mitochondrial function and glucose metabolism in the placenta with gestational diabetes mellitus: role of miR-143. Clin Sci (Lond) *130*, 931-941.

Nakano, N., Maeyama, K., Sakata, N., Itoh, F., Akatsu, R., Nakata, M., Katsu, Y., Ikeno, S., Togawa, Y., Vo Nguyen, T.T., *et al.* (2014). C18 ORF1, a novel negative regulator of transforming growth factor-beta signaling. J Biol Chem *289*, 12680-12692.

Neubauer, O., Sabapathy, S., Ashton, K.J., Desbrow, B., Peake, J.M., Lazarus, R., Wessner, B., Cameron-Smith, D., Wagner, K.H., Haseler, L.J., *et al.* (2014). Time course-dependent changes in the transcriptome of human skeletal muscle during recovery from endurance exercise: from inflammation to adaptive remodeling. Journal of applied physiology (Bethesda, Md : 1985) *116*, 274-287.

Neumann, A., Lindholm, L., Norberg, M., Schoffer, O., Klug, S.J., and Norstrom, F. (2017). The cost-effectiveness of interventions targeting lifestyle change for the prevention of diabetes in a Swedish primary care and community based prevention program. The European journal of health economics : HEPAC : health economics in prevention and care *18*, 905-919.

Newsholme, E.A., Leech, A.R., and Board, M. (2010). Functional biochemistry in health & disease : metabolic regulation in health and disease (Hoboken, N.J.; Chichester: Wiley ; John Wiley distributor).

Nielsen, S., Scheele, C., Yfanti, C., Akerstrom, T., Nielsen, A.R., Pedersen, B.K., and Laye, M.J. (2010). Muscle specific microRNAs are regulated by endurance exercise in human skeletal muscle. J Physiol *588*, 4029-4037.

Nikolic, N., Rhedin, M., Rustan, A.C., Storlien, L., Thoresen, G.H., and Stromstedt, M. (2012). Overexpression of PGC-1alpha increases fatty acid oxidative capacity of human skeletal muscle cells. Biochem Res Int *2012*, 714074.

Noguchi, S., Yasui, Y., Iwasaki, J., Kumazaki, M., Yamada, N., Naito, S., and Akao, Y. (2013). Replacement treatment with microRNA-143 and -145 induces synergistic inhibition of the growth of human bladder cancer cells by regulating PI3K/Akt and MAPK signaling pathways. Cancer Lett *328*, 353-361.

Nohata, N., Hanazawa, T., Enokida, H., and Seki, N. (2012). microRNA-1/133a and microRNA-206/133b clusters: dysregulation and functional roles in human cancers. Oncotarget *3*, 9-21.

Olson, E.N., Sternberg, E., Hu, J.S., Spizz, G., and Wilcox, C. (1986). Regulation of myogenic differentiation by type beta transforming growth factor. J Cell Biol *103*, 1799-1805.

Ong, J., Timens, W., Rajendran, V., Algra, A., Spira, A., Lenburg, M.E., Campbell, J.D., van den Berge, M., Postma, D.S., van den Berg, A., *et al.* (2017). Identification of transforming growth factor-beta-regulated microRNAs and the microRNA-targetomes in primary lung fibroblasts. PloS one *12*, e0183815.

Osler, M.E., Fritz, T., Caidahl, K., Krook, A., Zierath, J.R., and Wallberg-Henriksson, H. (2015). Changes in gene expression in responders and nonresponders to a low-intensity walking intervention. Diabetes care *38*, 1154-1160.

Pedersen, B.K., and Saltin, B. (2015). Exercise as medicine - evidence for prescribing exercise as therapy in 26 different chronic diseases. Scandinavian journal of medicine & science in sports *25 Suppl 3*, 1-72.

Pilegaard, H., Saltin, B., and Neufer, P.D. (2003). Exercise induces transient transcriptional activation of the PGC-1alpha gene in human skeletal muscle. J Physiol *546*, 851-858.

Poehlman, E.T., Melby, C.L., Badylak, S.F., and Calles, J. (1989). Aerobic fitness and resting energy expenditure in young adult males. Metabolism *38*, 85-90.

Polesskaya, A., Degerny, C., Pinna, G., Maury, Y., Kratassiouk, G., Mouly, V., Morozova, N., Kropp, J., Frandsen, N., and Harel-Bellan, A. (2013). Genome-wide exploration of miRNA function in mammalian muscle cell differentiation. PloS one *8*, e71927.

Popov, D.V., Lysenko, E.A., Vepkhvadze, T.F., Kurochkina, N.S., Maknovskii, P.A., and Vinogradova, O.L. (2015). Promoter-specific regulation of PPARGC1A gene expression in human skeletal muscle. Journal of molecular endocrinology *55*, 159-168.

Praet, S.F., and van Loon, L.J. (2008). Exercise: the brittle cornerstone of type 2 diabetes treatment. Diabetologia *51*, 398-401.

Puigserver, P., Wu, Z., Park, C.W., Graves, R., Wright, M., and Spiegelman, B.M. (1998). A cold-inducible coactivator of nuclear receptors linked to adaptive thermogenesis. Cell *92*, 829-839.

Qiao, Y.C., Chen, Y.L., Pan, Y.H., Ling, W., Tian, F., Zhang, X.X., and Zhao, H.L. (2017). Changes of transforming growth factor beta 1 in patients with type 2 diabetes and diabetic nephropathy: A PRISMA-compliant systematic review and meta-analysis. Medicine (Baltimore) *96*, e6583.

Ranallo, R.F., and Rhodes, E.C. (1998). Lipid metabolism during exercise. Sports Med *26*, 29-42.

Remels, A.H., Langen, R.C., Schrauwen, P., Schaart, G., Schols, A.M., and Gosker, H.R. (2010). Regulation of mitochondrial biogenesis during myogenesis. Mol Cell Endocrinol *315*, 113-120.

Richter, E.A., Turcotte, L., Hespel, P., and Kiens, B. (1992). Metabolic responses to exercise. Effects of endurance training and implications for diabetes. Diabetes care *15*, 1767-1776.

Roberts, C.K., Hevener, A.L., and Barnard, R.J. (2013). Metabolic syndrome and insulin resistance: underlying causes and modification by exercise training. Comprehensive Physiology *3*, 1-58.

Rochlin, K., Yu, S., Roy, S., and Baylies, M.K. (2010). Myoblast fusion: when it takes more to make one. Developmental biology *341*, 66-83.

Rodriguez, A., Griffiths-Jones, S., Ashurst, J.L., and Bradley, A. (2004). Identification of mammalian microRNA host genes and transcription units. Genome Res *14*, 1902-1910.

Romijn, J.A., Coyle, E.F., Sidossis, L.S., Gastaldelli, A., Horowitz, J.F., Endert, E., and Wolfe, R.R. (1993). Regulation of endogenous fat and carbohydrate metabolism in relation to exercise intensity and duration. Am J Physiol *265*, E380-391.

Ropka-Molik, K., Pawlina-Tyszko, K., Zukowski, K., Piorkowska, K., Zak, G., Gurgul, A., Derebecka, N., and Wesoly, J. (2018). Examining the Genetic Background of Porcine Muscle Growth and Development Based on Transcriptome and miRNAome Data. Int J Mol Sci *19*.

Ross, R. (1997). Effects of diet- and exercise-induced weight loss on visceral adipose tissue in men and women. Sports Med *24*, 55-64.

Rotwein, P., and Wilson, E.M. (2009). Distinct actions of Akt1 and Akt2 in skeletal muscle differentiation. J Cell Physiol *219*, 503-511.

Ruegsegger, G.N., and Booth, F.W. (2018). Health Benefits of Exercise. Cold Spring Harbor perspectives in medicine *8*.

Russell, A.P., Feilchenfeldt, J., Schreiber, S., Praz, M., Crettenand, A., Gobelet, C., Meier, C.A., Bell, D.R., Kralli, A., Giacobino, J.P., *et al.* (2003). Endurance training in humans leads to fiber type-specific increases in levels of peroxisome proliferator-activated receptor-gamma coactivator-1 and peroxisome proliferator-activated receptor-alpha in skeletal muscle. Diabetes *52*, 2874-2881.

Russell, A.P., and Lamon, S. (2015). Exercise, Skeletal Muscle and Circulating microRNAs. Progress in molecular biology and translational science *135*, 471-496.

Russell, A.P., Lamon, S., Boon, H., Wada, S., Guller, I., Brown, E.L., Chibalin, A.V., Zierath, J.R., Snow, R.J., Stepto, N., *et al.* (2013). Regulation of miRNAs in human skeletal muscle following acute endurance exercise and short-term endurance training. J Physiol *591*, 4637-4653.

Sabag, A., Way, K.L., Keating, S.E., Sultana, R.N., O'Connor, H.T., Baker, M.K., Chuter, V.H., George, J., and Johnson, N.A. (2017). Exercise and ectopic fat in type 2 diabetes: A systematic review and meta-analysis. Diabetes Metab *43*, 195-210.

Samocha-Bonet, D., Debs, S., and Greenfield, J.R. (2018). Prevention and Treatment of Type 2 Diabetes: A Pathophysiological-Based Approach. Trends in endocrinology and metabolism: TEM *29*, 370-379.

Sancak, Y., Peterson, T.R., Shaul, Y.D., Lindquist, R.A., Thoreen, C.C., Bar-Peled, L., and Sabatini, D.M. (2008). The Rag GTPases bind raptor and mediate amino acid signaling to mTORC1. Science *320*, 1496-1501.

Sapp, R.M., Shill, D.D., Roth, S.M., and Hagberg, J.M. (2017). Circulating microRNAs in acute and chronic exercise: more than mere biomarkers. Journal of applied physiology (Bethesda, Md : 1985) *122*, 702-717.

Sarabia, V., Lam, L., Burdett, E., Leiter, L.A., and Klip, A. (1992). Glucose transport in human skeletal muscle cells in culture. Stimulation by insulin and metformin. The Journal of clinical investigation *90*, 1386-1395.

Schabort, E.J., van der Merwe, M., Loos, B., Moore, F.P., and Niesler, C.U. (2009). TGF-beta's delay skeletal muscle progenitor cell differentiation in an isoform-independent manner. Experimental cell research *315*, 373-384.

Schiaffino, S., Dyar, K.A., Ciciliot, S., Blaauw, B., and Sandri, M. (2013). Mechanisms regulating skeletal muscle growth and atrophy. FEBS J *280*, 4294-4314.

Schiaffino, S., and Reggiani, C. (2011). Fiber types in mammalian skeletal muscles. Physiol Rev *91*, 1447-1531.

Sempere, L.F., Freemantle, S., Pitha-Rowe, I., Moss, E., Dmitrovsky, E., and Ambros, V. (2004). Expression profiling of mammalian microRNAs uncovers a subset of brain-expressed microRNAs with possible roles in murine and human neuronal differentiation. Genome Biol *5*, R13.

Shubrook, J.H., Chen, W., and Lim, A. (2018). Evidence for the Prevention of Type 2 Diabetes Mellitus. J Am Osteopath Assoc *118*, 730-737.

Shull, M.M., Ormsby, I., Kier, A.B., Pawlowski, S., Diebold, R.J., Yin, M., Allen, R., Sidman, C., Proetzel, G., Calvin, D., *et al.* (1992). Targeted disruption of the mouse transforming growth factor-beta 1 gene results in multifocal inflammatory disease. Nature *359*, 693-699.

Sin, J., Andres, A.M., Taylor, D.J., Weston, T., Hiraumi, Y., Stotland, A., Kim, B.J., Huang, C., Doran, K.S., and Gottlieb, R.A. (2016). Mitophagy is required for mitochondrial biogenesis and myogenic differentiation of C2C12 myoblasts. Autophagy *12*, 369-380.

Sjoberg, K.A., Frosig, C., Kjobsted, R., Sylow, L., Kleinert, M., Betik, A.C., Shaw, C.S., Kiens, B., Wojtaszewski, J.F.P., Rattigan, S., *et al.* (2017). Exercise Increases Human Skeletal Muscle Insulin Sensitivity via Coordinated Increases in Microvascular Perfusion and Molecular Signaling. Diabetes *66*, 1501-1510.

Smith, U., and Kahn, B.B. (2016). Adipose tissue regulates insulin sensitivity: role of adipogenesis, de novo lipogenesis and novel lipids. J Intern Med *280*, 465-475.

Sokilde, R., Newie, I., Persson, H., Borg, A., and Rovira, C. (2015). Passenger strand loading in overexpression experiments using microRNA mimics. RNA Biol *12*, 787-791.

Solomon, T.P., and Thyfault, J.P. (2013). Type 2 diabetes sits in a chair. Diabetes Obes Metab *15*, 987-992.

Solomon, T.P.J. (2018). Sources of Inter-individual Variability in the Therapeutic Response of Blood Glucose Control to Exercise in Type 2 Diabetes: Going Beyond Exercise Dose. Front Physiol *9*, 896.

Soriano-Arroquia, A., McCormick, R., Molloy, A.P., McArdle, A., and Goljanek-Whysall, K. (2016). Age-related changes in miR-143-3p:Igfbp5 interactions affect muscle regeneration. Aging Cell *15*, 361-369.

Soyal, S.M., Felder, T.K., Auer, S., Hahne, P., Oberkofler, H., Witting, A., Paulmichl, M., Landwehrmeyer, G.B., Weydt, P., Patsch, W., *et al.* (2012). A greatly extended PPARGC1A genomic locus encodes several new brain-specific isoforms and influences Huntington disease age of onset. Hum Mol Genet *21*, 3461-3473.

Sparks, L.M. (2017). Exercise training response heterogeneity: physiological and molecular insights. Diabetologia *60*, 2329-2336.

Sparks, L.M., Johannsen, N.M., Church, T.S., Earnest, C.P., Moonen-Kornips, E., Moro, C., Hesselink, M.K., Smith, S.R., and Schrauwen, P. (2013). Nine months of combined training improves ex vivo skeletal muscle metabolism in individuals with type 2 diabetes. J Clin Endocrinol Metab *98*, 1694-1702.

Stephens, N.A., and Sparks, L.M. (2015). Resistance to the beneficial effects of exercise in type 2 diabetes: are some individuals programmed to fail? J Clin Endocrinol Metab *100*, 43-52.

Stephens, N.A., Xie, H., Johannsen, N.M., Church, T.S., Smith, S.R., and Sparks, L.M. (2015). A transcriptional signature of "exercise resistance" in skeletal muscle of individuals with type 2 diabetes mellitus. Metabolism *64*, 999-1004.

Suzuki, H.I. (2018). MicroRNA Control of TGF-beta Signaling. Int J Mol Sci *19*.

Suzuki, H.I., Katsura, A., Yasuda, T., Ueno, T., Mano, H., Sugimoto, K., and Miyazono, K. (2015). Small-RNA asymmetry is directly driven by mammalian Argonautes. Nat Struct Mol Biol *22*, 512-521.

Taft, R.J., and Mattick, J.S. (2003). Increasing biological complexity is positively correlated with the relative genome-wide expansion of non-protein-coding DNA sequences. Genome Biology *5*, P1.

Thompson, D.B., Pratley, R., and Ossowski, V. (1996). Human primary myoblast cell cultures from non-diabetic insulin resistant subjects retain defects in insulin action. The Journal of clinical investigation *98*, 2346-2350.

Thomson, D.W., Bracken, C.P., Szubert, J.M., and Goodall, G.J. (2013). On measuring miRNAs after transient transfection of mimics or antisense inhibitors. PloS one *8*, e55214.

Thota, P., Perez-Lopez, F.R., Benites-Zapata, V.A., Pasupuleti, V., and Hernandez, A.V. (2017). Obesity-related insulin resistance in adolescents: a systematic review and meta-analysis of observational studies. Gynecol Endocrinol *33*, 179-184.

Tiano, J.P., Springer, D.A., and Rane, S.G. (2015). SMAD3 negatively regulates serum irisin and skeletal muscle FNDC5 and peroxisome proliferator-activated receptor gamma coactivator 1-alpha (PGC-1alpha) during exercise. J Biol Chem *290*, 11431.

Tuomilehto, J., Lindstrom, J., Eriksson, J.G., Valle, T.T., Hamalainen, H., Ilanne-Parikka, P., Keinanen-Kiukaanniemi, S., Laakso, M., Louheranta, A., Rastas, M., *et al.* (2001). Prevention of type 2 diabetes mellitus by changes in lifestyle among subjects with impaired glucose tolerance. The New England journal of medicine *344*, 1343-1350.

Tureckova, J., Wilson, E.M., Cappalonga, J.L., and Rotwein, P. (2001). Insulin-like growth factor-mediated muscle differentiation: collaboration between phosphatidylinositol 3-kinase-Akt-signaling pathways and myogenin. J Biol Chem *276*, 39264-39270.

Ueki, K., Yamamoto-Honda, R., Kaburagi, Y., Yamauchi, T., Tobe, K., Burgering, B.M., Coffer, P.J., Komuro, I., Akanuma, Y., Yazaki, Y., *et al.* (1998). Potential role of protein kinase B in insulin-induced glucose transport, glycogen synthesis, and protein synthesis. J Biol Chem *273*, 5315-5322.

Vacante, F., Denby, L., Sluimer, J.C., and Baker, A.H. (2019). The function of miR-143, miR-145 and the MiR-143 host gene in cardiovascular development and disease. Vascul Pharmacol *112*, 24-30.

Vaidya, T.B., Rhodes, S.J., Taparowsky, E.J., and Konieczny, S.F. (1989). Fibroblast growth factor and transforming growth factor beta repress transcription of the myogenic regulatory gene MyoD1. Mol Cell Biol *9*, 3576-3579.

Valcourt, U., Kowanetz, M., Niimi, H., Heldin, C.H., and Moustakas, A. (2005). TGF-beta and the Smad signaling pathway support transcriptomic reprogramming during epithelial-mesenchymal cell transition. Mol Biol Cell *16*, 1987-2002.

van Rooij, E., Quiat, D., Johnson, B.A., Sutherland, L.B., Qi, X., Richardson, J.A., Kelm, R.J., Jr., and Olson, E.N. (2009). A family of microRNAs encoded by myosin genes governs myosin expression and muscle performance. Dev Cell *17*, 662-673.

Wang, Y., Yu, Y., Tsuyada, A., Ren, X., Wu, X., Stubblefield, K., Rankin-Gee, E.K., and Wang, S.E. (2011). Transforming growth factor-beta regulates the sphere-initiating stem cell-like feature in breast cancer through miRNA-181 and ATM. Oncogene *30*, 1470-1480.

Weber, M., Hellmann, I., Stadler, M.B., Ramos, L., Paabo, S., Rebhan, M., and Schubeler, D. (2007). Distribution, silencing potential and evolutionary impact of promoter DNA methylation in the human genome. Nature genetics *39*, 457-466.

Weiss, A., and Attisano, L. (2013). The TGFbeta superfamily signaling pathway. Wiley Interdiscip Rev Dev Biol *2*, 47-63.

Wibom, R., Hultman, E., Johansson, M., Matherei, K., Constantin-Teodosiu, D., and Schantz, P.G. (1992). Adaptation of mitochondrial ATP production in human skeletal muscle to endurance training and detraining. Journal of applied physiology (Bethesda, Md : 1985) *73*, 2004-2010.

Wightman, B., Ha, I., and Ruvkun, G. (1993). Posttranscriptional regulation of the heterochronic gene lin-14 by lin-4 mediates temporal pattern formation in C. elegans. Cell *75*, 855-862.

Winbanks, C.E., Wang, B., Beyer, C., Koh, P., White, L., Kantharidis, P., and Gregorevic, P. (2011). TGF-beta regulates miR-206 and miR-29 to control myogenic differentiation through regulation of HDAC4. J Biol Chem *286*, 13805-13814.

Winett, R.A., Davy, B.M., Savla, J., Marinik, E.L., Winett, S.G., Baugh, M.E., and Flack, K.D. (2014). Using response variation to develop more effective, personalized behavioral medicine?: evidence from the Resist Diabetes study. Transl Behav Med *4*, 333-338.

Xie, X., Gao, H., Zeng, W., Chen, S., Feng, L., Deng, D., Qiao, F.Y., Liao, L., McCormick, K., Ning, Q., *et al.* (2015). Placental DNA methylation of peroxisome-proliferator-activated receptor-gamma co-activator-1alpha promoter is associated with maternal gestational glucose level. Clin Sci (Lond) *129*, 385-394.

Xu, T., Zhou, Q., Che, L., Das, S., Wang, L., Jiang, J., Li, G., Xu, J., Yao, J., Wang, H., *et al.* (2016). Circulating miR-21, miR-378, and miR-940 increase in response to an acute exhaustive exercise in chronic heart failure patients. Oncotarget *7*, 12414-12425.

Yates, T., Davies, M.J., Edwardson, C., Bodicoat, D.H., Biddle, S.J., and Khunti, K. (2014). Adverse responses and physical activity: secondary analysis of the PREPARE trial. Medicine and science in sports and exercise *46*, 1617-1623.

Yu, Y., Kanwar, S.S., Patel, B.B., Oh, P.S., Nautiyal, J., Sarkar, F.H., and Majumdar, A.P. (2012). MicroRNA-21 induces stemness by downregulating transforming growth factor beta receptor 2 (TGFbetaR2) in colon cancer cells. Carcinogenesis *33*, 68-76.

Zentella, A., and Massague, J. (1992). Transforming growth factor beta induces myoblast differentiation in the presence of mitogens. Proc Natl Acad Sci U S A *89*, 5176-5180.

Zhang, D., Li, X., Chen, C., Li, Y., Zhao, L., Jing, Y., Liu, W., Wang, X., Zhang, Y., Xia, H., *et al.* (2012). Attenuation of p38-mediated miR-1/133 expression facilitates myoblast proliferation during the early stage of muscle regeneration. PloS one *7*, e41478.

Zhang, Y.E. (2009). Non-Smad pathways in TGF-beta signaling. Cell Res *19*, 128-139.

Zheng, Y., Ley, S.H., and Hu, F.B. (2018). Global aetiology and epidemiology of type 2 diabetes mellitus and its complications. Nature reviews Endocrinology *14*, 88-98.

Zhou, S., Li, S., Zhang, W., Tong, H., Li, S., and Yan, Y. (2018). MiR-139 promotes differentiation of bovine skeletal muscle-derived satellite cells by regulating DHFR gene expression. J Cell Physiol *234*, 632-641.

Zimmet, P., Alberti, K.G., and Shaw, J. (2001). Global and societal implications of the diabetes epidemic. Nature *414*, 782-787.

Zurlo, F., Larson, K., Bogardus, C., and Ravussin, E. (1990). Skeletal muscle metabolism is a major determinant of resting energy expenditure. The Journal of clinical investigation *86*, 1423-1427.

6 Acknowledgements

Zu guter Letzt möchte ich noch all denen danken, die meine Arbeit der letzten Jahre möglich und angenehm gemacht haben. An oberster Stelle danke ich Martin Hrabe de Angelis für die Möglichkeit an seinem Institut unter sehr guten Rahmenbedingungen zu promovieren. Zusammen mit Cora Weigert und Stefanie Hauck gab es in meinem Thesis Committee immer hilfreiche und unterstützende Fragen, danke dafür!

Cora Weigert gilt als direkter Betreuerin mein ganz besonderer Dank. Danke für die bestmögliche Fernbetreuung die man sich vorstellen kann – immer erreichbar, wenn es dringend war, sehr schnelle und hilfreiche Korrekturen, Unterstützung auf Konferenzen und wo angemessen auch Lob und Kritik. Danke auch an die anderen Tübinger, vor allem Christoph Hoffmann und Heike Runge, für die Telefonhilfe bei größeren und kleineren Problemen!

Vielen Dank auch an meine Arbeitsgruppe in München, Danke Lucia, Bernd und Annett für die Unterstützung in und ums Labor! Dankeschön an Johannes Beckers und seine Arbeitsgruppe, besonders Martin Irmler und Peter Huypens für die gemeinsamen Projekte, das Initiieren weiterer Kooperationen mit der TUM und den Bioinformatikern Tim Jeske und Max Hastreiter. Danke an Sibylle für aufmunternde Worte und bürokratische Unterstützung.

Vielen Dank auch an alle auf „unserem Stockwerk“ für die angenehmen Stunden zwischen der Laborarbeit, die Unterstützung und alles was dazu gehört! Danke an Sandra für all die Schokolade, an Dani, Anna, Nirav, aber auch Max, Raf und Marina für beste Kaffeepäuschen, von Dampf ablassen bis zum Führen intellektueller Gespräche. Vielen Dank auch an die DINIs und HeJus für gemeinsames soziales und politisches Engagement. Das alles hat meine Promotionszeit auch außerhalb vom Labor zu einer Zeit gemacht, die ich nicht missen möchte!

Abseits vom Campus möchte ich mich bei meiner neuen Heimat dem Unterwasserhockey München e.V. bedanken, all die Trainingslager, Turniere und damit verbundenen Fahrten auf denen ich wirklich richtig abschalten konnte um montags mal mehr, mal weniger erholt zurück in die Arbeit zu kommen! Vielen Dank geht auch an meine Familie und Flo für bedingungslose Unterstützung!

Danke euch allen!